3-26-2020

Enhanced Surface Electrical Neurostimulation (eSENS): A Non-invasive Platform for Peripheral Neuromodulation

Andres Eduardo Pena
Florida International University, apena009@fiu.edu

FLORIDA INTERNATIONAL UNIVERSITY

Miami, Florida

ENHANCED SURFACE ELECTRICAL NEUROSTIMULATION (eSENS):

A NON-INVASIVE PLATFORM FOR PERIPHERAL NEUROMODULATION

A dissertation submitted in partial fulfillment of the

requirements for the degree of

DOCTOR OF PHILOSOPHY

in

BIOMEDICAL ENGINEERING

by

Andres Pena

2020

To: Dean John Volakis
    College of Engineering and Computing

This dissertation, written by Andres Pena, and entitled Enhanced Surface Electrical Neurostimulation (eSENS): A Non-Invasive Platform for Peripheral Neuromodulation, having been approved in respect to style and intellectual content, is referred to you for judgment.

We have read this dissertation and recommend that it be approved.

_____
James J. Abbas

_____
Kenneth W. Horch

_____
Jacob McPherson

_____
Anthony S. Dick

_____
Ranu Jung, Major Professor

Date of Defense: March 26, 2020

The dissertation of Andres Pena is approved.

_____
Dean John Volakis
College of Engineering and Computing

_____
Andrés G. Gil
Vice President for Research and Economic Development
and Dean of the University Graduate School

Florida International University, 2020

ii

ACKNOWLEDGMENTS

ABSTRACT OF THE DISSERTATION

ENHANCED SURFACE ELECTRICAL NEUROSTIMULATION (eSENS):

A NON-INVASIVE PLATFORM FOR PERIPHERAL NEUROMODULATION

by

Andres Pena

Florida International University, 2020

Miami, Florida

Professor Ranu Jung, Major Professor

Electrical stimulation of peripheral afferents has been used to study the sensory neural code and restore lost sensory function after amputation. Recently, implantable neural interfaces have prompted multiple breakthroughs in artificial somatosensory feedback for individuals with amputation, resulting in functional and psychological benefits. Although promising, the invasive nature of these approaches limits wide clinical applications, hindering the development of advanced neuromodulation strategies for intuitive sensory feedback. Transcutaneous (surface) stimulation is a potential non-invasive alternative. However, traditional surface stimulation methods are hampered by inadequate electrode and stimulation parameter fitting, localized discomfort, poor selectivity, and limited percept modulation.

An enhanced surface electrical neurostimulation platform has been developed to address the need for a non-invasive approach capable of selectively eliciting

comfortable tactile percepts with a wide range of intensities, that could be used to complete functional tasks. Several strategies were developed and implemented within the platform to achieve these features. First, a novel channel-hopping interleaved pulse scheduling strategy was developed to elicit enhanced tactile percepts while avoiding the discomfort associated with localized charge densities. This strategy was evaluated with able-bodied human subjects and compared with traditional methods. Second, a bio-inspired charge-rate encoding strategy was implemented to enhance the range and gradation of evoked percept intensities. The encoding strategy was evaluated during psychophysical studies with surface stimulation in able-bodied subjects and intrafascicular stimulation in an individual with a transradial amputation. Finally, a series of functional studies with able-bodied subjects evaluated the functional benefits afforded by the enhanced feedback on their ability to determine the size and hardness of virtual objects and perform graded control of virtual grasp force without visual feedback.

Results of these studies suggest that the strategies implemented within the stimulation platform can address the comfort and selectivity limitations of traditional methods and deliver a wide range of graded percepts that can be utilized to complete precise functional tasks. Overall, the use of this platform may eventually allow wide adoption of surface neurostimulation for chronic restoration of sensory function in individuals with amputation and could serve as a testbed for developing more natural neuromodulation strategies before deployment in implantable systems.

TABLE OF CONTENTS

LIST OF TABLES

LIST OF FIGURES

LIST OF ABBREVIATIONS AND ACRONYMS

AQR   Activation charge-rate

AP   Action potential

CHIPS   Channel-hopping interleaved pulse scheduling

CNS   Central Nervous System

DIME   Distributed intrafascicular multi-electrode

EMG   Electromyogram

eSENS   Enhanced surface electrical neurostimulation

FEM   Finite element model

LIFE   Longitudinal intrafascicular electrode

PA   Pulse amplitude

PF   Pulse frequency

PNS   Peripheral Nervous System

PW   Pulse width

SENS   Surface electrical neurostimulation

UiTL   User in the loop

CHAPTER 1

INTRODUCTION

1.1 Overview

Loss of sensory function caused by a life-changing event such as amputation after limb trauma or peripheral neuropathies after nerve injury, can have substantial effects on work, leisure, social life, and daily living activities as well as on psychological well-being. People rely on sensory feedback for everyday function, including planning and control of even simple movements, such as reaching for an object (Miall et al., 2019). For individuals with upper-limb amputation, the functionality of commercially available prosthetic technology is limited, which impacts quality of life and often leads to prosthesis abandonment (Biddiss and Chau, 2007b, Peerdeman et al., 2011a). The lack of sensory feedback from the prosthesis increases reliance on visual cues and attentional demand from the user, resulting in substantial functional deficits (Antfolk et al., 2013, Cordella et al., 2016). Because of this, sensory feedback is one of the most desired design priorities independent of the type of prosthesis and level of limb loss (Pylatiuk et al., 2007). The provision of sensory feedback may enable the user to better control the prosthesis and perform precise tasks with lower attentional demands; thereby improving quality of life (Carey et al., 2015). It also has the potential to promote prosthesis embodiment (Marasco et al., 2011, D'Alonzo et al., 2015).

For decades, the development of artificial sensory feedback systems has mostly centered on the activation of cutaneous mechanoreceptors through mechanical or electro-tactile stimulation to convey somatotopically-mismatched information (sensory substitution), and the activation of sensory fibers in peripheral nerves to evoke somatotopically-matched, distally referred sensations in the phantom hand. Non-invasive mechanical (Colella et al., 2019, Pena et al., 2019) and electro-tactile (Franceschi et al., 2017, Geng et al., 2018) sensory substitution approaches encode the missing sensory information (e.g. grasp force) through an alternate sensory channel by delivering tactile information at specific locations on the user's skin. Although these approaches offer an opportunity for conveying some information about prosthesis usage, they are often unable to evoke intuitive sensations due to percept modality and location mismatch. This limits the efficacy of the sensory feedback and increases the user's cognitive load and response time (Zhang et al., 2015, Pena et al., 2019). Alternatively, electrical stimulation of peripheral nerve afferents has been used to study the sensory neural code and restore lost sensory function after amputation. Recently, deployment of implantable neuromodulation systems has prompted multiple breakthroughs in artificial somatotopically-matched sensory feedback for individuals with amputation (Horch et al., 2011, Schiefer et al., 2018, Ortiz-Catalan et al., 2019, Clemente et al., 2019), resulting in functional and psychological benefits. Although promising, the invasive nature of these approaches limits wide clinical applications (Resnik et al., 2019).

Transcutaneous electrical neurostimulation is a potential non-invasive alternative for providing somatotopically-matched sensory feedback. In this approach, surface electrodes applied on the skin are used to deliver electrical pulses to nearby peripheral nerves, activating afferent pathways. Earlier studies have shown that transcutaneous stimulation can be used to elicit distally referred sensations when targeting the median and ulnar nerves at the forearm (D'Anna et al., 2017) or at the elbow level (Shin et al., 2018). However, inadequate electrode and stimulation parameter fitting, localized discomfort, poor selectivity, and limited percept modulation have precluded wide adoption of traditional transcutaneous neurostimulation as a viable sensory feedback approach (Kuhn et al., 2010, Forst et al., 2015, D'Anna et al., 2017, Shin et al., 2018).

An enhanced surface electrical neurostimulation (eSENS) platform was developed to elicit comfortable distally-referred percepts that could serve as intuitive non-invasive somatotopically-matched sensory feedback. The platform utilizes a novel Channel-hopping Interleaved Pulse Scheduling (CHIPS) strategy that leverages the combined influence of short, sub-threshold interleaved current pulses to deliver supra-threshold stimulation levels within the tissue, while reducing the total charge per pulse delivered by any given electrode on the skin. The platform also utilizes "User-in-the-loop" (UiTL) calibration routines developed to streamline the stimulation parameter fitting process. A bio-inspired charge-rate encoding strategy was implemented to enhance the range and gradation of percept intensities evoked by the stimulation. The eSENS platform was developed and characterized in psychophysical and functional studies with able-bodied human subjects. These

studies showed that the strategies used within this platform could elicit a wide range of percept intensities that are meaningful and could be readily utilized to complete functional tasks while avoiding the local sensations and skin discomfort, associated with the large charge densities in traditional methods. This suggests that the eSENS platform can be used to study the neural mechanisms of natural touch and offers a viable alternative to invasive approaches for delivering intuitive, somatotopically-matched sensory feedback to individuals with amputation. Additionally, it may be possible to expand the capabilities of this platform be used during remote operation of robotic devices (e.g. military explosive disposal, remote surgery), interactions within virtual and augmented reality environments (e.g. gaming, surgical training, social interactions), and to deliver targeted neuromodulation therapies for peripheral neuropathies, including neuropathic pain and sensory deficits secondary to intermediate carpal tunnel syndrome injury.

1.2 Rationale

Transcutaneous electrical neurostimulation has been investigated as a non-invasive approach for providing somatotopically-matched sensory feedback (D'Anna et al., 2017, Shin et al., 2018). Although promising, local sensations and skin discomfort associated with large charge densities and poor stimulation fitting have precluded wide adoption of this approach as a viable alternative to more invasive systems. The stimulation strategy implemented in this work was designed to avoid the discomfort associated with localized charge densities by leveraging the spatiotemporal summation of sub-threshold current pulses interleaved across a set of distributed electrodes, to deliver functional (supra-threshold) stimulation

levels within the tissue while reducing the total charge per pulse delivered by any given electrode. This strategy is based on the idea that the "RC recovery time interval" could enable the membrane to store some of the charge of the first pulse, making it easier for the fiber to depolarize after the second pulse (Rutten et al., 1991, Geng et al., 2011). This strategy was developed and tested around the peripheral nerves of able-bodied subjects at the wrist level. This location provides a flexible, yet stable platform for exploring the feasibility of the strategy since the target nerves are closer to the ventral skin surface, and allows access to mostly afferent fibers that innervate the hand digits while avoiding most of the efferent (motor) fibers. Implementation of this stimulation strategy within an array of spatially distributed electrodes may improve targeting and fitting (Shin et al., 2018). The ability to deliver enhanced tactile percepts enables the use of this platform to study the neural mechanisms of natural touch and explore multiple neuromodulation strategies for conveying intuitive and discriminable percepts. For instance, the transcutaneous electrical neurostimulation platform can be used to assess the benefits of modulating fiber population recruitment and firing rate to enhance the range and gradation of percept intensities (Graczyk et al., 2016). Bio-inspired sensory encoding strategies such as charge-rate modulation could be used to provide relevant sensory information that may be readily utilized to complete precise functional tasks with lower attentional demands. If the sensory encoding performance and functional control benefits of the eSENS platform is comparable to that of more invasive methods, it may eventually allow wide adoption of transcutaneous neurostimulation for restoration of sensory function in

individuals with amputation, and could serve as a testbed for developing more natural neuromodulation strategies in able-bodied subjects before deployment in implantable systems.

1.3 Design goals

The overall goal of the thesis presented here was to develop, characterize, and test an enhanced surface electrical neurostimulation (eSENS) platform capable of eliciting a wide range of percept intensities that are comfortable and meaningful, and could be readily utilized to complete functional tasks. A set of strategies were developed and implemented within the eSENS platform to satisfy the following features:

- Elicit distally referred tactile percepts while avoiding the local sensations and skin discomfort associated with the large charge densities in traditional methods.

- Convey a wide range of discriminable levels of tactile intensities

- Streamline the stimulation parameter fitting process

- Deliver intuitive haptic feedback that can be utilized during functional tasks

The performance of the platform was assessed with consenting able-bodied adult subjects and a consenting subject with a transradial amputation. The specific aims listed below served to accomplish these goals.

1.4 Specific aims

1.4.1 Specific aim 1

Specific Aim 1 was to develop an enhanced surface electrical neurostimulation (eSENS) platform capable of activating sensory afferents within the peripheral nerves in the upper arm to evoke distally referred sensations more comfortably and efficiently than traditional surface stimulation strategies. This specific aim can be subdivided into the following sub aims:

a) Develop a computational platform based on a median nerve sensory axon activation model in which the Channel-hopping interleaved pulse scheduling (CHIPS) strategy can be developed and assessed before implementation in the neurostimulation platform.

b) Evaluate the performance of the CHIPS strategy, and compare it with traditional surface stimulation configurations: able-bodied human subject trials.

c) Evaluate the steerability of the referred percept area with an array of distributed surface electrodes.

1.4.2 Specific aim 2

Specific aim 2 was to assess the ability of the eSENS platform to convey a wide range of discriminable levels of tactile intensities for haptic feedback. Specific Aim 2 is subdivided into the following sub aims:

a) Characterize the dependency of percept intensity range and gradation on different pulse frequency and charge modulation schemes in able-bodied subjects with the non-invasive neurostimulation platform, and a subject with a transradial amputation receiving intrafascicular stimulation.

b) Establish a streamlined parameter fitting strategy to convey a wide range of discriminable levels of tactile intensities.

1.4.3 Specific aim 3

Specific aim 3 was to assess the ability of the eSENS platform and the charge-rate encoding scheme to convey graded and discriminable levels of sensory information for intuitive haptic feedback during functional tasks. Specific Aim 3 is subdivided into the following sub aims:

a) Develop experimental paradigms for functional tasks

    a. Virtual object grasping tasks

    b. Graded control tasks

b) Assess the functional benefits afforded by the enhanced haptic feedback on the subject's ability to grasp and classify virtual objects with different size and hardness characteristics.

c) Assess the functional benefits afforded by the enhanced haptic feedback on the subject's ability to perform graded control of an external device's force output.

1.5 Organization of the dissertation

This dissertation is divided into six chapters. Chapter 1 serves as an introduction to the dissertation and discusses the rationale, design goals, specific aims, and organization of the dissertation. Chapter 2 consists of a review of the pertinent literature and rationale for the neurostimulation platform and strategy development. Chapter 3 describes the development and assessment of the eSENS platform to deliver comfortable distally referred sensory feedback. Chapter 4 describes a series of psychophysical trials that explored the discriminability and dynamic range of percept intensity under different parameter maps to develop a streamlined parameter fitting strategy to convey a wide range of discriminable levels of tactile intensities. Chapter 5 describes a study to assess whether the eSENS platform delivers intuitive and discriminable information to perform functional tasks. A summary of the work, its significance and limitations as well as future directions are presented in Chapter 6.

CHAPTER 2

LITERATURE REVIEW

Loss of sensory function caused by amputation after limb trauma or peripheral neuropathies after nerve injury can have substantial effects on work, leisure, social life, and daily living activities as well as on psychological well-being. People rely on sensory feedback for everyday function, including communication as well as planning and control of even simple movements, such as reaching for an object (Redmond et al., 2010, Miall et al., 2019). Loss of sensation can be especially devastating when the hands are affected. Our hands and fingers play an important role during dexterous motor tasks and sensory appreciation of object properties thanks to their fine sensory capacity. Loosing tactile sensation from our hands and fingers may result in motor deficits such as weakness, stiffness, or clumsiness, thus affecting our manual dexterity.

In 2005, in the United States of America, approximately 541,000 Americans had some level of upper limb loss and over 30% of them experience some level of depression and/or anxiety. This number is expected to double by the year 2050 (Ziegler-Graham et al., 2008). Amputation of a limb implies the complete transection of the sensory and motor nerves that innervated the removed limb. This results in a severe sensory impairment from the missing limb.

As commercially available prosthetic technology is limited by the lack of sensory feedback from the prosthesis, individuals with upper-limb amputation have to rely on visual and sound cues to perform simple control tasks such as grasping an object without crushing it. This results in substantial functional deficits (Pylatiuk et al., 2007, Antfolk et al., 2013, Cordella et al., 2016) which impacts quality of life and often leads to prosthesis abandonment (Biddiss and Chau, 2007a, Peerdeman et al., 2011b). Because of this, artificial sensory feedback is one of the most desired design priorities independent of the type of prosthesis and level of limb loss (Pylatiuk et al., 2007, Biddiss et al., 2007).

2.1 Physiology of Tactile Perception

Before discussing artificial sensory feedback, it is useful to first understand the mechanisms of human tactile perception. Somatosensory information is a main component of human perception. This includes tactile information received from the skin (i.e. sense of touch, pressure, pain) and proprioceptive information received from the limbs and joints (i.e. movement and position) (Kandel et al., 2000, Johansson and Flanagan, 2009). The sense of touch is important when exploring and acting on the physical world. We receive information about our mechanical interactions with the environment through the responses of specialized receptors that respond to physical deformation, known as mechanoreceptors. These include cutaneous receptors for touch, receptors that monitor muscle length and tension, as well as pain receptors, or nociceptors. Mechanoreceptors are sensitive to specific aspects of local tissue distortion, transforming the stimulus energy into electrical impulses (action potentials) that are transmitted through

afferent fibers that come together in the peripheral nervous system (PNS). This information is then carried to the central nervous system (CNS), where activity from thousands of receptors is integrated and processed for cognition by both primary somatosensory cortex and secondary cortical areas of the brain (Cruccu et al., 2008). The modality of the sensation that is experienced typically depends on the combined outputs of different receptor types. Stimuli delivered to the skin, for instance, can evoke sensations of pressure, tickle, light touch, or vibration.

2.1.1 Cutaneous Mechanoreceptors

Tactile sensations in the human hand involves the integration of more than one kind of stimulus and more than one kind of tactile mechanoreceptor (Kandel et al., 2000). The sense of touch can be understood as the combined result of the output of four primary receptors innervating the human skin: Merkel cells, Meissner corpuscles, Pacinian corpuscles, and Ruffini endings. Each of these receptors respond to stimuli differently depending on its location, structure and innervation pattern. They can be classified as type 1 or type 2 fibers, based on how deep they are located beneath the skin. Type 1 fibers terminate in clusters of small receptors at the dermal-epidermal margin while type 2 fibers terminate in single large receptors in the deeper dermal and sub-dermal tissues (Kandel et al., 2000, Johansson and Flanagan, 2007).

Most receptors show some type of adaptation, which means they become less sensitive during the course of a maintained stimulus. They can be classified as either rapidly or slowly adapting depending on their rate of adaptation. Receptors

innervated by slowly adapting (SA) afferent fibers, for instance, respond best to unchanging stimuli such as static position or sustained skin deformation. In contrast, receptors innervated by rapidly adapting (RA) fibers respond best to changing stimuli, giving a constant output during the dynamic phases of tissue deformation. Some rapidly adapting receptors (e.g., the Pacinian corpuscles) adapt so quickly that they respond only at the beginning and end of a stimulus (Kandel et al., 2000, Johansson and Flanagan, 2007). While adaptation is known to be a receptor-level process, the CNS also has ways to regulate the sensitivity of receptors when needed (Vanderah and Gould, 2015). The relationship between receptors and their afferent fibers is complex; single fibers can innervate multiple receptors and single receptors can be innervated by multiple fibers (Cauna, 1956, Paré et al., 2002).

Cutaneous receptors are not uniformly distributed throughout the skin. The number and type receptors vary by location based on the need for sensory feedback. Some areas such as the hands, fingertips and lips are much more densely innervated than others such as the back. This close packing of receptors in our fingertips are important for tactile discrimination and dexterous manipulation of the environment. In fact, there are about 2,000 receptors in each fingertip and about 10,000 receptors in the glabrous skin on the volar surface of the hand (Johansson and Flanagan, 2007).

2.1.2 Mechanoreceptor types

Meissner corpuscles consist of rapidly adapting type 1 (RA1) fibers. They are elongated, encapsulated endings located closer to the skin surface, just beneath the epidermis. They innervate the skin more densely than any other mechanoreceptor type, and are more abundant in the skin of fingertips. These receptors allow us to perform fine tactile discriminations with our fingertips, and are well suited for the perception of low frequency vibrations and grip control (Nelson, 2001, Kandel et al., 2000).

Merkel Cells consist of slowly adapting type 1 (SA1) fibers situated in the basal layer of the epidermis, close to the surface. These receptors have small receptive fields, and are sensitive to local stimulation but not to a uniform skin indentation (Kandel et al., 2000, Nelson, 2001). They are involved in form and texture perception as they have high spatial resolution (~0.5 mm) and are very sensitive to curves, points, corners, and edges.

Pacinian corpuscles are probably the most rapidly adapting receptors we have. Pacinian fibers are rapidly adapting type 2 (RA2) fibers that end in single Pacinian corpuscles, which are located deep in the dermis and are composed of multiple layers of fluid-filled membranes. The elastic properties of the capsular layers act as high-pass filters, allowing quickly applied forces to reach the nerve ending while maintained forces do not. Therefore, they are poor receptors for pressure but good ones for the rapidly changing mechanical stimulation that we perceive as high frequency stimulation. These corpuscles are very sensitive due to their large

receptive fields and unmyelinated endings; they can respond to skin indentations as small as 1 µm (Nelson, 2001, Vanderah and Gould, 2015).

Ruffini endings are encapsulated mechanoreceptors that consist of slowly adapting type 2 (SA2) fibers, and are located deep near the base of the epidermis in both glabrous and hairy skin. These receptors have significantly larger receptive fields than Merkel cells, with no clear borders. They are less sensitive to cutaneous indentation but more sensitive to directional strain such as skin stretch and deformations within joints, providing valuable feedback for gripping objects and controlling hand position and movement (Johansson and Flanagan, 2007).

Pain information is conveyed by **nociceptors** in two different stages corresponding to the two different size classes of axons involved. After a painful stimulus is applied, an initial sensation of sharp, pricking, well-localized pain is carried by rapidly conducting, thinly myelinated Aδ fibers followed by a slow aching pain carried by the more slowly conducting, unmyelinated C fibers (Kandel et al., 2000, Vanderah and Gould, 2015). Other receptors, known as proprioceptors, detect muscle status and limb position to provide proprioceptive and kinesthetic signals from limbs. **Muscle spindles**, which are unique to muscle, detect the amount and velocity of muscle stretch, or lengthening. **Golgi tendon organs,** which are similar to Ruffini endings, are tension receptors that detect force changes during muscle contraction (Kandel et al., 2000, Vanderah and Gould, 2015).

2.1.3 Peripheral Nerve Afferents

The diverse modalities of tactile sensations are mediated by several types of peripheral nerve fibers with different electrophysiological behaviors and anatomical distinctions in terms of myelination, diameter, and conduction velocities (Table 1). Myelinated fibers are categorized as group I, II, or III in order of decreasing size, while unmyelinated fibers are placed in group IV. The highly myelinated Aα fibers (primary afferents) have the largest diameter. They also have the highest conduction velocity and a relatively low threshold level to external stimuli. These fibers typically carry proprioceptive information such as muscle stretch velocity from muscle spindles, and muscle tension changes from Golgi tendon organs. Aβ fibers are smaller and slower than Aα, and carry both tactile (fine touch) as well as secondary proprioceptive information (position sense of a static muscle). Smaller myelinated and unmyelinated fibers (Aδ and C) are slow, with high activation thresholds, and mostly carry pain and temperature information.

Table 1. Classification of Peripheral Nerve Afferents*

Fiber Type	Sensory Function	Characteristics	Diameter (μm)	Conduction Velocity (m/sec)	Chronaxie (μsec)	Sensory Stimulation Threshold
Myelinated						
Aα	Proprioception	Ia: muscle spindle primary endings (sense muscle stretch and velocity) Ib: Golgi tendon organs (sense muscle tension)	12-22	60-120	40-100	Low ↓
Aβ	Tactile, proprioception	II: muscle spindle secondary endings (static length), fine touch, 2-point discrimination, joint position	6-12	30-70	40-100	↓
Aδ	Pain, cold	III: Fast, sharp pain & temperature, light touch	2-5	12-30	150	↓
Unmyelinated						
C	Pain, thermal, Mechanical	IV: dull, burning, poorly localized pain; primary thermal afferent	0.3-1.3	0.5-2	400	High

* (Fix, 1995, Kandel et al., 2000, Micera and Navarro, 2009)

2.2 Sensory Coding

In the past, it was widely assumed that morphologically distinct types of receptors are uniquely responsible for specific sensations (Johnson et al., 2000). However, recent efforts to elucidate the neural coding in touch have shown that the perceived sensation is probably determined by the responses of multiple fiber types and across different receptors (Goodwin and Wheat, 2004, Muniak et al., 2007, Saal and Bensmaia, 2014). The stimulus information conveyed in the signals of multiple fiber types with different output dynamics, results in spatiotemporal patterns of activity which are integrated at higher stages of processing. These patterns encode specific aspects of the stimulus using different neural coding schemes such as rate coding and population coding (Kandel et al., 2000, Johansson and Flanagan, 2007).

In rate or frequency coding, the adaptation properties of the afferents allow them to encode changes in the stimuli as changes in the pattern of neural activity. In this case, the transmitted information could be decoded by counting the number of pulses generated for a given stimulus. During population coding, changes in the stimuli are conveyed by the total number of active fibers (recruitment) in the receptor population. One of the most basic sensory dimensions that is conveyed by firing rate and population recruitment is the perceived intensity of a tactile stimulus (Muniak et al., 2007). For instance, the firing rate of sensory afferents increases proportionally to the intensity of the stimulus. At the same time, the number of afferents responding to the stimulus increases, first recruiting fibers with lower thresholds followed by higher threshold fibers.

While intensity is encoded by the amount of activity in the nerve, information about the nature or modality of a stimulus is believed to be determined by spatiotemporal patterning of this activity and conveyed through separate neural codes (Tan et al., 2014). For example, texture perception relies on spatial code signals from SA1 afferents and temporal code signals from RA and PC afferents (Weber et al., 2013). In spatial code, the information conveyed by the fiber population is encoded by the relative activation of the fibers it contains. For example, when touching braille characters or similar embossed dots patterns, SA1 and RA fibers produce spatial patterns that encode the location (presence or absence) of the dots (Phillips et al., 1990). On the other hand, the sparsely distributed PC fibers would not be suited to convey information in this way due to their lower spatial resolution.

In temporal code, the information conveyed by the fibers is encoded in the temporal sequence of the pulses. For example, information about specific textures could be conveyed in temporal pulse patterns evoked in RA and PC fibers when exploring a given texture (Weber et al., 2013). On the other hand, the temporal patterning of the slower SA1 fibers does not convey as much information as their pulse rate (Weber et al., 2013).

2.3 Artificial sensory feedback

For decades, researchers and engineers have been challenged with restoring the missing sensory function after amputation, closing the loop between the prosthesis and the user. Although the full sensation of a healthy hand is a complex feature which may not be possible to completely replace (Moberg, 1964), the provision of

intuitive and relevant artificial tactile percepts may help improve the functionality of prosthetic limbs (Antfolk et al., 2013, Cordella et al., 2016), enabling individuals with amputation to perform precise tasks with lower attentional demands and potentially promote prosthesis embodiment (Marasco et al., 2011, D'Alonzo et al., 2015); thereby improving quality of life. The development of artificial sensory feedback systems for prostheses has mostly centered on the activation of cutaneous mechanoreceptors through mechanical or electro-tactile stimulation to convey somatotopically-mismatched information (sensory substitution), and neural activation in the brain or in peripheral nerves to evoke somatotopically-matched, distally referred sensations in the phantom hand.

2.3.1 Sensory Substitution

Non-invasive mechanical (Colella et al., 2019, Pena et al., 2019) and electro-tactile (Franceschi et al., 2017, Geng et al., 2018) sensory substitution approaches encode the missing sensory information (e.g. grasp force) through an alternate sensory channel by delivering tactile information at specific locations on the user's skin. Although these approaches offer an opportunity for conveying some information about prosthesis usage, they are often unable to evoke intuitive sensations due to percept modality and location mismatch. This limits the efficacy of the sensory feedback and increases the user's cognitive load and response time (Zhang et al., 2015, Pena et al., 2019).

2.3.2 Electrical Neurostimulation

Electrical stimulation to the central and peripheral nervous system has shown potential for delivering somatotopically-matched feedback. Intracortical microstimulation of the somatosensory cortex has previously studied to restore tactile sensation to individuals with spinal cord injury (Flesher et al., 2016). This is an invasive approach in which direct stimulation within the hand area of the primary somatosensory cortex evokes referred tactile sensations on the hand. In intact sensory systems, tactile information is transmitted through peripheral and central pathways to sub-cortical areas of the brain before conscious perception occurs (Kandel et al., 2000). However, direct cortical stimulation bypasses all pre-processing by sub-cortical areas, resulting in significantly slower response times than natural touch, despite being perceived on the hand (Godlove et al., 2014, Caldwell et al., 2019). On the other hand, direct stimulation of the residual nerves of individuals with amputation leverages the natural peripheral pathways to reach the correct sub-cortical areas before the stimulus is consciously perceived, resulting in more natural sensory processing. Implantable neuromodulation systems have been used to activate sensory fibers in the median and ulnar nerves to evoke graded distally referred tactile and proprioceptive sensations in the phantom hand (Horch et al., 2011, Davis et al., 2016, Schiefer et al., 2018, Ortiz-Catalan et al., 2019, Clemente et al., 2019). For instance, recent studies showed discrete, graded sensations of touch/pressure, joint position or movement of the phantom hand, generated by longitudinal intra-fascicular electrodes (LIFE) in the median and ulnar nerves (Horch et al., 2011). Other studies employing different

neural interfaces such as nerve cuffs (Tan et al., 2014), transverse intrafascicular electrodes (Clemente et al., 2019), and penetrating multi-electrode arrays (Davis et al., 2016) have shown similar results evoking sensations of touch or pressure. These direct stimulation methods are characterized by high selectivity and sensation quality features that facilitate the delivery of more intuitive sensory feedback from prosthetic limbs, resulting in functional and psychological benefits (Dhillon et al., 2005, Schiefer et al., 2015, Wendelken et al., 2017, Petrini et al., 2018). However, the invasive nature of device implantation procedures is not acceptable to all (Resnik et al., 2019).

2.4 Surface Electrical Neurostimulation

Surface electrical neurostimulation (SENS) is a potential non-invasive alternative for providing somatotopically-matched sensory feedback. In this approach, surface electrodes applied on the skin are used to deliver electrical pulses transcutaneously to evoke a motor or sensory event (Behrens, 2006). While this technique is often used in the realm of pain management and physical therapy, some studies have shown that SENS can be used to elicit distally referred sensations when activating afferent pathways in peripheral nerves such as the median and ulnar nerves at the forearm (D'Anna et al., 2017) or at the elbow level (Shin et al., 2018).

2.4.1 Mechanism of Stimulation

Electrical stimulation can be delivered to the peripheral nerves transcutaneously through self-adhesive hydrogel electrodes applied to the skin (Behrens, 2006).

Traditional electrode configurations used in sensory feedback studies with SENS include monopolar (single stimulating electrode over the target area, with a distant return electrode), or bipolar (two stimulating electrodes from one channel over the target area) (Behrens, 2006, Reilly and Diamant, 2011). Conventionally, these electrodes deliver stimulation in the form of charge-balanced biphasic rectangular pulses generated by either voltage-controlled or current-controlled stimulation channels (Peckham and Knutson, 2005). When voltage is controlled, current levels are dependent on the impedance at the electrode interface. This can cause the sensory responses to change as the electrode impedance changes. Alternatively, when the stimulator controls the current output, the quality of the stimulation is not affected by changes in the electrode-tissue impedance, keeping the quantity of charge delivered per pulse constant. Voltage-control is sometimes used to avoid sudden increases in current densities due to loss of adhesion surface electrodes, which result in an unexpected increase of electrode-skin interface impedance.

Electrical stimulation works by either depolarizing or hyperpolarizing nerve fibers, depending on the stimulation characteristics (Kandel et al., 2000, Merrill et al., 2005). Nerve fibers typically have a membrane potential (resting potential) of about -90 mV. Surface stimulation using a negative polarity (cathodic) stimuli removes the extracellular positive charge, reducing the potential across the membrane. Voltage-gated sodium channels activate in response to these changes in membrane potential, making the inside of the membrane more positive (depolarization). If the depolarization threshold is crossed, an action potential is triggered, or a series of action potentials are triggered which propagate in both

22

directions along the length of the nerve fiber, starting at the cathode. On the other hand, when the membrane potential is decreased from its resting state, the voltage-gated sodium channels are less likely to become active. This causes the inside of the cell to become more negative, or hyperpolarized. This is usually caused by the application of positive (anodic) stimuli near the site of hyperpolarization. When electrical stimuli are applied in the direction of the nerve, the tangentially oriented fibers depolarize under the cathode, and hyperpolarize under the anode. If the hyperpolarization is large enough, an action potential may only propagate in one direction, away from the region of hyperpolarization. However, when fibers are aligned orthogonally to the axis between the cathode and anode, they activate more efficiently under anodic stimuli than cathodic stimuli (Sato and Tachi, 2010, Anderson et al., 2019). The neural signals triggered by the stimulation travel to the brain and evoke subjective experience of the stimulus and produce a sensation.

Multiple parameters can be manipulated to control the characteristics of sensations evoked with SENS: current pulse amplitude (PA), pulse width (PW) or duration, pulse frequency (PF) (Merrill et al., 2005). The current PA refers to how much current is delivered by each stimulation pulse. Most human-approved stimulators for sensory activation with SENS can deliver peak output current amplitudes between 3 to 15 mA. The PW is the time over which the current is delivered during a single pulse. Typical durations used in SENS studies span from 0.1 to 1 ms. The stimulation PF is the rate at which pulses are delivered over time. For instance,

stimulation could be delivered at frequencies ranging from 75 to 200 Hz to evoke fused (not pulsating) percepts.

The effect of electrical stimulation on the membrane potential decreases as a function of distance from the stimulating electrode (Merrill et al., 2005). Simply put, fibers closer to the stimulating electrode require lower PA to activate. In contrast, fibers located farther away require larger PA to activate, which generally means fibers between the stimulating electrode and the target fibers are also activated. Fiber morphology also plays a role in the way they respond to electrical stimulation. For instance, fibers with large diameter and long internodal distances experience greater changes in the membrane potential and are more likely to activate at lower current PA (Rattay, 1989).

2.4.2 Strength-Duration Relationships

In order to reach the threshold level for excitation and trigger an action potential, a certain minimum PA is required at a given PW (Mogyoros et al., 1996). These two stimulation parameters have an inversely proportional relationship, which is illustrated in the strength–duration (SD) curve (Figure 1A). The lowest threshold current that can activate a fiber at very long pulse durations is called the rheobase (PA_{rh}). Typically, there is a PW at which specific nerve fibers are most excitable at relatively low amplitudes. This value is called chronaxie (τ_{ch}; Figure 1) and is defined as the PW found at double the rheobase current. The Lapicque-Weiss's theoretical model (Eq. 1) is an experimentally derived relationship used to quantify the SD curve values (Lapicque, 1909, Weiss, 1990).

$$PA_{th} = PA_{rh}\left(1 + \frac{\tau_{ch}}{PW}\right)$$

(1)

In addition, the charge–duration (QD) curve (Figure 1B) illustrates the relationship between the charge (Eq. 2-3) and PW.

$$Q_{th} = PA_{rh}(PW + \tau_{ch})$$

(2)

$$Q_{th} = PA_{th} \times PW$$

(3)

The minimum charge (Q_{min}) occurs as PW approaches zero. In practice, the threshold charge (Q_{th}) is near Q_{min} when PW values are around tens of microseconds.
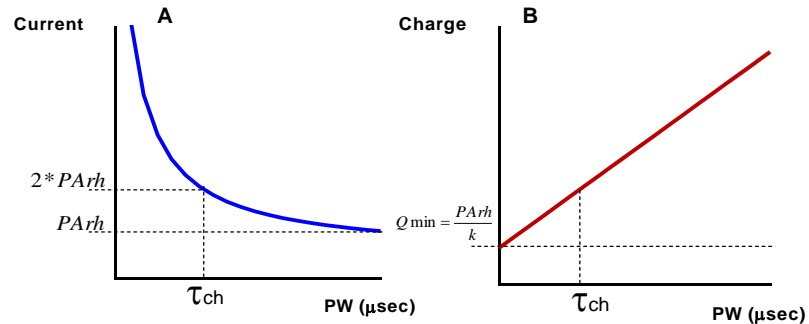
Figure 1. Strength–duration and charge–duration curves for initiation of an action potential. The rheobase current PArh is the current required to initiate an action potential at very long pulse durations. The chronaxie time τch is the pulse width corresponding to two times the rheobase current.

These relationships apply to perception thresholds as well as the upper threshold (pain) limits. These values depend on the stimulation technique used. For instance, in surface electrical neurostimulation, significantly high tissue impedances and large distances between the electrode and the target fibers are expected to result in a much higher rheobase as compared to direct peripheral nerve stimulation (Merrill et al., 2005, Forst et al., 2015). It is considered best practice to keep the PW short in order to minimize concentration of charges between the skin and the

25

electrode surface (Reilly and Diamant, 2011), which can cause discomfort and electrochemical reactions that could damage the electrode. On the other hand, the minimum PW is often limited by the amount of current that can be delivered by a stimulator (Merrill et al., 2005).

2.4.3 Stimulation Evoked Percepts

Percept intensity is one of the most basic sensory dimensions needed in artificial feedback. In intact sensory systems, intensity is encoded by fiber firing rate and population recruitment (Muniak et al., 2007, Graczyk et al., 2016). While these activation patterns have been thoroughly studied and are well understood, replicating these patterns or modulating individual receptor modalities with electrical stimulation is still a challenge. However, electrical stimulation can still be used to influence the sensory codes responsible for intensity perception by creating the illusion of changes in intensity. For instance, firing rate can be influenced with electrical stimulation by varying the PF, where higher frequencies result in stronger percepts. Concurrently, fiber population recruitment can be influenced by varying the charge (Q) delivered during the stimulation. The charge of rectangular pulses can be expressed as the product of PA and PW (Eq. 3). Increasing either parameter increases fiber recruitment, which also increases percept intensity. Previous studies have used PF modulation to elicit changes in percept intensity with surface stimulation (George et al., 2020). However, modulation of PF alone does not seem to evoke consistent percepts (D'Anna et al., 2017) and is likely to narrow the full range of discriminable levels of intensity that could be provided (Graczyk et al., 2016). Stimulation studies with implanted

electrodes in the residual nerves of individuals with amputation have shown that in fact, intensity of the perceived sensation is in part determined by the activation rate across the entire population of activated fibers (Graczyk et al., 2016), and simultaneous modulation of PF and Q can enhance the range and gradation of evoked intensities.

Percept modality is also an important dimension of artificial feedback. Traditional surface stimulation with constant parameters has been shown to elicit sensations often reported as artificial or unnatural electrical tingling, or paresthesia. These sensations are believed to be the result of synchronous activation within a population of different fibers (Mogyoros et al., 2000, Ochoa and Torebjörk, 1980) which contrast with the more complex spatiotemporal patterns recognized during natural sensory perception (Weber et al., 2013). Previous studies with direct nerve stimulation (Tan et al., 2014) and surface stimulation (P. Slopsema et al., 2018) have implemented spatiotemporal patterning strategies, with some reports of more natural pressure and tapping percepts.

2.4.4 Comfort and Selectivity Limitations

Traditional SENS methods are hampered by poor selectivity and uncomfortable sensations at the stimulation site (Kuhn et al., 2010, Forst et al., 2015, D'Anna et al., 2017, Shin et al., 2018). The comfort and selectivity of SENS are often associated with electrode size and charge density (Kuhn et al., 2010). Large electrodes help dissipate the charge over the skin to prevent discomfort, reducing selectivity. On the other hand, reducing the size of the electrode can help focalize

the stimulation within a given region of tissue, while introducing charge densities that could cause skin discomfort. In recent studies, surface stimulation of the median and ulnar nerves resulted in distracting local sensations due to large charge densities activating tactile afferents in the skin close to the electrodes (D'Anna et al., 2017, Shin et al., 2018). These sensations sometimes mask the distally referred sensations and can be hard to ignore, thus affecting the overall performance of the feedback approach. Improving comfort and selectivity in SENS would require the use of small electrodes to deliver focal stimuli while somehow avoiding large concentrations of charge at any given location on the skin. One way to reduce the charge densities at the electrode interface is to reduce the PW of the stimuli delivered by any given electrode without the need to increase the PA (Merrill et al., 2005). This could be achieved by delivering short current pulses across independent stimulation channels, such that the target tissue experiences the combined influence of all the pulses thanks to the charge-storing properties of the tissue (Geng et al., 2011, Brunton et al., 2019).

CHAPTER 3

CHANNEL-HOPPING DURING SURFACE ELECTRICAL

NEUROSTIMULATION: EVIDENCE OF ENHANCED SENSORY RESPONSES

3.1 Introduction

Loss of sensory function caused by a life-changing event such as amputation after limb trauma or peripheral neuropathies after nerve injury can have substantial effects on work, leisure, social life, and daily living activities as well as on psychological well-being. People rely on sensory feedback for everyday function, including planning and control of even simple movements, such as reaching for an object (Miall et al., 2019). In 2005, in the United States of America, approximately 541,000 Americans had some level of upper limb loss and over 30% of them experienced some level of depression and/or anxiety (Ziegler-Graham et al., 2008). This number is expected to double by the year 2050 (Ziegler-Graham et al., 2008). Individuals with upper limb amputation may use a myoelectric prosthesis. However, despite recent technological advances, the prostheses are still limited in their ability to provide direct sensory feedback to users (Antfolk et al., 2013), thereby requiring an increased reliance on visual cues and attentional demand from the user (Antfolk et al., 2013), and resulting in substantial functional deficits. Because of this, sensory feedback is one of the most desired design priorities independent of the type of prosthesis and level of limb loss (Pylatiuk et al., 2007).

The provision of sensory feedback may enable the user to better control the prosthesis and perform precise tasks with lower attentional demands (Antfolk et al., 2013, Cordella et al., 2016); thereby improving quality of life. It also has the potential to promote prosthesis embodiment (Marasco et al., 2011, D'Alonzo et al., 2015).

For decades, the development of artificial sensory feedback systems has mostly centered on the activation of cutaneous mechanoreceptors through mechanical or electro-tactile stimulation to convey somatotopically-mismatched information (sensory substitution), and the activation of sensory fibers in peripheral nerves to evoke somatotopically-matched, distally referred sensations in the phantom hand. Non-invasive mechanical (Colella et al., 2019, Pena et al., 2019) and electro-tactile (Franceschi et al., 2017, Geng et al., 2018) sensory substitution approaches encode the missing sensory information (e.g. grasp force) through an alternate sensory channel by delivering tactile information at specific locations on the user's skin. Although these approaches offer an opportunity for conveying some information about prosthesis usage, they are often unable to evoke intuitive sensations due to percept modality and location mismatch. This limits the efficacy of the sensory feedback and increases the user's cognitive load and response time (Zhang et al., 2015, Pena et al., 2019).

Alternatively, electrical stimulation of peripheral nerve sensory fibers has shown potential for delivering somatotopically-matched feedback. Implantable neuromodulation systems have been used to activate sensory fibers in the median

and ulnar nerves to evoke graded distally referred tactile and proprioceptive sensations in the phantom hand of individuals with amputation (Horch et al., 2011, Schiefer et al., 2018, Clemente et al., 2019). These direct stimulation methods are characterized by high selectivity and sensation quality features that facilitate the delivery of more intuitive sensory feedback from prosthetic limbs. However, the invasive nature of device implantation procedures is not acceptable to all (Resnik et al., 2019).

Surface electrical neurostimulation (SENS) is a potential non-invasive alternative for providing somatotopically-matched sensory feedback. In this approach, surface electrodes applied on the skin are used to deliver transcutaneous electrical pulses to nearby peripheral nerves, activating afferent pathways. Earlier studies have shown that single-channel SENS can be used to elicit distally referred sensations when targeting the median and ulnar nerves at the forearm (D'Anna et al., 2017) or at the elbow level (Shin et al., 2018). However, traditional methods for single-channel stimulation are hampered by inadequate electrode fitting, poor selectivity, motion dependency, and localized discomfort associated with large charge densities (Kuhn et al., 2010, Forst et al., 2015, D'Anna et al., 2017, Shin et al., 2018).

An enhanced surface electrical neurostimulation (eSENS) platform has been developed to overcome these drawbacks through the implementation of a Channel-hopping Interleaved Pulse Scheduling (CHIPS) strategy. CHIPS is a novel multi-channel approach designed to deliver interleaved current pulses from

independent stimulation channels, hopping across multiple strategically distributed surface electrodes. By leveraging the combined influence of the interleaved current pulses, each independent channel can be set to stimulate at shorter pulse widths than single-channel stimulation, thus reducing the total charge per pulse delivered by any given electrode, while maintaining net charge delivery to the target nerve at functional levels. In other words, the stimulation is sub-threshold for cutaneous activation near each electrode, but supra-threshold at the level of the nerve due to the spatiotemporal summation of the interleaved pulses (Geng et al., 2011, Brunton et al., 2019).

The CHIPS strategy was first developed and characterized *in silico*, where the sensory activation performance of this novel pulse scheduling scheme was evaluated using a computational model before implementation within the stimulation platform. Human studies were then performed to evaluate the performance of the CHIPS strategy and to determine whether this novel multi-channel approach could evoke distally referred sensations more efficiently and comfortably than single-channel stimulation. Able-bodied subjects received stimulation from either one-electrode pair at a time (single-channel) or interleaved between two-electrode pairs (multi-channel) placed around their right wrist. Percept thresholds were characterized for various pulse widths under each configuration, where the total duration was divided amongst the two active channels during multi-channel stimulation. We performed additional multi-channel stimulation threshold trials in which various delay values were introduced between the interleaved pulses to determine whether delays attenuate pulse summation

and affect sensory activation performance. A psychophysical questionnaire was used to interrogate the perceived modality, quality and location (MQL) of the evoked sensations under each configuration. Summation of interleaved current pulses delivered from multiple, strategically distributed surface electrodes can result in selective activation of afferent pathways while avoiding the local sensations and skin discomfort associated with the large charge densities from traditional single-channel stimulation. Our findings show that the CHIPS strategy can evoke stronger, more comfortable, distally-referred sensations without local sensations in able-bodied subjects, maintaining activation thresholds comparable to single-channel stimulation, while delivering shorter pulses per channel. This novel strategy has the potential to address some of the issues that have precluded wide adoption of surface stimulation as a viable alternative for intuitive, somatotopically-matched sensory feedback.

3.2 Methods

3.2.1 Computational Evaluation of the CHIPS Strategy

A finite element model (FEM) of the wrist was developed to predict extracellular potential changes due to stimulation from traditional single-channel stimulation and from stimulation using the CHIPS strategy. The model design included surface electrodes distributed around the ventral and dorsal surfaces and electrical properties for each tissue domain. The extracellular potential profiles were applied to a validated sensory axon model in NEURON (v7.3, (Hines and Carnevale, 1997)) to predict whether or not a sensory axon would fire at different locations

within the wrist geometry. Several simulations were performed to assess the activation performance for different pulse durations and pulse delays to generate strength-duration profiles for each stimulation condition.

Potential Field Computation (Wrist FEM Model)

A simplified cross-section of the human wrist was assembled in a 2D drawing in SolidWorks®. The geometry characteristics were based on published anthropometric data (Standring et al., 2005), and included the radius and ulna embedded within a 53x41mm oval-shaped muscle region, surrounded by a 2.5mm fat layer and a 1mm skin layer (Figure 2A). Two pairs of surface electrodes were distributed around the ventral and dorsal surfaces. Two small stimulating (s) electrodes were placed on the ventral aspect of the wrist while two large return (r) electrodes were placed on the opposite (dorsal) side. Stimulating electrodes were 15mm long arcs separated by 1mm each. These represented the cross-section of neighboring electrodes with a surface area of $275mm^2$. The return electrodes were 20mm long arcs separated by 1mm each. These represented the cross-section of neighboring electrodes with a surface area of $460mm^2$.

The drawing was exported as a segmented 2D geometry and imported into COMSOL Multiphysics (COMSOL AB, Stockholm, Sweden). Electrical conductivity and relative permittivity values (Gabriel, 1996) were applied to each tissue layers (Table 2) in order to compute the potential field distribution within the wrist generated by current-controlled stimulation by solving the Poisson's equation relating electric potential to source current density and the tissue electrical

properties (Joucla et al., 2014). In this simplified model, the skin and fat were assumed to be homogenous materials, and the different layers of the skin were combined and treated as one. Since this model only had one muscle component, it was assumed to be entirely longitudinal and transverse components were disregarded. Bone was assumed to be homogeneous and the properties for cortical bone were used (Gabriel, 1996). Each stimulating electrode on the ventral surface was assigned to a return electrode on the dorsal surface such that each "s-r" pair would be an independent stimulation channel (source and sink, respectively) configured such that their current paths would cross each other. Time dependent simulations were performed using the COMSOL Electric Currents (EC) physics on a finely meshed geometry with a minimum element size of 18.9μm and a maximum element size of 1000μm (Figure 2B). These mesh characteristics were determined during convergence testing, ensuring that the calculations are consistent throughout the model. The EC module required a ground boundary condition to run the simulations. A ground point was placed within the ulna and radius in order to satisfy this requirement while using the poor conductivity of the bone to minimize the effect of the ground points on the stimulation currents.

Table 2. Electrical Properties of Tissues (Gabriel, 1996)

	Electrical Conductivity (σ)	Relative Permittivity (ε)
Skin	0.013 S/m	990.8
Fat	0.044 S/m	50.8
Muscle	0.50 S/m	1836.4
Bone	0.024 S/m	144.5

Two stimulation configurations were simulated for different stimulation parameters (Figure 2C). During traditional single-channel (SC) stimulation, a 500µs long current regulated square pulse was delivered across a single stimulation channel (configuration pattern 1A or 2B), with a pulse amplitude PA at the source, and -PA at the sink. For the multi-channel (MC) configurations used to test the CHIPS strategy, two 250µs long current regulated square pulses were interleaved from two independent stimulation channels (from 1A to 2B, or from 2B to 1A) so that the pulses were delivered from each channel consecutively, resulting in a total pulse duration of 500µs. The extracellular potential distributions were calculated for each configuration and exported to MATLAB R2019b (Mathworks, Natick MA) with a 0.1 mm grid resolution.

Neuron Response Computation (Sensory Axon Model)

The axon fiber model used in this study was based on a previously published sensory axon model (Gaines et al., 2018), derived from the McIntyre Richardson Grill (MRG) model (McIntyre et al., 2002) and implemented in a NEURON programming environment (Hines and Carnevale, 1997). The sensory axon model was a double-cable model consisting of nodes separated by internodal segments coated in myelin (Figure 3). Each internode was divided into ten segments: two paranodal myelin attachment segments (MYSA); two paranodal main segments (FLUT); and six internodal segments (STIN). The sensory axon parameters used are the same as described in the published model (Gaines et al., 2018), with ion channels modeled as voltage dependent resistors, including fast K^+, slow K^+, and hyperpolarization-activated cyclic-nucleotide gated (HCN) channels, with leak

resistance and internodal capacitance within the internodal segments. Each node has fast K^+, slow K^+, fast Na^+, persistent Na^+, and leak channels, with nodal capacitance. For these simplified neuron response simulations, a single sensory axon (12µm diameter, 21 nodes and 20 internodes) was used.

The calculated extracellular potential distribution over the stimulation time was used to generate a spatiotemporal matrix of voltages at 5 different points of interest (POI) within the wrist cross-section (Figure 2C), depending on the distance between the stimulation source and the point of interest. These voltages were applied along the length of the sensory axon to determine its activation threshold at each POI. An activation region (AR) was derived to spatially describe where the axons are likely to be activated within the cross-section of the wrist. The AR was determined for each configuration from the 2D activation distribution that resulted in activation of a single sensory axon located each POI. The boundary of an AR represents the farthest point from the stimulation source that is above the sensory axon threshold. Performance for each of the stimulation configurations was assessed by comparing the stimulation amplitudes required to activate a sensory axon located at each of the 5 POIs near the stimulating electrodes. The activation thresholds were obtained for each configuration under 5 different pulse width values (300µs to 700µs, at 100µs intervals) to compute their strength-duration (SD) curves.

3.2.2 Able-bodied Subjects

Written informed consent was obtained from 10 adult subjects (4 males, 6 females, mean age ±SD: 34.9±15.3) in compliance with the Institutional Review Board of Florida International University which approved this study protocol. All prospective subjects were screened prior to the study to determine eligibility. Subjects were able-bodied, with no sensory disorders or any self-reported condition listed as a contraindication for surface stimulation (pregnancy, epilepsy, lymphedema, or cardiac pacemaker) (Rennie, 2010).

3.2.3 Experiment Setup

Subjects were seated on a chair with both arms on a table in front of them (Figure 4A). Their right forearm was thoroughly cleaned with an alcohol wipe and placed on a support pad on the table, with their right hand's palmar surface parallel to the vertical plane. Subjects were encouraged to drink water before and during the experiment to increase skin hydration.

Each subject received electrical stimulation from a distributed set of surface electrodes around their right wrist to activate their median nerve sensory fibers, evoking distally referred sensations in their right hand. Median nerve stimulation was delivered by four self-adhesive hydrogel electrodes (Rhythmlink International LLC, Columbia, SC) placed around the subject's right wrist, allowing superficial access to the median nerve's sensory fibers from the index, middle, and part of the ring finger. Two small stimulating (s) electrodes (15x20mm) were placed on the ventral aspect of the wrist (~3cm from the distal radial crease) and two large return

(r) electrodes (20x25mm) on the opposite (dorsal) side (Figure 4B). Each "s-r" electrode pair was assigned to an independent channel and configured such that their current paths would cross each other and intersect the median nerve transversally (Figure 4B). Placement of each "s-r" pair was determined by exploring various locations around the median nerve while providing brief, 1s long stimulation bursts (500μs biphasic, anode-first pulses at 30Hz) at various amplitude levels between 1.5mA and 3mA, in increments of 0.1mA, until a distinct referred sensation was reported by the subject.

A custom 3-button keyboard was placed on the table in front of the subject's left hand. Subjects used this keyboard to trigger the delivery of the electrical stimuli (Go) and provide percept responses (Yes/No). Subjects were fitted with a pair of noise cancelling headphones playing soft white noise to reduce distracting noises and deliver sound queues at various stages of the study. Subjects were instructed to relax and maintain a fixed arm position throughout the experiment but were encouraged to stretch and move their hand during periodic breaks to prevent discomfort. Subjects were asked about their comfort levels, or if additional breaks were needed after each task.

3.2.4 Stimulation Configurations

A multi-channel programmable, optically isolated benchtop bio-stimulator (TDT IZ2-16H, Tucker-Davis Technologies, Alachua FL USA) was used to deliver the electrical stimuli. A custom TDT Synapse stimulation control environment running on the TDT RZ5D base processor was used to schedule charge-balanced, current-

controlled biphasic rectangular pulses with pulse amplitudes (PA) between ±3mA per channel, with 1µA/step resolution, and a pulse width (PW) resolution of 21µs/step. Anode-first pulses were used throughout the study, as they have been shown to activate orthogonally oriented fibers more efficiently than cathode-first pulses (Sato and Tachi, 2010, Anderson et al., 2019). The TDT Synapse environment was interfaced to a custom MATLAB program (v2018b, MathWorks Inc, Natick, MA) designed to run and monitor the various study conditions and modulate the stimulation parameters based on subject responses.

Two stimulation configurations were used in this study (Figure 4B). During traditional single-channel (SC) stimulation, biphasic current pulses with a 100µs inter-phase gap (IPG) and a given PW were delivered to the median nerve from only one channel at a time (configuration pattern 1A or 2B). For the multi-channel (MC) configurations used to test the CHIPS strategy, biphasic pulses were interleaved from two independent stimulation channels (from 1A to 2B, or from 2B to 1A) so that the anodic phases of each channel were delivered consecutively, followed by their respective charge-balancing phases after a 100µs IPG. In this case, the pulse width for each channel was set to half of the pulse width used during single-channel stimulation. The pulses were interleaved to prevent channel interactions. During some experiments, various delays (Del) were tested between the first (leading) channel and the second (trailing) channel.

3.2.5 Experimental Procedures

Performance for each of the stimulation configurations was assessed by comparing the percept threshold measurements and the results from the psychophysical evaluation of the elicited percepts. Figure 5 summarizes the experimental protocols completed in this study.

Percept Threshold Measurements

Percept thresholds (PT) were obtained from all subjects for each SC (1A, 2B) and MC (3AB, 4BA) configuration under 5 different pulse width values (300μs to 700μs, at 100μs intervals). Additional MC stimulation trials were completed by a subset of subjects (n=4) under various interleaved pulse delay values (0μs, 20μs, 40μs, 60μs, 200μs, 500μs). The order of the stimulation configuration, pulse width and delays was randomized across all subjects. All trials were completed twice under every condition. The PT determination procedure used was a combination of the Parameter Estimation by Sequential Testing (PEST) method (Taylor and Creelman, 1967) and a randomly alternating dual staircase method (Cornsweet, 1962). This combination was meant to reduce variability and user bias, allowing for fast and accurate estimation of percept thresholds. An example of a stimuli presentation sequence is shown in Figure 6. A custom algorithm was designed and integrated into a MATLAB program that controlled the delivery of electrical stimuli and collected information about the subject's sensory responses. Subjects triggered the delivery of the stimuli by pressing the "Go" button on a keyboard, and then provided a positive or negative response by pressing the "Yes" or "No" button, depending on whether each stimulus was detected. Positive responses were

followed by a decrease in PA while negative responses were followed by an increase in PA. The step size was halved after every positive response, or doubled after two successive negative responses. The direction of the trials was always changed after a response reversal. The order of occurrence of the staircases was randomized in advance. The two sequences always started apart and eventually came together, crossing and re-crossing each other thereafter until 6 response reversals per sequence were reached.

The subject responses were analyzed for each sequence independently since they could be considered as two replicates of the same condition. Threshold values were computed by fitting the Wichmann and Hill psychometric function (Wichmann and Hill, 2001) and finding the stimulation amplitude value with a 50% probability of having a positive or negative response for each sequence. The final threshold amplitude for a given pulse width was computed by taking the average of the thresholds found from each sequence. The experimental PT measures (2 reps per pulse width) were fitted to the Lapicque-Weiss's theoretical model (Lapicque, 1909, Weiss, 1990) to compute individual strength-duration (SD) curves for each subject under each stimulation configuration.

For trials comparing the traditional single-channel (1A, 2B) and novel multi-channel (3AB, 4BA) configurations, each subject's SD curves were normalized to the rheobase (Weiss, 1990) of the best performing SC configuration (with the lowest overall threshold). To compare across configurations, the normalized threshold values for each tested pulse width were scaled to the % of the threshold from the

42

best performing SC configuration. A theoretical "no summation" reference SD curve was calculated by assuming only half of the PW was delivered under the best performing SC configuration. For trials comparing MC stimulation under various interleaved pulse delays, each subject's SD curves under each delay were normalized to the rheobase of the tested MC configuration without any delay, and adjusted for PW. Furthermore, the performance of each of the configurations was assessed by comparing their effect on the normalized threshold measurements with a one-way ANOVA (SPSS 21, IBM, Armonk, NY). Post-hoc multiple comparisons between configurations were made using the Tukey-Kramer test at an alpha level of 0.05 for significance.

Assessing Elicited Percepts: MQL Questionnaire.

To evaluate the characteristics of the sensations evoked by the stimulation, subjects were instructed to complete a multiple-choice psychophysics questionnaire (Q1-Q3 in Figure 7) about the Modality, Quality, and Location (MQL) of the sensations under each configuration. The order of the configuration used during this assessment was randomized across all subjects.

While completing the questionnaire, subjects received 1sec long bursts (30Hz, 100µs IPG) under each configuration tested. Subjects were allowed to trigger the stimulation burst as many times as they needed to answer all the questions. Stimulation amplitude was set to 25% above the percept threshold (1.25xPT) at a pulse width of 500µs. This duration was chosen since it allowed for a wide range

of amplitudes to be used. No pulse delays were used during multi-channel stimulation in this procedure.

The sensation modality was evaluated from a list of 16 pre-defined options (i.e. touch, pressure, needle prick, tingling, vibration, etc). The sensation quality was evaluated as comfortable or uncomfortable, as well as sharp, blunt, soft, mild or strong. The perceived location of the sensations was evaluated as local (at the stimulation site), spreading (from one site to another), or referred (in the hand). All options in the questionnaire were explained to the subjects before the experiment. Subjects were instructed to choose one or more options that best described the elicited sensation, or to report a different word if none of the options accurately described the sensation.

Assessing Percept Location.

The subject reported the percept location by drawing the localized region of the sensation on standardized paper diagrams of the palmar and dorsal surfaces of the right hand (Q4 in Figure 7). The subject completed a percept map for each configuration, under the same stimulation parameters used during the MQL questionnaires. Each percept map was scanned and loaded into individual layers in Adobe Photoshop CS2. The percept regions were digitized by tracing a solid shade within the area drawn by the subject with an Intuos Pro drawing tablet (Wacom Co., Ltd. Saitama, Japan). The same hand contour image provided to the subject was used as a base layer during the digitization process. All digitized percept areas from each configuration were stacked in MATLAB, and overlapping

44

pixels were aggregated to calculate the frequency of location reports for all subjects.

3.3 Simulation Results

A finite element model of the wrist was developed and used to predict extracellular potentials due to stimulation from the CHIPS strategy and traditional single-channel stimulation. These voltage distributions were applied to a validated sensory axon model in NEURON to determine activation of a sensory axon located at different points of interest that represented possible locations of the median nerve within the wrist cross-section.

3.3.1 Activation Regions

Activation regions (AR) were obtained to spatially describe where the axons were likely to be activated within the cross-section of the wrist. Figure 8A depicts the regions of activation generated by each configuration when triggering a sensory axon located closer to A than B (POI 2 in Figure 2C) with 500µs long stimulation pulses (250µs for each channel with CHIPS). This point of interest was chosen to simulate a condition in which one channel is better positioned to activate the sensory axon than the other. The AR under single-channel configuration 2B was found to be larger than 1A, as the stimulation source is farther from the point of interest. Stimulation under both multi-channel configurations with the CHIPS strategy (3AB and 4BA) resulted in activation regions that reach the sensory fiber at the point of interest while delivering current amplitudes comparable to single-

channel stimulation and only half of the pulse width from each of the stimulation channels.

3.3.2 Activation Thresholds

Activation threshold values were computed for 500μs long stimulation pulses (250μs for each channel with CHIPS) across 5 POIs representing different possible locations for the median nerve (Figure 8B). The stimulation amplitudes required to activate a sensory axon under single-channel stimulation increased as the distance between the stimulation source and the point of interest increased. However, the activation performance of the CHIPS strategy was found to be relatively stable for the different points of interest tested. More detailed activation threshold computations were performed for multiple pulse durations to obtain the strength-duration (SD) profiles for each simulated configuration when activating a sensory axon located at the second POI. At this location, multi-channel stimulation with the CHIPS strategy (configurations 3AB and 4BA) resulted in PT values comparable to single-channel stimulation (between configurations 1A and 2B), while delivering shorter pulses per channel (Figure 8C).

3.4 Human Studies Results

Able-bodied subjects received electrical stimulation from a distributed set of surface electrodes around their right wrist, evoking distally referred sensations in the general area innervated by the sensory fibers in the median nerve (palmar surface, index, middle, and part of the ring finger). The sensory activation performance and elicited percept characteristics were evaluated and compared for

all configurations tested. All surface electrodes had impedance values (mean ± SD) of around 26.4 ± 0.5 kΩ, which remained stable for all subjects throughout the study (Figure 9). No side effects like irritation or redness of the skin were observed in any of the subjects.

3.4.1 Percept Thresholds

Strength-duration profiles obtained from the percept threshold (PT) measures of an individual subject under each stimulation configuration were normalized to the rheobase of configuration 1A, which was the best performing (lowest PT) single-channel configuration, as compared to configuration 2B. Figure 10A shows the mean SD curves across all participants, where multi-channel stimulation with the CHIPS strategy (configurations 3AB and 4BA) resulted in PT values comparable to single-channel stimulation (between configurations 1A and 2B), and far below the "no summation" (N-S) reference (dashed-line) while delivering shorter pulses per channel.

Figure 10B compares the sensory activation performance of each configuration. Stimulation under configuration 1A resulted in significantly lower PT's than configurations 2B ($p<0.005$) and 3AB ($p<0.05$), while no significant differences were found between configurations 1A and 4BA, making 4BA the best-performing multi-channel configuration.

The sensory activation performance of multi-channel stimulation appeared to decrease with the introduction of delays between interleaved pulses, especially for large delays (i.e. 500µs). As shown in Figure 10C, PT values for both

configurations 3AB and 4BA increased as delays were increased, suggesting an attenuation in the net charge delivery due to a reduction in pulse summation.

3.4.2 Elicited Percepts

Results from the MQL questionnaire about percept modality (Figure 11A) show that all stimulation configurations evoked sensations that were mostly described as "Tingling", with only a few reports of "needle prick". Only SC stimulation resulted in numb, unnatural or painful sensations. In contrast, only MC stimulation evoked sensations of vibration, pressure or light touch. As shown in Figure 11B, most subjects (n=9) reported comfortable sensations after MC stimulation, while three participants reported them as uncomfortable after SC. Percept location responses in Figure 11C show that most participants felt referred sensations for all configurations, while local sensations (under the electrodes) were only reported after SC stimulation (n=7).

3.4.3 Percept Location

All participants reported distally referred sensations across the area of the hand including the ring, index, middle fingers and the thumb. As shown in Figure 12A-B, local sensation under the electrodes were reported by seven participants for both SC configurations only. Only one subject reported a tingle-like sensation on the lateral surface of the wrist (between electrodes, not under) with configuration 3AB (Figure 12C). Finally, Figure 12D shows that stimulation under configuration 4BA resulted in the most consistent reports of distally-referred sensations on the ring and middle fingers as well as the palm of the hand, without local sensations.

3.5 Discussion

This work presents an evaluation of the performance of a novel Channel-hopping Interleaved Pulse Scheduling (CHIPS) strategy for multi-channel surface stimulation to determine whether it could evoke distally referred sensations, more efficiently and comfortably than single-channel stimulation. Able-bodied subjects received interleaved current pulses from surface electrodes strategically distributed around their right wrist, resulting in more comfortable, distally-referred tingle-like sensations in the areas of the hand that are innervated by the sensory fibers in the median nerve, with lower incidence of local sensations than single-channel stimulation. These results show that the CHIPS strategy is capable of enhancing the performance of surface electrical stimulation for delivering non-invasive sensory feedback.

3.5.1 Computational modeling: limitations and implications

One of the challenges of traditional surface electrical stimulation studies is obtaining consistent and reliable responses due to differences in electrode placement within and across subjects, skin movement, position dependency and physiological variables that effect the electrical properties of the tissue. Computational modeling can be used to avoid some of these challenges during the research and development phases to predict neural activation performance under different stimulation conditions before implementation in clinical applications. Before the CHIPS strategy was implemented and tested with able-bodied subjects, a simplified hybrid computational model of neural activation within the human wrist was used to first predict extracellular voltage distributions in a

simplified 2D anatomically-based finite element model, and axon activation within the human wrist due to surface stimulation using different electrode configurations and pulse scheduling strategies. Implementation of this model resulted in strength-duration profiles and activation thresholds comparable to experimental results with human subjects. The model predicted activation thresholds for multi-channel stimulation in between those found under single-channel stimulation when the target nerve is somewhere between the current paths of the two stimulating electrodes (Figure 8). The model also predicted that implementation of the CHIPS strategy would result in activation areas that were smaller than the combined activation areas produced by each independent channel (Figure 8A), suggesting that the CHIPS strategy could result in more focal activation than single-channel stimulation.

The main building blocks of this simplified wrist cross-section geometric structure used in this model include structures and parameters that have the largest influence on the potential distribution and neural activation, while those with a small influence were neglected or approximated as simpler or lumped structures. This model incorporates two homogeneous cortical bony structures (ulna and radius), a large longitudinal muscle structure, and homogeneous fat and skin layers. While the electrical properties of the skin and fat layers have been shown to have little influence on nerve activation when using current-controlled stimulation, the electrical properties of muscle, as well as the location and diameter of the sensory axon do have a major influence (Kuhn et al., 2010). The influence of the sensory axon location implies that the thickness of the skin and fat layers seen in humans

is a critical factor for predicting neural activation. Other tissues and in-homogeneities not included in this model can affect the voltage distribution. For instance, blood vessels or interstitial fluids have low resistivity and could act as shunts, while tendons that connect muscles to bony structures have high resistivity (Gabriel, 1996). The close vicinity of these tissues to nerves may also have an influence on nerve activation during surface stimulation. Additionally, the FEM model of surface stimulation used time dependent simulations in an effort to include the effect of tissue capacitance which is known to affect the shape and amplitude of the stimulation pulses within the tissue (Dorgan and Reilly, 1999, Kuhn et al., 2009). However, this model neglects the properties of electrode-skin interface components such as the hydrogel layer, which could have major effects on the potential distribution due to its capacitance. The specific contribution of the capacitive properties of this layer in this model needs further investigation.

Another limitation of this model is that the neural response simulations only involved a single sensory axon at each point of interest. This was done to reduce simulation time. More complex simulations could be performed to investigate the effect of the different configurations and scheduling strategies on axonal population recruitment to determine whole nerve activation profiles under each condition. This can be done by expanding the NEURON model to include multiple fascicles within the median nerve, with each fascicle containing a distribution of sensory axons with a random assignment of axon diameters following known axonal population proportions (Tackmann et al., 1976, Wesselink et al., 1999). The model could be expanded even further to include the somatotopic targets such as

51

the hand digits and palm. This would allow for the computational evaluation of activation region steering strategies with an electrode array.

While the model used in this study could be optimized to simulate more realistic conditions, the overall effects of these limitations on the extracellular potential distribution should be the same for all stimulation configurations and sensory axons at the different points of interest. Therefore, the analysis and conclusions drawn about the relative activation of the sensory axon based on its location and approach used should provide some information about how the different stimulation configurations and pulse scheduling strategies would perform under those specific conditions. The behaviors observed in this model served as the basis for designing the stimulation protocols used during human studies and developing more streamlined fitting strategies. For example, simulation results showed lower activation thresholds for both independent channels when the sensory axon was located between both channels (Figure 8B). This information can be used to guide selection of electrode pairs in an array in order to optimize the shape of the activation region. For instance, choosing the electrode pairs with the lowest single-channel thresholds assures that the target nerve would be in between the two stimulating electrodes when stimulating with the CHIPS strategy, thus avoiding unnecessarily larger activation regions for either of the channels. This model could also be used to guide the development of stimulation fitting algorithms that would allow for real-time adjustment of stimulation parameters such as stimulation amplitude and combination of electrodes within an array to achieve targeted activation of different parts of the nerve and steer the location of the

evoked sensations. By making the appropriate adjustments, this model could potentially be used to explore different stimulation methods and predict neural activation responses when using cuff-like electrodes or delivering intraneural stimulation to target both sensory or motor axons.

3.5.2   Sensory activation performance in humans

Multi-channel stimulation with the CHIPS strategy resulted in percept thresholds that were within the range of thresholds found under both single-channel configurations (Figure 10A), while delivering lower charges per pulse under any given electrode. We believe this is the result of the summation of interleaved pulses during the "RC recovery time interval", in which the membrane still contains some of the charge of the leading pulse (bringing it close to the fibers' activation threshold), making it easier for the fiber to depolarize after the trailing pulse (Rutten et al., 1991, Geng et al., 2011). Interestingly, the CHIPS strategy seemed to perform better when leading-trailing pulses were interleaved from high-threshold to low-threshold channels (worst-to-best), or from configuration 2B to 1A (4BA) as seen in Figure 10B. It is possible that the summation of the leading and trailing pulses is not perfect. While the leading pulse's effect on the membrane potential could be momentarily sustained, it could decay slightly during the transition to the trailing pulse. Since the trailing pulse plays a more critical role in crossing the fiber's activation threshold, the most efficient sequence would be the one where the trailing pulse is delivered from the best configuration. Finally, we observed that while the introduction of small delays between interleaved pulses does not seem to compromise the performance of the CHIPS strategy, large delays resulted in

increased threshold amplitudes (Figure 10C), especially for the worst performing multi-channel configuration (3AB). This is consistent with the idea of pulse summation, since large delays would be expected to attenuate the effect of the leading pulse on the nerve membrane at the time of arrival of the trailing pulse.

3.5.3 Percept enhancement

The comfort and selectivity of surface stimulation are often associated with electrode size and charge density (Kuhn et al., 2010). Large electrodes help dissipate the charge over the skin to prevent discomfort, reducing selectivity. On the other hand, reducing the size of the electrode can help focalize the stimulation within a given region of tissue, while introducing charge densities that could cause skin discomfort. In recent studies, surface stimulation of the median and ulnar nerves also resulted in distracting local sensations due to the activation of the tactile afferents in the skin close to the electrodes (D'Anna et al., 2017, Shin et al., 2018). These sensations can be hard to ignore, affecting the overall performance of the stimulation approach. In contrast, the novel strategy evaluated in this study allowed us to deliver focal stimulation to the median nerve using small surface electrodes while avoiding the large charge densities associated with local sensations and skin discomfort. In fact, analysis of the MQL questionnaire responses revealed that stimulation under configuration 4BA evoked the most consistent reports of stronger, more comfortable distally-referred sensations (Figure 11) on the ring and middle fingers as well as the palm of the hand (Figure 12), without local sensations. These results suggest that implementation of the CHIPS strategy allowed for focal activation of a specific parts of the nerve (partial

recruitment) resulting in sensations on the areas of the hand innervated by sensory fibers within the recruited section. More specifically, since the electrodes were placed so their current paths would interfere near the center of the wrist ventral surface, the median nerve would be expected to receive stimulation mostly near its ventral and medial aspect (the side closest to the ulna). Because of this, percepts are evoked more predominantly on the ring and middle fingers as well as the palm of the hand, matching the expected somatotopy of the median nerve at this location (Tackmann et al., 1976).

3.5.4 Limitations

One of the limitations of this study is that the initial electrode fitting parameters were determined through trial and error, and the electrode placement often had to be adjusted until each individual channel elicited the desired sensations. Because of this, it is possible that each individual channel's alignment with the median nerve was not optimal. This would explain the significant differences in percept thresholds found between the two single-channel configurations (Figure 10B). To overcome this issue, the stimulation fitting process could be enhanced by implementing a spatially distributed set of electrodes (an electrode array) in which subsets of electrodes are selected to optimize the stimulation effectiveness and comfort. The combinations and location of active electrodes, as well as the characteristics of the stimulation pulses can be adjusted to reshape the spatiotemporal distribution of charge within the array (Kuhn et al., 2009, Spencer et al., 2018). This would allow for spatial steering of the stimulation focus to target specific tissue regions to modulate percept areas and intensity, and help reduce

or mitigate the effect of arm motion on the stimulation. Another limiting aspect of this study is the long duration of the iterative processes used to determine percept thresholds. On average, it took about an hour for subjects to complete all basic threshold determination blocks using the modified dual staircase. While these procedures are designed to determine percept thresholds accurately for research objectives, they are not sustainable for stimulation parameter fitting in the real world. Accurate and efficient stimulation fitting could be achieved through interactive user-controlled fitting paradigms (user-in-the-loop) to help determine and optimize the stimulation parameter ranges, accelerate identification of the target nerve branches, and create user-specific stimulation profiles. These strategies could further improve the efficiency and efficacy of this stimulation platform compared to traditional methods.

Other factors to consider in our percept assessment results are the technical constraints of the stimulation system. For instance, MQL questionnaires were completed with pulse amplitudes set to 25% above the mean percept threshold at 500µs. The wide range of amplitudes at this pulse width helped keep the stimulation from reaching the maximum current output of 3mA while avoiding some of the uncomfortable sensations associated with long pulse widths. In contrast, shorter pulse widths would have required pulse amplitudes much higher than the output limit. An additional constraint within the pulse sequencing algorithm used during our percept assessment procedures limited the stimulation frequency to 30Hz. As a consequence, the percept characteristics reported in this study should be viewed in the context of these specific stimulation parameters. It is not yet

known whether different percept characteristics would be reported between the stimulation approaches at various pulse widths and frequencies. For this, further studies should be conducted to investigate whether modulation of different stimulation parameters can affect the stimulation approaches differently.

Lastly, this study evaluated the performance of our stimulation approach in able-bodied subjects at the wrist level. In its current form, this approach could be further evaluated in people with wrist disarticulation or transradial amputations. Future studies should also investigate whether this approach could be translated to the general population of individuals with upper-limb amputation by designing an electrode array that would fit around or above the elbow joint, where some nerve branches are more superficial. Conditions for implementing this stimulation approach could be further improved for patients undergoing pre-planned amputations, as they could be eligible for nerve reassignment procedures (Valerio et al., 2019), relocating residual nerve branches to make them more accessible via surface electrodes.

3.5.5 Implications and future directions

This novel strategy has the potential to selectively elicit referred sensations that are comfortable, thus addressing some of the issues hampering traditional non-invasive neuromodulation approaches, making it a viable alternative for individuals who may not be eligible, or chose not to undergo, surgical procedures for invasive neuromodulation, as the latter carries risks of adverse effects such as infection and persistent implant site pain (Eldabe et al., 2015). Another innovative aspect of this

approach is the potential to deliver targeted neuromodulation therapies for peripheral neuropathies. Surface stimulation has been previously explored as a non-pharmacological alternative for patients with neuropathic pain symptoms secondary to nerve injury or amputation (Johnson et al., 2015, Petersen et al., 2019). Although the neural mechanisms underlying the analgesic effects of conventional surface stimulation are complex and incompletely understood, they are generally consistent with the gate control theory (Melzack and Wall, 1965). In this context, our approach could be used to deliver focal stimulation to non-pain-related sensory fibers to prevent, or "gate," nociceptive signals from being relayed from the spinal cord or brainstem to the brain.

3.6 Conclusions

This work evaluated the performance of a novel multi-channel neurostimulation approach against traditional single-channel stimulation. Able-bodied subjects reported enhanced distally-referred percepts when receiving interleaved current pulses from multiple channels strategically distributed around the wrist. The performance of this approach was characterized for various interleaved pulse orders and delays to identify the most optimal configuration and to inform the development of advanced fitting procedures. The results presented here demonstrate that our stimulation strategy addresses some of the primary issues that have hindered the use of non-invasive neural stimulation to elicit meaningful sensations. This strategy offers a potential alternative not only for delivering enhanced tactile feedback, but also for stimulation therapies to treat various pain conditions.

FIGURES
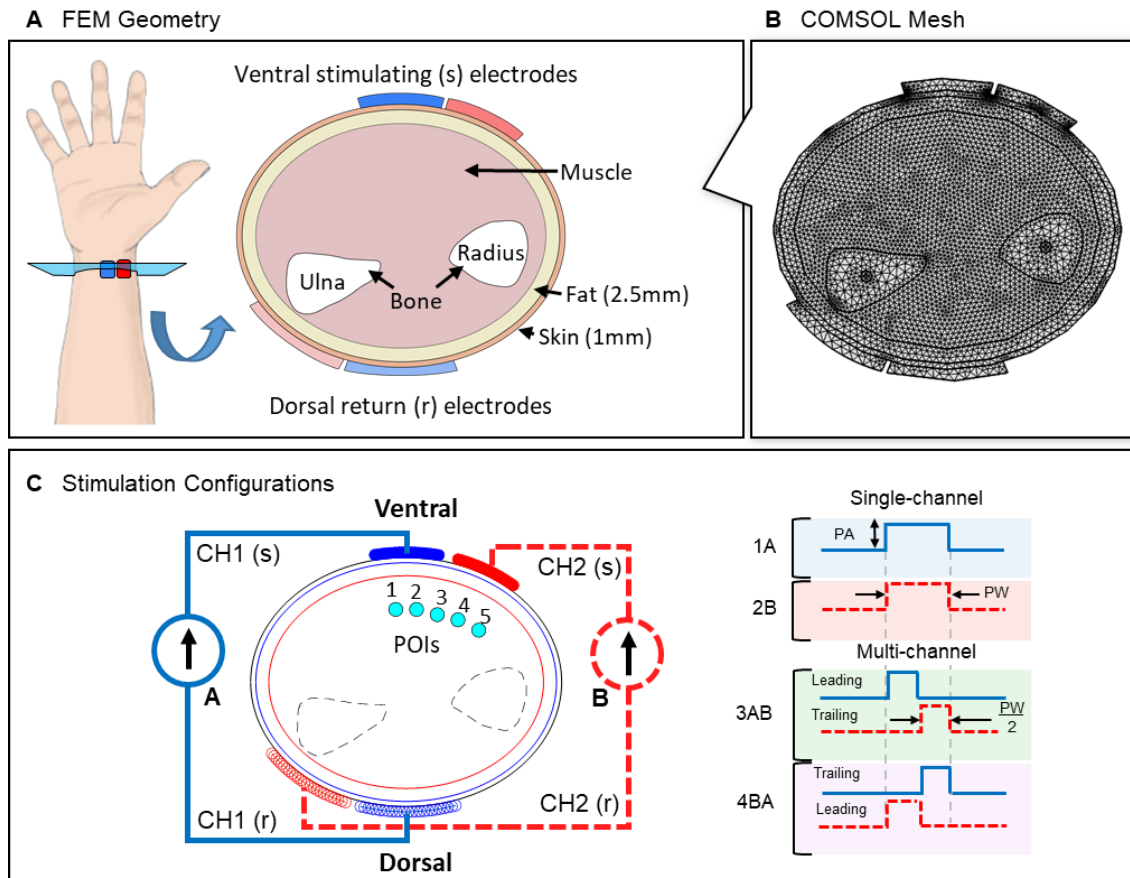
Figure 2. Finite element model of surface stimulation in a simplified cross-section of the human wrist. (A) Segmented 2D geometric structure of a simplified cross-section of the human wrist. Two cortical bone segments representing the ulna and radius were embedded within a 53x41mm oval-shaped longitudinal muscle region, and surrounded by a 2.5mm homogeneous fat layer and a 1mm homogeneous skin layer. Two ventral stimulating (s) electrodes and two dorsal return (r) electrodes were placed on the outer surface of the skin layer with a 1mm inter-electrode gap. (B) Fine mesh of the imported geometric structure of the model using free triangular elements in COMSOL. (C) Computation of extracellular potential distribution under different stimulation configurations. Each stimulating electrode on the ventral surface was assigned to a return electrode on the dorsal surface such that each "s-r" pair would be an independent stimulation channel (source and sink, respectively) configured such that their current paths would cross each other. Two stimulation configurations were simulated for different stimulation parameters. Single-channel (SC) stimulation was delivered with only one channel (1A or 2B) while multi-channel (MC) stimulation was interleaved from 1A to 2B (3AB) or from 2B to 1A (4BA).
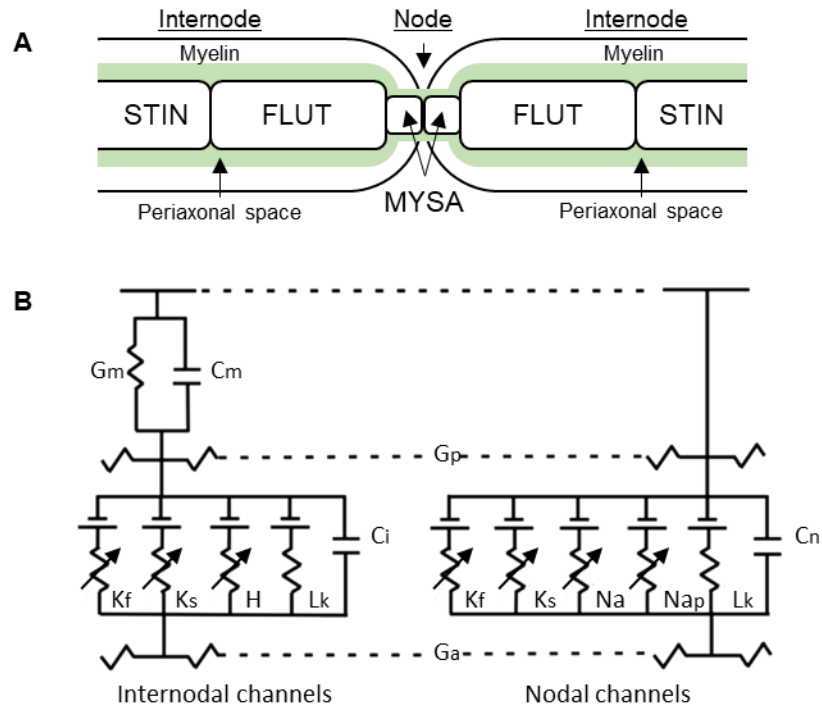
Gaines et al 2018, McIntyre et al. 2002

Figure 3. Overview of the sensory axon model implemented in NEURON. (A) The overall structure of the sensory axon model consisted of 21 nodes separated by 20 internodes coated in myelin. Each internode consisted of two MYSA segments, two FLUT segments, and six STIN segments located between each node of Ranvier. The axon was modeled with 12μm diameter. (B) The ion channels were modeled as voltage dependent resistors. This modified MRG model includes fast K^+, slow K^+, and HCN channels, with leak resistance and internodal capacitance within the internodal segments. Each node has fast K^+, slow K^+, fast Na^+, persistent Na^+, and leak channels, with nodal capacitance. Also represented are the conductance and capacitance of the myelin (Gm and Cm), the axoplasmic conductance (Ga), and the periaxonal conductance (Gp).

60

A Experiment Setup

B Stimulation Configurations
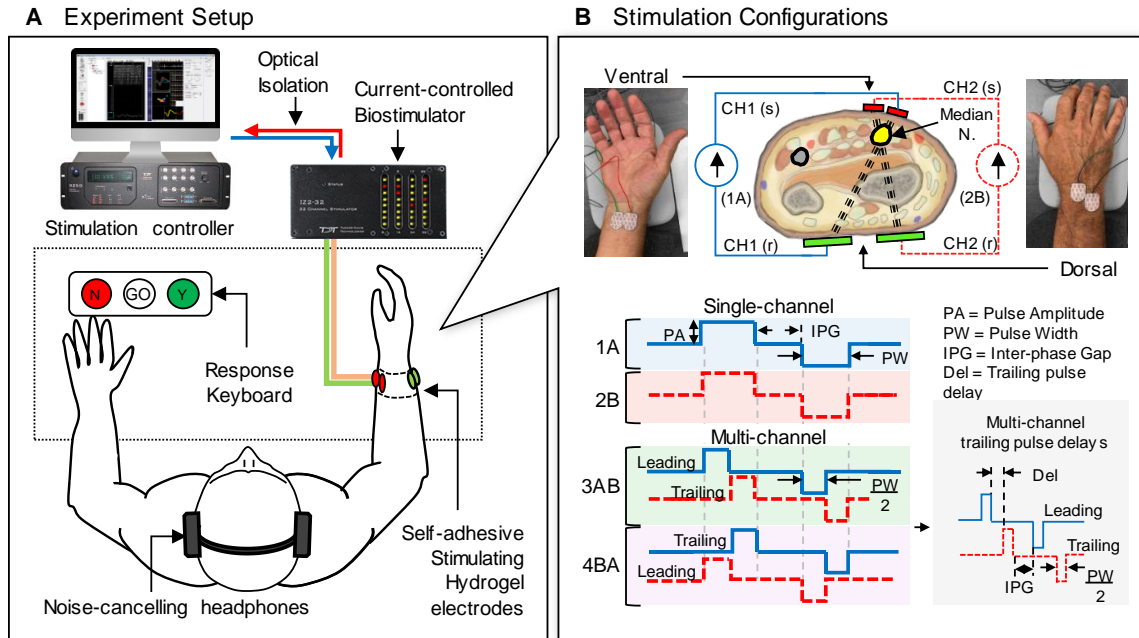
Figure 4. Experiment setup and stimulation configurations for human studies.(A) Experimental setup schematic showing stimulation being delivered by an optically isolated, current-controlled biostimulator (TDT RZ5 / IZ2H-16) through up to two surface electrode pairs placed around the subject's right forearm (~3cm from the distal radial crease). Percept responses (Yes/No) were collected using a custom keyboard. (B) Each electrode pair was assigned to an independent current source (CH1 & CH2) to deliver charge-balanced biphasic pulses to the median nerve. Two stimulating (s) electrodes were placed on the ventral aspect of the wrist, and two return (r) electrodes on the dorsal aspect. Single-channel (SC) stimulation was delivered with only one channel (1A or 2B) while multi-channel (MC) stimulation was interleaved from 1A to 2B (3AB) or from 2B to 1A (4BA) using the CHIPS strategy.
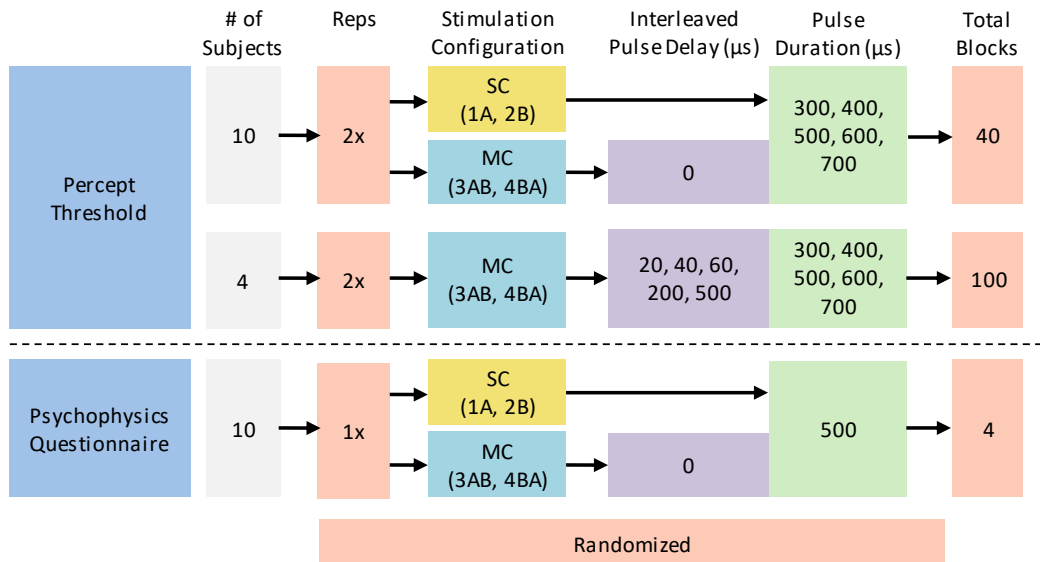
Figure 5. Experiment sequence diagram for the human study protocols. All subjects completed 40 threshold measurement blocks, randomized across 2 reps of 5 pulse width and 4 stimulation configurations. A subset of randomly selected subjects completed 100 additional threshold measurement blocks, randomized across 2 reps of 5 pulse widths, 5 interleaved pulse delays and 2 stimulation configurations. Each threshold measurement block took between 30-45s on average. Short breaks between blocks were at least 10s, and extended as much as the subjects needed. Finally, all subjects completed four randomized questionnaires for all configurations tested. SC=Single-channel; MC=Multi-channel
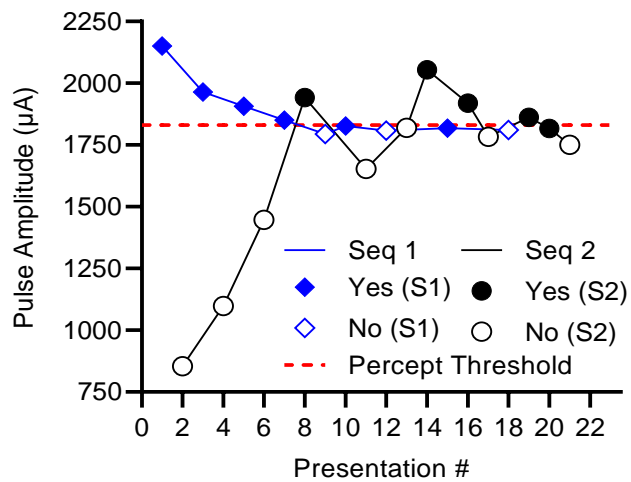
Figure 6. Modified dual staircase procedure to determine percept threshold (example from one subject). Pulse amplitude is changed (y-axis) at each trial to elicit sensation based on randomly alternating dual staircase sequences (Sq.1, Sq.2) while collecting Yes or No responses from the subject.

Q1   Please indicate the **modality** of the sensations you feel by checking the appropriate boxes below

     ☐ Fist closed   ☐ Pressure   ☐ Hot   ☐ Deep Pain

     ☐ Fist open   ☐ Needle Prick   ☐ Sharp Pain   ☐ Other

     ☐ Finger bent   ☐ Tingling   ☐ Diffuse Pain   (Describe)

     ☐ Fingers spread   ☐ Cool   ☐ Numb

     ☐ Light Touch   ☐ Warm   ☐ Unnatural

Q2   Please describe the **quality** of the sensations you feel by checking the appropriate boxes below

     ☐ Comfortable   ☐ Sharp   ☐ Soft   ☐ Strong

     ☐ Uncomfortable   ☐ Blunt   ☐ Mild   ☐ Other (Describe)

Q3   Please indicate the **location** of the sensations you feel by checking the appropriate boxes below

     ☐ Local   ☐ Spreading   ☐ Referred   ☐ Other (Describe)

Q4   Please illustrate in the diagrams below the areas where you feel the sensation
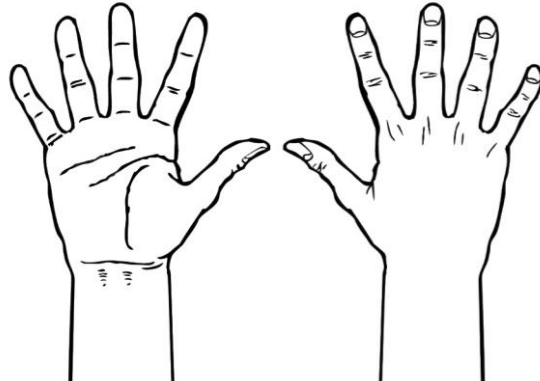
Figure 7. The MQL Questionnaire to assess the Modality (Q1), Quality (Q2) and Location (Q3) of the elicited percepts. A diagram of the palmar and dorsal surfaces of the right hand (Q4) was used to assess the elicited percept areas.
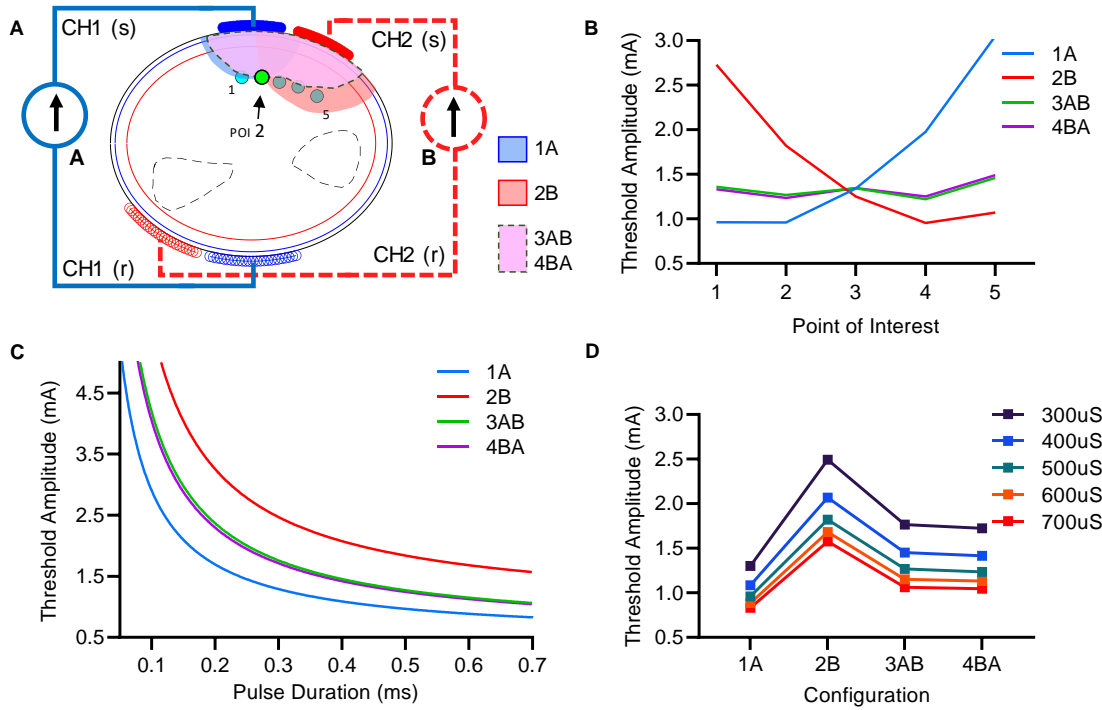
Figure 8. Activation performance across stimulation configurations in a computational model. (A) Activation regions describing the areas where the axons are likely to be activated within the cross-section of the wrist. Depicted are the regions generated by each configuration when triggering a sensory axon located at the second point of interest (Blue: 1A, Red: 2B, Violet with green dashed lines: 3AB and 4BA). (B) Activation threshold across 5 points of interest. Single-channel stimulation with 1A and 2B at PW:500µs; Multi-channel stimulation with CHIPS 3AB and 4BA at PW:250µs per channel. (C) Strength-duration curves for each simulated configuration (Weiss–Lapicque fit) when activating a sensory axon located at the second point of interest. In B and C, Blue: 1A; Red: 2B; Green: 3AB, Violet: 4BA. (D) Activation thresholds for each simulated configuration under various pulse durations when activating a sensory axon located at the second point of interest.
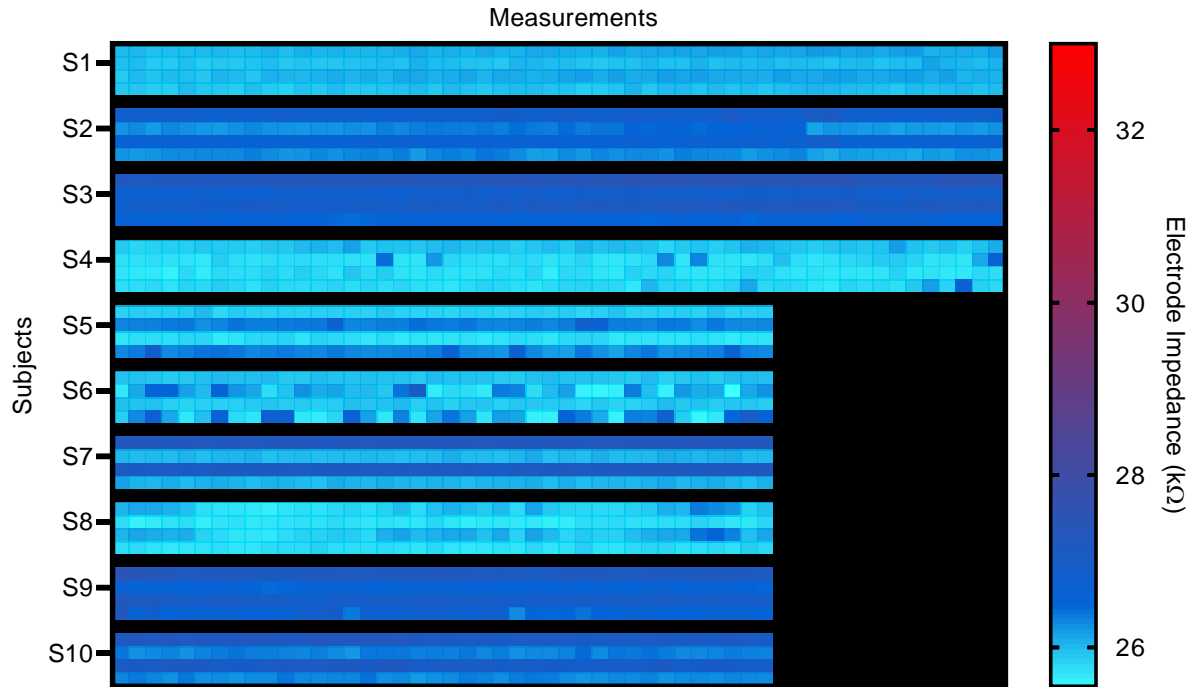
Figure 9. Surface electrode impedances were stable throughout the study. The impedance measurements (kΩ) for each electrode recorded at the start of every block during the regular threshold measurement trials. Additional impedance measurements were done with 4 subjects over 14 trials spread across the additional pulse delay trials. Each colored square is an individual impedance value collected at different measurement times (x-axis). All electrode impedance values were less than 30 kΩ (26.4 ± 0.5 kΩ; mean ± SD) for all subjects.
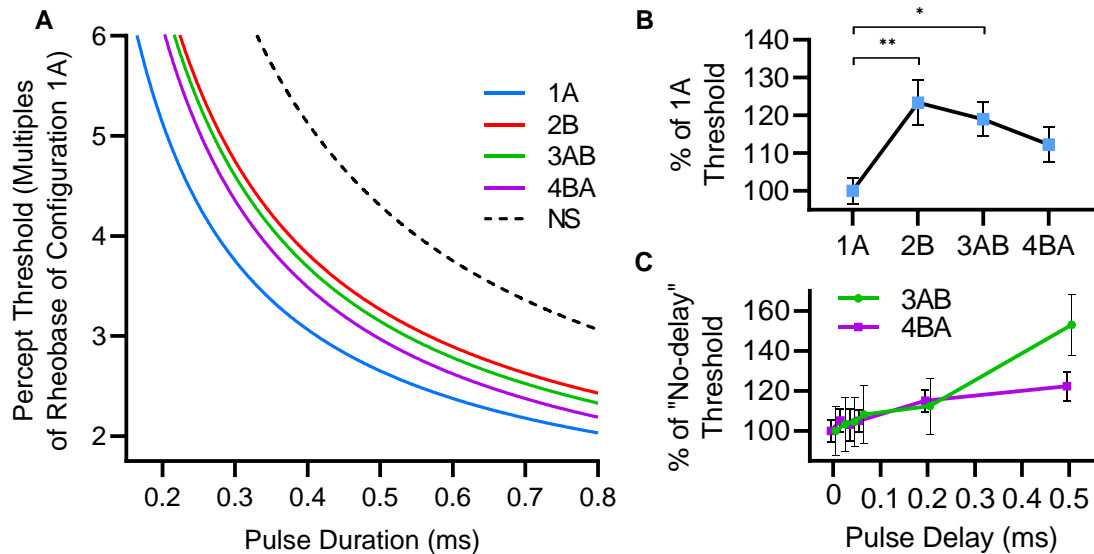
Figure 10. Sensory activation performance in human subjects. (A) Mean strength-duration curves from all participants (Weiss–Lapicque fit) normalized for each subject to the rheobase of the best performing (lowest PT) SC configuration, 1A (blue) as compared to 2B (red). A black-dashed reference SD profile represents the lowest theoretical PT that would be seen if there was no summation (N-S) of interleaved pulses. (B) Mean normalized PT values adjusted to the % of 1A across all PW values tested (* $p < 0.05$, ** $p < 0.005$ post-hoc Tukey test). (C) Threshold differences under various trailing pulse delays. Mean PT for 3AB (green) and 4BA (violet), normalized to their rheobase at 0µs delay, and adjusted for all PW values tested.
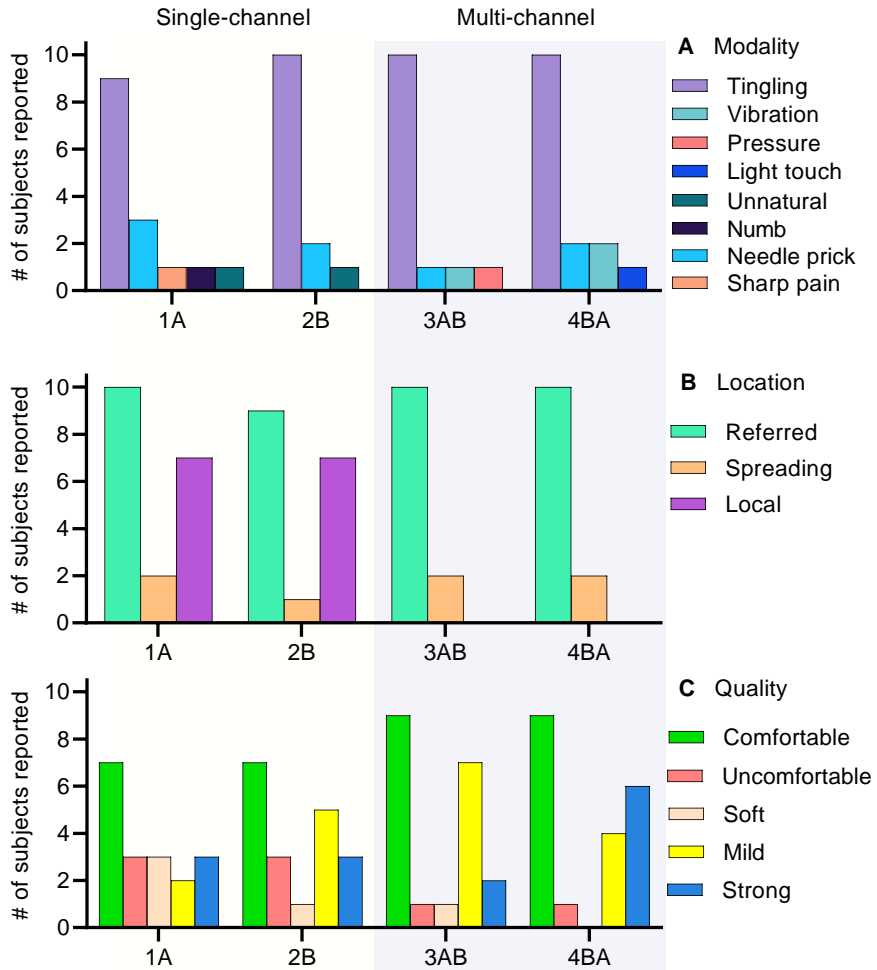
Figure 11. Questionnaire responses across all stimulation configurations. The bar plots represent the number of subjects that reported a given (A) percept modality, (B) percept quality, and (C) percept location. The maximum possible number of reports for any given percept descriptor was 10.
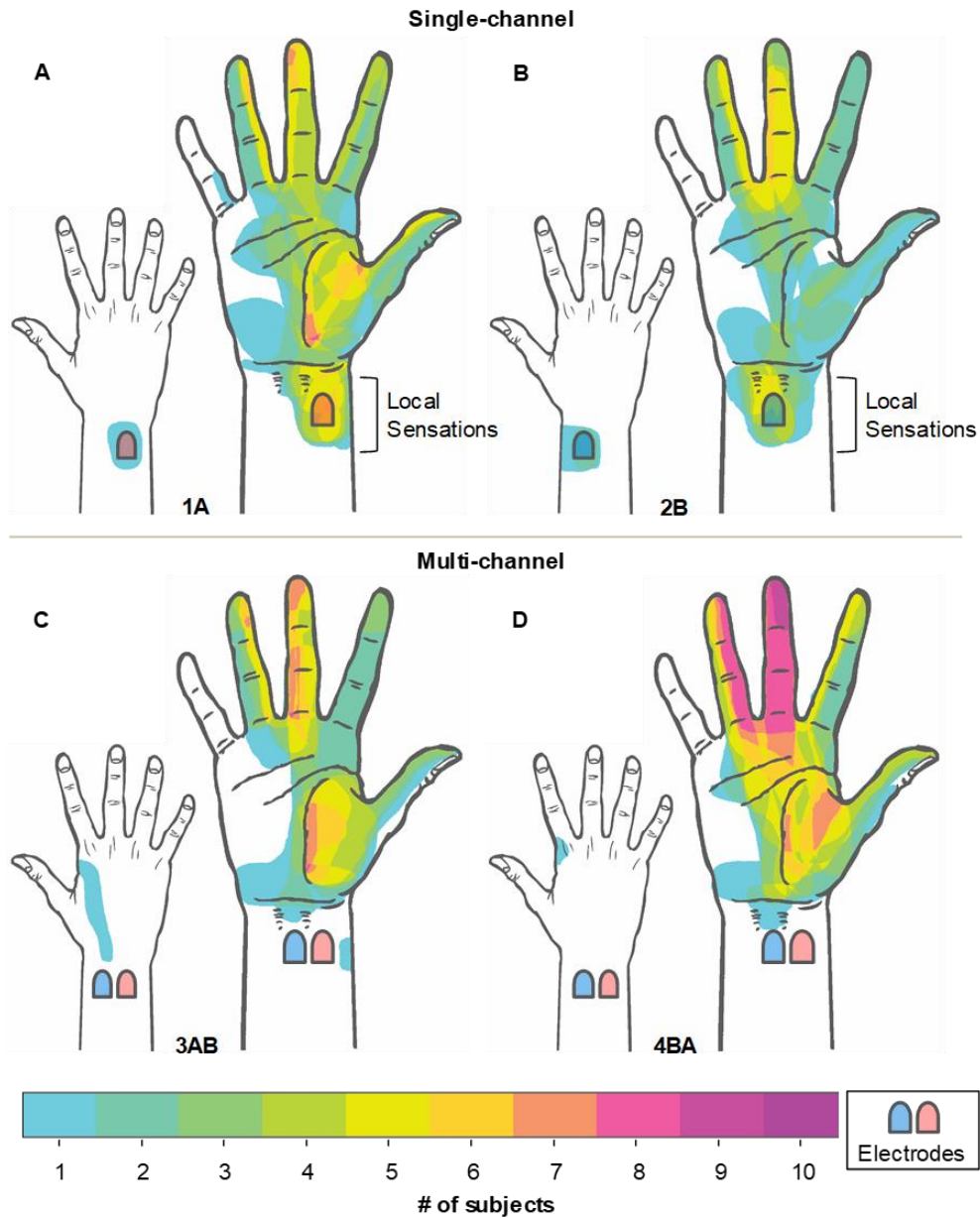
Figure 12. Location of the percept regions drawn by all subjects on diagrams of the palmar and dorsal surfaces of the right hand. All subjects reported distally referred sensations across the area of the hand including the ring, middle, index fingers and the thumb. The color scale represents the number of subjects that reported a percept in any given location. (A, B) Local sensations under the electrodes were reported by 7 subjects under configurations 1A and 2B. (C) A tingle-like sensation was reported by 1 subject on the lateral surface of the wrist under configuration 3AB (between electrodes, not under). (D) Sensations on the ring and middle fingers, and the palm of the hand were most consistently reported under configuration 4BA. The red/blue pads on the wrist represent approximate electrode locations for each stimulation configuration.

CHAPTER 4

CHARGE-RATE SENSORY ENCODING WITH AN ENHANCED SURFACE
ELECTRICAL NEUROSTIMULATION PLATFORM

4.1 Introduction

For individuals with upper-limb amputation, the functionality of commercially
available prosthetic technology is limited, which impacts quality of life and often
leads to prosthesis abandonment (Biddiss and Chau, 2007b, Peerdeman et al.,
2011a). The lack of sensory feedback from the prosthesis necessitates a high level
of visual attention and limits the quality of control (Antfolk et al., 2013, Cordella et
al., 2016). It has been demonstrated that electrical stimulation of residual nerves
with implantable electrodes can evoke distally referred sensations in the phantom
hand. This has been used to provide amputees with intuitive sensory feedback,
resulting in functional and psychological benefits (Dhillon et al., 2005, Schiefer et
al., 2015, Wendelken et al., 2017, Petrini et al., 2018). However, the invasive
nature of the device implantation procedures is not acceptable to all (Resnik et al.,
2019).

Surface electrical neurostimulation is a potential non-invasive alternative for
providing somatotopically-matched sensory feedback. In this approach, surface
electrodes applied on the skin are used to deliver electrical pulses to nearby
peripheral nerves, activating afferent pathways. Earlier studies have shown that
transcutaneous stimulation can be used to elicit distally referred sensations when
targeting the median and ulnar nerves at the forearm (D'Anna et al., 2017) or at

the elbow level (Shin et al., 2018). However, localized discomfort, poor selectivity, inadequate electrode and stimulation parameter fitting, and limited percept modulation have precluded wide adoption of traditional methods for surface stimulation as a viable sensory feedback approach (D'Anna et al., 2017, Shin et al., 2018).

An enhanced surface electrical neurostimulation (eSENS) platform that is able to selectively elicit comfortable, distally referred percepts has been previously developed and is described in Chapter 3. The eSENS platform utilizes a novel Channel-hopping Interleaved Pulse Scheduling (CHIPS) strategy to address some of the primary issues that have hindered the use of transcutaneous stimulation to deliver intuitive sensory feedback. The CHIPS strategy leverages the combined influence of short, sub-threshold current pulses from independent channels, interleaved across a set of distributed electrodes, to deliver functional (supra-threshold) stimulation levels within the tissue while reducing the total charge per pulse delivered by any given electrode. This novel approach has been shown to elicit enhanced tactile percepts while avoiding the local sensations and skin discomfort associated with the large charge densities in traditional methods. In addition to comfort and selectively, another important requirement for an intuitive artificial sensory feedback platform is the ability to convey discriminable levels of tactile intensities. The intensity of a tactile stimulus is one of its most basic sensory dimensions. It can be used to provide relevant sensory information such as grasping force when manipulating an object (Graczyk et al., 2016, Schiefer et al., 2016).

Thus, it is essential for the eSENS platform to be able to convey a wide range of discriminable percept intensities in order to serve as a viable option for intuitive sensory feedback during functional tasks.

Tactile sensations in neurologically intact individuals involves the integration of more than one kind of stimulus and more than one kind of tactile mechanoreceptor to form a coherent percept (Johansson and Flanagan, 2007). The dynamics of the receptor output convey important information about the properties of the stimulus through rate coding and population coding. In rate coding, the frequency of the action potentials generated by the sensory receptors is proportional to the intensity of the stimulus. In population coding, changes in stimuli intensity is conveyed by the total number of active neurons in the receptor population. When the stimulus intensity increases, receptors with lower thresholds are first recruited, followed by receptors with higher thresholds (Kandel et al., 2000). The contributions of firing rate and population recruitment to percept intensity are believed to be closely intertwined (Muniak et al., 2007).

In the context of electrical stimulation, firing rate and fiber population recruitment can be influenced by varying the stimulation Pulse Frequency (PF) and Pulse Charge (Q), respectively (Graczyk et al., 2016). When the stimulation pulses are square, the pulse charge can be expressed as the product of Pulse Amplitude (PA) and the Pulse Width (PW). Previous studies with electrical stimulation of residual nerves in amputees have modulated PF or Q independently to elicit changes in percept intensity (Horch et al., 2011, Schiefer et al., 2016, Charkhkar et al., 2018,

George et al., 2020). However, since rate and recruitment are both linked to percept intensity, modulation of only one of these two parameters could have resulted in a narrow range of discriminable levels of intensity that could be provided. To further understand this relationship, Graczyk *et al.* evaluated the effect of these two parameters on percept intensity gradation in amputees receiving direct electrical stimulation around their residual nerves. They found that PF and Q had systematic, cooperative effects on perceived tactile intensity, which supports the idea that the intensity of the perceived sensation is in part determined by the activation rate across the entire population of activated afferent neurons, weighted by fiber type. Based on these findings Graczyk et al. proposed an activation charge-rate (AQR) model, which unifies these two parameters into a single quantity that predicts percept intensity when delivering direct peripheral nerve stimulation.

The ability to convey a wide range of discriminable levels of intensity could be achieved with the eSENS platform by combining these two aspects of neural response. However, it is not known whether the AQR model would predict intensity perception for transcutaneous neurostimulation in the same way as it has for direct peripheral nerve stimulation. To answer this, in the present study classical psychophysical methods were applied to investigate the effect of these stimulation parameters on percept intensity gradation in able-bodied subjects receiving non-invasive stimulation from the eSENS platform, and in a subject with a transradial amputation receiving direct peripheral nerve stimulation with implanted intrafascicular electrodes. This characterization of the influence of charge and

frequency on percept intensity requires careful exploration of the parameter space and accurate stimulation parameter fitting, which includes the determination of optimal stimulation amplitudes and selection of the operating ranges for each modulated parameter. Stimulation parameter fitting has been traditionally done over iterative procedures involving psychophysics measures or verbal reports from subjects (Strauss et al., 2019, Geng et al., 2019). These procedures are time-consuming and can take a large portion of an experimental session. To address this bottleneck, this study implemented subject-controlled calibration routines that were developed to streamline the determination of stimulation amplitude thresholds and selection of the operating ranges for stimulation parameters such as pulse charge and pulse frequency, based on real-time input from the subjects.

In this study, a series of forced-choice tasks probed the subjects' ability to discriminate changes in percept intensity, while percept intensity rating tasks were used to assess how the range of percept intensities vary as stimulation parameters change. All experiments were completed across three parameter mapping schemes: modulation of pulse frequency alone, charge alone, and modulation of charge-rate (QR) in which both PF and Q are adjusted simultaneously. This newly acquired understanding could serve as the foundation for establishing a streamlined parameter fitting strategy to enable the eSENS platform to convey a wide range of graded percept intensities during functional tasks.

4.2 Methods

This study examines the dependency of percept intensity range and gradation on stimulation pulse frequency and pulse charge in able-bodied subjects with non-invasive median nerve stimulation, and in a subject with a transradial amputation receiving intrafascicular ulnar nerve stimulation. The discriminability and dynamic range of percept intensity were assessed for all subjects in a series of forced-choice tasks and open-ended intensity estimation tasks. All experiments were double-blinded with a randomized stimulus presentation order.

4.2.1   Subjects

Written informed consent was obtained from 10 adult subjects (7 males, 3 females, mean age ±SD: 29±3.5) in compliance with the Institutional Review Board of Florida International University. All prospective subjects were screened prior to the study to determine eligibility. Subjects were able-bodied, with no sensory disorders or any self-reported condition listed as a contraindication for transcutaneous electrical stimulation (pregnancy, epilepsy, lymphedema, or cardiac pacemaker) (Rennie, 2010).

Written informed consent was obtained from an individual with a unilateral left-arm transradial amputation (40-year-old male, 7-years post traumatic amputation) and was enrolled in an early feasibility clinical trial, Neural Enabled Prosthesis for Upper Limb Amputees (ClinicalTrials.gov: NCT03432325). Briefly, in March 2018 an investigational neural stimulator with a distributed intrafascicular multi-electrode (DIME) (Thota et al., 2015, Pena et al., 2017), comprising 15 longitudinal

intrafascicular electrodes (LIFEs) (Dhillon and Horch, 2005) that are arranged in three bundles of five electrodes was implanted subcutaneously in the deltoid region of the left upper-arm of the subject. Ten LIFEs were implanted in the median nerve (two sets of five at each of two sites along the nerve) and five were implanted in the ulnar nerve.

4.2.2 Experiment Setup

Subjects were seated in front of a table with a computer screen, a custom 3-button keyboard and a control knob (Figure 13 and Figure 14). The screen displayed instructions for the subject at different stages of the study. The subjects used the keyboard to provide percept responses, and the knob to adjust various stimulation parameters at different stages of the study. The knob was set to control stimulation parameter values within safe levels. Subjects were instructed to concentrate throughout the experiment but were encouraged to stretch and move their hand during periodic breaks to prevent discomfort. Subjects were asked about their comfort levels, or if additional breaks were needed after each task.

4.2.3 Peripheral Nerve Stimulation

Surface Electrical Neurostimulation in Able-bodied subjects

Each subject received transcutaneous electrical stimuli from four self-adhesive hydrogel electrodes (Rhythmlink International LLC, Columbia, SC) placed around the right wrist. This location allowed superficial access to the median nerve, which contains afferent fibers innervating the radial aspect of the palm, and the tips of the thumb, index and middle fingers.

Their right forearm was thoroughly cleaned with a wet wipe and placed on a support pad on the table, with their right hand's palmar surface parallel to the vertical plane. Two small stimulating (s) electrodes (15x20mm) were placed on the ventral aspect of the wrist (~3 cm from the distal radial crease) and two large return (r) electrodes (20x25mm) placed on the opposite (dorsal) side. Each "s-r" electrode pair was assigned to an independent stimulation channel (A and B) and configured such that their current paths would cross each other and intersect the median nerve transversally (Figure 13B). Placement of each "s-r" pair was determined by exploring different locations around the median nerve while providing brief, 1s long stimulation bursts (500µs biphasic, anode-first pulses at 30Hz) at different amplitude levels between 1.5mA and 3mA, in increments of 0.1mA, until a distinct referred sensation was reported by the subject.

A multi-channel programmable, optically isolated benchtop bio-stimulator (TDT IZ2-16H, Tucker-Davis Technologies, Alachua FL USA) was used to deliver charge-balanced, current-controlled biphasic rectangular pulses. The stimulator was controlled by a custom TDT Synapse stimulation control environment interfaced to a custom MATLAB (v2019b, MathWorks Inc, Natick, MA) program designed to run and monitor the different study conditions and adjust the stimulation parameters based on subject responses.

The stimulation was delivered to the median nerve following the CHIPS strategy (Figure 13B), in which two short biphasic anode-first pulses were interleaved from two independent stimulation channels (hopping from A to B) so that the anodic

77

phases of each channel were delivered consecutively, followed by their respective

balancing phases after a 100µs inter-phase gap (IPG). The stimulation PW was

defined as the sum of the individual interleaved phase durations (Figure 13B). The

interleaved pulses did not overlap in time to prevent channel interactions.

Additional information regarding the transcutaneous stimulation procedure can be

found in Chapter 3.

Stimulation Parameters

Pulse Amplitude thresholds were obtained from all able-bodied subjects under 5

different Pulse Width values (300µs to 700µs, at 100µs intervals). The order of the

pulse widths was randomized across all subjects. During the PA threshold

determination procedure, subjects interacted with a custom MATLAB algorithm

designed to control the delivery of electrical stimuli and collect the subject's

responses. Subjects triggered the delivery of a constant 5Hz pulse train by

pressing the "Go" button on a keyboard, and then used a custom control knob to

adjust the PA (from 0µA to 3000µA) to find the lowest possible level that evoked a

percept. This procedure was performed twice, and the PA was averaged for each

PW. The subject responses were fitted to the Lapicque-Weiss's theoretical model

(Lapicque, 1909, Weiss, 1990) to derive the strength-duration (SD) profile. The

stimulation pulse amplitude used throughout this study was set to 50% above the

percept threshold (1.5xPA_{th}) at a PW of 500µs. This duration was chosen since it

lay beyond the nonlinear region of the SD profile, thus allowing for a wide range of

PW to be used at this PA.

A similar subject-controlled calibration routine was used to determine the operating ranges for Q and PF that would be used throughout the study. For able-bodied subjects, modulation of Q was achieved by fixing PA and adjusting PW. First, stimulation was delivered at a fixed PF of 100Hz while instructing the subjects to use the knob to explore a wide range of PW (from 100μs to 800μs) to find the lowest possible level that evoked a reliable percept, and the highest possible level that did not cause discomfort. Lastly, the stimulation PW was set to the midpoint of the recently obtained PW range, and the subjects were again instructed to use the knob to explore a wide range of PF (from 30Hz to 300Hz) to find the lowest possible frequency that was not perceived as pulsating (fusion), and the level at which the perceived stimulation intensity did not change (saturation).

Modulation of QR was achieved by adjusting both PF and Q simultaneously, along their operating ranges. The pulse charge at perception threshold (Q_{th}) of each subject was derived from their SD profile and was used with the AQR model ($AQR = (Q - Q_{th}) \times PF$ where $Q = PA \times PW$) to calculate the equivalent QR range values that would result from each PF and Q adjustment.

Intrafascicular Stimulation in a Subject with a Transradial Amputation

The subject with the transradial amputation had a fully implantable, wireless multi-channel neurostimulator based on the design of the CI24RE (Cochlear Ltd., Sydney, Australia) with lead wires attached to 15 LIFE electrodes implanted longitudinally inside fascicles of the median and ulnar nerves (Figure 14A). The stimulator received wireless transcutaneous communication of stimulation pulse

parameters and power through an RF coil, from a custom stimulation control software and delivers charge-balanced biphasic stimulation pulses with pulse-by-pulse control of PA, PW, IPG and pulse timing, which provides control of PF. Additional information regarding the neurostimulator, electrodes, and implantation procedure used for this subject can be found in (Thota et al., 2015, Pena et al., 2017).

During this study, the implanted stimulator delivered biphasic, cathode-first rectangular pulses with a fixed PW of 300µs and an IPG of 57µs. The stimulation was delivered through an intrafascicular electrode located in the ulnar nerve. Stimulation on this electrode evoked a tingling sensation that was felt on the anterior side of pinky, from the distal interphalangeal crease to the distal palmar crease.

Stimulation Parameters

Pulse Amplitude (PA) thresholds were obtained from the subject under 10 different PW values (75µs to 300µs, at 25µs intervals). During the PA threshold determination procedure, the subject used a custom control knob to adjust the PA (from 20.22µA to 76.94µA) to find the lowest possible level that evoked a percept. This procedure was performed three times, and the PA was averaged for each PW. The strength-duration (SD) profile was also derived for this subject by fitting the detection responses to the Lapicque-Weiss's model. The stimulation PW used throughout this study was set to 300µs to allow for a wide range of PA values to be explored.

A similar subject-controlled calibration routine was used to determine the operating ranges for Q and PF that would be used throughout the study. In this case, modulation of Q was achieved by fixing PW to 300μs and adjusting PA. First, stimulation was delivered at a fixed PF of ~76Hz while instructing the subject to use the knob to explore a wide range of PA (from 20.22μA to 76.94μA) to find the lowest possible level that evoked a reliable percept, and the highest possible level that did not cause discomfort. Lastly, the stimulation PA was set to the midpoint of the recently obtained PA range (~37.36μA), and the subject was again instructed to use the knob to explore a wide range of PF (from 5Hz to 333Hz) to find the lowest possible frequency that was not perceived as pulsating (fusion), and the level at which the perceived stimulation intensity did not change (saturation).

Modulation of QR was achieved by adjusting both PF and Q simultaneously, along their operating ranges. The pulse charge at perception threshold (Q_{th}) was derived from the subject's SD profile and was used with the AQR model to calculate the equivalent QR range values that would result from each PF and Q adjustment.

4.2.4   Intensity Discrimination Tasks

A series of forced-choice tasks were completed to assess the subject's ability to discriminate different stimulation intensity levels. On each trial, a pair of stimulation bursts were presented, and the subjects were instructed to report whether the second burst felt softer, same or stronger than the first burst by responding on a custom 3-button keyboard. Each burst lasted for 1 second, with a 0.5 second pause in between. Subjects were instructed to focus on the intensity or magnitude

of the evoked sensation when deciding how to respond. A single experimental block consisted of 45 randomized burst pair presentations (9 unique stimulus pairs presented 5 times) with short breaks after every 10 presentations. All subjects completed 3 experimental blocks: modulating PF, Q, or both (QR). In each block, each burst pair differed in the parameter being tested. The first burst was always the reference, in which the tested parameter was set to the midpoint of its range. The reference burst was compared to 9 unique test bursts that included 4 equally spaced values below and above the reference, with a step size no larger than 25% from the reference value. The just noticeable difference (JND) was determined for each parameter tested by fitting the subject's responses to a cumulative normal distribution to obtain the psychometric function. The JND was calculated by averaging the 75% correct performance points for both ends of the psychometric function. To compare discriminability across conditions, the Weber ratios were computed by dividing the JND by the reference value for each parameter tested.

Statistical Analysis

The discrimination performance under each stimulation conditions was assessed by comparing their effect on the weber ratios with a one-way ANOVA using GraphPad Prism 8 (v8.3.1 for Windows, GraphPad Software, San Diego, California USA). Post-hoc multiple comparisons between stimulation conditions were made using the Tukey-Kramer test at an alpha level of 0.05 for significance. One sample t-tests were performed to compare discrimination performances between transcutaneous and intrafascicular stimulation.

4.2.5 Intensity Estimation Tasks

Intensity estimation was recorded using a free magnitude scaling paradigm or open-ended scale to test the span of evoked percept intensities and allow relative comparison of the perceived strength levels. This method has been traditionally used in psychophysics to perform direct quantitative assessments of subjective magnitudes or intensities (Stevens, 1956, Banks and Coleman, 1981). For each intensity estimation trial, a 1-second-long stimulation burst was delivered, and the subject was asked to state a number that represented the perceived intensity or magnitude of the evoked sensation by comparing it with the previous burst. For instance, if one stimulus feels half or twice as intense as the previous one, it could be given a score that is half or twice as large (Stevens, 1956). A score of 0 was used when no sensation is perceived. All subjects completed 3 experimental blocks, each consisting of up to 30 randomized trials (up to 10 equally spaced levels per test condition). Three test conditions were intermixed in each experimental block: During Q modulation, Q was changed while PF was fixed at its range midpoint. During PF modulation, PF was changed while Q was fixed at its range midpoint. Finally, during QR modulation, both Q and PF were changed simultaneously. Ratings were normalized by dividing the values by the grand mean rating on their respective blocks.

Statistical Analysis

Simple linear regressions were performed to assess the relationship between percept intensity ratings and each stimulation condition used. The perceived intensity ranges under the different stimulation condition were compared with a

one-way ANOVA (GraphPad Prism 8). Post-hoc multiple comparisons of the intensity ranges between stimulation condition were made using the Tukey-Kramer test at an alpha level of 0.05 for significance.

4.3 Results

Ten able-bodied subjects received transcutaneous stimulation from the eSENS platform enhanced by the novel CHIPS strategy. This approach evoked comfortable distally referred sensations of tingle, pressure and light touch in the general area innervated by the sensory fibers in the median nerve (palmar surface, index, middle, and part of the ring finger). A subject with a transradial amputation received intrafascicular stimulation through an electrode located in the ulnar nerve. Stimulation on this electrode evoked comfortable distally referred tingling sensations that were felt on the anterior side of little finger, from the distal interphalangeal crease to the distal palmar crease. The discriminability and dynamic range of percept intensity were assessed for all subjects across three parameter mapping schemes. No uncomfortable or local sensations, and no side effects like irritation or redness of the skin were observed in any of the able-bodied subjects.

All subjects were able use a control knob to determine percept threshold values and define an operating range for both PF and Q from a wide range of parameter values. In average, these calibration routines were completed in less than 10 minutes. Able-bodied subjects reported an operating range for Q spanning from $0.77 \pm 0.19 \mu C$ to $1.42 \pm 0.32 \mu C$ with surface stimulation, while the operating range

for PF spanned from 56.07±15.76Hz (fusion) to 185.38±38.06Hz (saturation). Simultaneous adjustment of PF and Q over these ranges resulted in a wide QR range spanning from 1.48±2.26µA to 107.97±42.30µA. The reference value used for discrimination tasks was 52.13±21.89µA, averaged across all subjects. All values are reported as mean ±SD.

The subject with the transradial amputation reported an operating range for Q between 9.88nC and 11.83nC with intrafascicular stimulation, and a PF range between 36.0Hz and 91.0Hz. Simultaneous adjustment of PF and Q over these ranges resulted in a wide QR range spanning from 91.0nA to 490.8nA. The reference values used for discrimination tasks were 348nA, 305nA, and 281nA for PF, Q and QR modulation respectively.

4.3.1 Subjects reliably discriminated small increments of QR

All subjects performed intensity discrimination tasks to determine how much change in a given stimulation parameter was required for the subjects to report a change in the perceived intensity of the evoked percept. In general, all were able to perceive changes in percept intensity across stimulation conditions, as evidenced by the psychometric curves that were obtained (Figure 15). For consistency, and to compare across stimulation conditions, all references and JND values are reported in terms of QR, defined as the total charge per second (µA). All results from able-bodied subjects are reported as mean ±SD.

For able-bodied subjects (Figure 15A), the JND during PF modulation was 9.71±4.04µA, and the Weber ratio was 0.21±0.1. The JND for Q modulation was

6.70±4.31µA, with a Weber ratio of 0.13±0.07. Simultaneous modulation of both

PF and Q resulted in intensity discrimination performance that was between that

found when either was adjusted in isolation. The JND during QR modulation was

9.74±6.55µA, with a Weber ratio of 0.19±0.11. While the Weber ratio for Q

modulation was visibly lower than PF and QR, they were all statistically

indistinguishable (one-way ANOVA, $F_{(2,27)}=1.935$, $p=0.1639$).

The subject with the amputation was able to discriminate intensity changes in

percepts evoked by intraneural stimulation, with a performance comparable to that

of able-bodied subjects (Figure 15B). The JND for PF modulation was 36.33nA,

and the Weber ratio was 0.27. The JND for Q modulation was 36.34nA, with a

Weber ratio of 0.12. The JND during QR modulation was 47.03nA, with a Weber

ratio of 0.17.

4.3.2 Subjects perceived a wider range of intensities with QR modulation

While discrimination performance provides the minimum required change in

stimulation parameter to produce a noticeable change in percept intensity, it does

not elucidate the actual range of intensities that are possible with a given

stimulation parameter range. To address this, the dynamic ranges of percept

intensity for each stimulation condition were assessed for all able-bodied subjects

and the subject with the transradial amputation over a series of intensity estimation

trials. Intensity ratings given by the subjects were normalized for comparison. As

expected, the perceived intensity increased when Q or PF were increased over

their operational range. Modulation of QR was strongly correlated to percept

intensity during non-invasive stimulation in able-bodied subjects: r=0.87; p<0.0001, and during intraneural stimulation in the subject with the amputation: r=0.85; p<0.0001. In both cases, the range of intensities that were perceived during QR modulation spanned wider than for the other parameters (Figure 16A and C).

Linear regressions were performed to predict perceived intensity as a function of charge-rate for all subjects. A one-way analysis of variance (ANOVA) on the perceived intensity ranges found for able-bodied subjects revealed significant differences between the stimulation conditions, F(2,27)=101.8, p<0.0001 (Figure 16B; inset). A post hoc Tukey test showed that the perceived intensity ranges found for PF modulation spanned significantly narrower than for Q and QR modulation (both p<0.0001), but no significant differences in intensity ranges were found between Q and QR modulation (p=0.13). The regression slopes however were significantly different depending on which parameter was modulated (F(2,23)=6.584, p=0.0055). The slopes were steepest for Q, shallowest for PF, and intermediate for QR (Figure 16B).

Responses from the subject with the amputation showed a similar trend where the intensity range found during QR was about 3.5 times the range of PF modulation, and about 1.3 times the range of Q modulation (Figure 16C; inset). The regression slopes were significantly different from each other, F(2,20)=4.202, p=0.03. In this case, Q and QR modulation also showed the steepest and intermediate regression slopes, respectively. Also, the slope for PF modulation was the shallowest, to the point where it was not significantly different from zero (F(1,6)=2.365, p=0.1750).

4.4 Discussion

An enhanced surface electrical neurostimulation (eSENS) platform was previously develop to selectively elicit comfortable, distally-referred percepts that could be used as sensory feedback. While comfort and selectively are important, the platform's ability to convey a wide range of discriminable levels of tactile intensities is a critical requirement in order for it to be a viable non-invasive option for intuitive sensory feedback during functional tasks. This work presents the first evaluation of activation charge-rate (AQR) to enhance the percept intensity mapping with surface electrical neurostimulation. The charge-rate relationship was leveraged to develop subject-controlled calibration routines that streamlined the stimulation parameter fitting process.

A series of psychophysical tests were used to probe the effect of different parameter modulation strategies on the range and gradation of percept intensities elicited in able-bodied subjects with the eSENS platform, and in a subject with transradial amputation receiving intrafascicular neurostimulation. In both cases, simultaneous modulation of charge and frequency resulted in fine intensity discrimination and a wider dynamic range of intensities. This is consistent with the concept that percept intensity is driven by the total firing rate evoked in the recruited mechanoreceptive afferent population (Muniak et al., 2007, Graczyk et al., 2016). While the intensity ranges obtained during modulation of charge and charge-rate were similar, charge-rate modulation provided a greater modulation resolution as the parameter map used implies changes in both frequency and charge values. Subjects also reported smoother transitions as charge-rate

increased as compared to the more drastic step-wise changes from charge modulation alone. In contrast, frequency modulation alone resulted in lower discrimination performance and a significantly narrower intensity range. In this case, stimulation charge was fixed to the mid-point of its operating range while frequency was changed. Because of this, the stimulation was always supra-threshold, which explains why the lowest intensity value reported during frequency modulation never reached zero.

Implementation of this sensory encoding strategy within the eSENS platform showed that it is possible to artificially influence the intensity code transcutaneously with psychophysical responses comparable to more invasive methods. These results serve as the foundation for creating a parameter-percept mapping strategy that can be used for delivering graded sensory feedback during functional tasks.

4.4.1 A streamlined parameter fitting strategy for wide range, graded sensation intensity mapping

Previous studies have performed percept characterization procedures in which stimulation parameters are varied to elicit a range of percept intensities and psychophysics measures or verbal reports are gathered from the subjects (Strauss et al., 2019). Determination of activation thresholds, as well as lower and upper limits for different parameters is often done over lengthy iterative processes (Geng et al., 2019). While these procedures yield a detailed map between percept and stimulation parameter, they are time-consuming and can take a large portion of an

experimental session. Therefore, more efficient stimulation parameter fitting procedures are needed.

In this study, the activation charge-rate model (Graczyk et al., 2016) was found to be a strong predictor for graded intensity perception during both transcutaneous and intrafascicular neurostimulation. This relationship was leveraged to enable fast and accurate stimulation parameter fitting with minimal intervention from the experimenter. Modulation of charge-rate was accomplished by adjusting pulse charge and pulse frequency simultaneously, along their operating ranges. These ranges were obtained through a subject-controlled calibration routine that was developed to simplify the exploration of the parameter-space. All subjects were able use a control knob to determine activation thresholds and define the operating range of pulse charges and pulse frequencies used throughout the study. The threshold determination procedures used in previous studies implemented a modified dual staircase designed to determine percept thresholds accurately for research objectives. In this case, it took an average of 5 minutes for each subject to find the threshold amplitudes for a single strength-duration profile. In contrast, the subject-controlled calibration routine used in this study allowed subjects to determine up to four strength-duration profiles (one for each configuration), and define two operating ranges in less than 10 minutes. This calibration routine can be used to streamline the parameter fitting process for additional studies using the eSENS platform, and possibly other neurostimulation approaches. Implementation of the charge-rate encoding scheme could thus enhance the intensity mapping of functional information such as grasping force.

4.4.2 Limitations

The intensity discrimination performance during frequency modulation, and by consequence during charge-rate modulation, could have been masked by potentially narrow operating ranges in pulse frequency due to the fusion-saturation limits. Other studies have shown that frequency discrimination performance is often better with low frequency references since subjects often use the timing of individual pulses as supplementary cues. However, as the intent of the study was to pay attention to the perceived intensity and not the frequency, subjects were instructed to pick the lower end of the operational frequency range as the point where individual pulses are no longer detectable (fusion). This helped avoid the presence of low frequency references and test bursts during the discrimination trials, which could have also increased the difficulty of the task.

Another limitation of this study is that it only focused on percept intensity. However, percept modality is also an important dimension of artificial feedback. While intensity is encoded by rate and population recruitment, modality seems to be encoded by the spatiotemporal patterning of this activity (Tan et al., 2014). Traditional surface stimulation methods have been shown to elicit sensations often reported as artificial or unnatural electrical tingling, or paresthesia. These sensations are believed to be the result of synchronous activation within a population of different fibers (Ochoa and Torebjörk, 1980, Mogyoros et al., 2000) which contrast with the more complex spatiotemporal patterns recognized during natural sensory perception (Weber et al., 2013). Previous studies with direct nerve stimulation (Tan et al., 2014) and surface stimulation (P. Slopsema et al., 2018)

have implemented time-variant patterning strategies in which a sinusoidal or pseudorandom jitter is added to the charge and/or frequency. These strategies have shown some reports of more natural pressure and tapping percepts. In this study, subjects were asked to explore the full range of intensities available through charge-rate modulation before the end of the experimental session. When asked to describe the percept modality, most subjects reported feeling comfortable distally referred sensations of tingle, pressure, vibration and light touch. This could be due to the fact that subjects swept the range of intensities, causing changes in both temporal and spatial recruitment during charge-rate modulation. While this is not exactly the type of time-variant patterning used in other studies, the continuous changes in charge and rate may have resulted in more "natural" activation patterns than in traditional methods. Future work could implement neuromorphic models that mimic healthy receptor behavior (Saal and Bensmaia, 2015) to generate time-variant patterns for both charge and frequency, to evoke more natural sensations.

4.4.3 Implications for neuromodulation strategy development

Electrical stimulation of peripheral afferents has been used for decades to formulate an understanding of neural coding and to restore lost sensory function (Anani et al., 1977). Recently, deployment of implantable peripheral nerve interfaces has prompted multiple breakthroughs in artificial somatosensory feedback and the neural basis of touch (Graczyk et al., 2016). Although promising, these approaches have only been tested on a small number of subjects, and wide clinical applications are limited due to the required surgery procedure and long-

term care (Resnik et al., 2019), thus hindering development of advanced neuromodulation strategies for intuitive sensory feedback.

The percept intensity rating and discrimination performance of able-bodied subjects with the eSENS platform was comparable to the subject with transradial amputation receiving intrafascicular neurostimulation. Moreover, these results were consistent with studies of amputees with implanted cuff electrodes (Graczyk et al., 2016). One of the key differences between transcutaneous and intrafascicular stimulation was selectivity. This can be seen in the differences in charge threshold and comfort limits between able-bodied subjects and the subject with transradial amputation, which were consistent with the nature of the stimulation method used in each case. Transcutaneous activation of afferent fibers within a superficial nerve such as the median nerve in the wrist required ~1000nC, which activated a larger portion of the nerve, evoking percepts on larger areas of the hand. In contrast, intrafascicular stimulation required lower charge (~10nC) to activate smaller groups of axons within the fascicle. Although this difference may play a role in the location and span of the referred percept, it does not seem to affect the way intensity is encoded. This suggests that the eSENS platform is capable of influencing and modulating the sensory code, and deliver information in a way that is comparable to implantable systems. The eSENS platform could thus serve as a testbed for studying the neural mechanisms of natural touch and developing advanced neuromodulation strategies for intuitive sensory feedback in able-bodied subjects before deployment in implantable systems.

FIGURES

A Experiment Setup

B Surface Electrical Stimulation
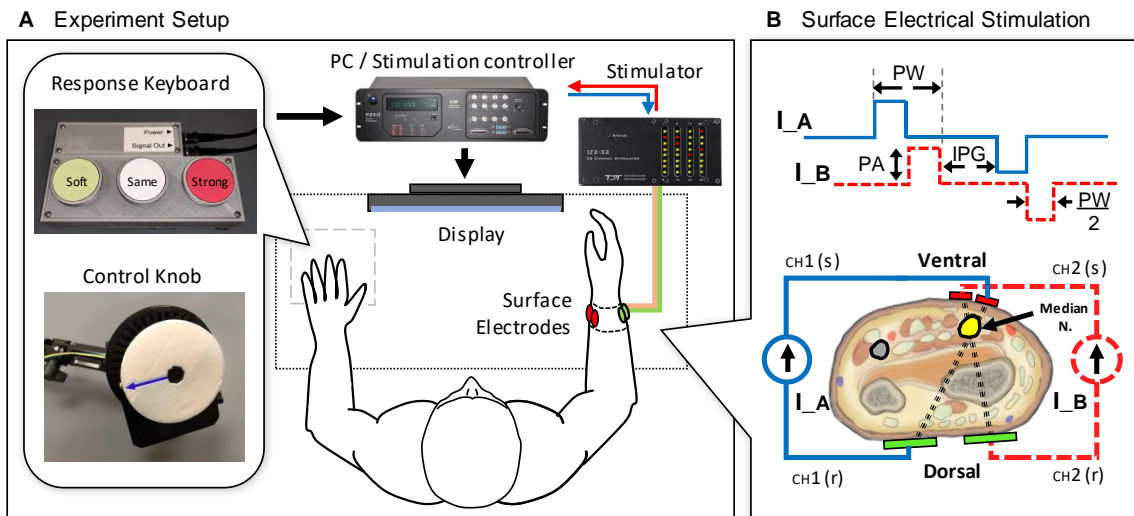
Figure 13. Experiment setup for surface stimulation. (A) Able-bodied subjects were seated on a chair with both arms on a table in front of them. A custom 3-button keyboard and a control knob were placed next to the subject's left hand. A computer screen was placed in front of them at eye level. The keyboard was used to provide percept responses, while the knob was used to adjust various stimulation parameters at different stages of the study. (B) Charge-balanced biphasic stimulation pulses were delivered by a current-controlled biostimulator (TDT RZ5 / IZ2H-16) from two independent current sources (CH1 & CH2) to two stimulating (s) surface electrodes on the ventral aspect of the wrist (~3cm from the distal radial crease), and two return (r) electrodes on the dorsal aspect. PA=Pulse Amplitude; PW=Pulse Duration; IPG=Inter-phase Gap.
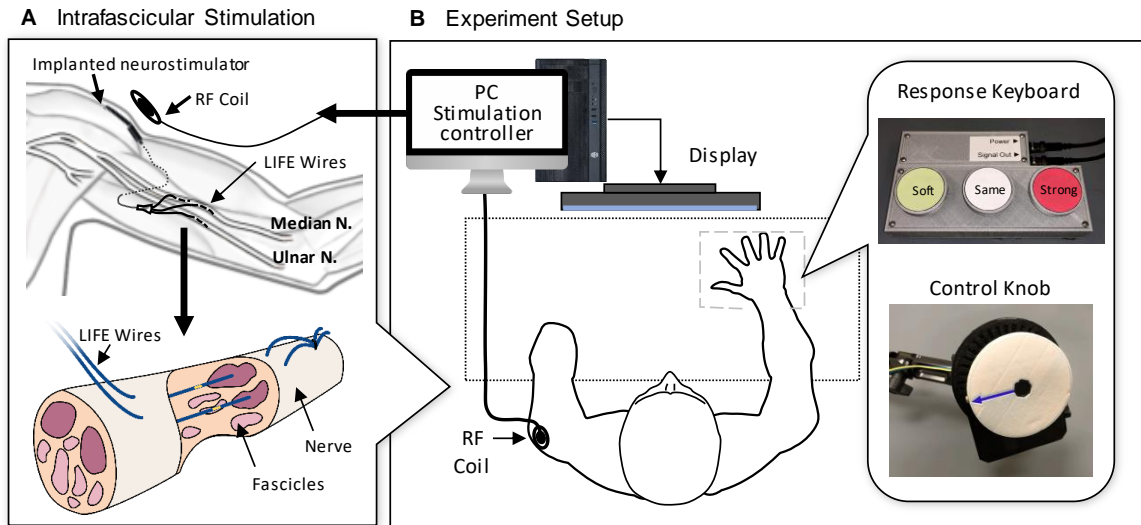
Figure 14. Setup for intrafascicular stimulation. (A) Implanted multi-channel neurostimulator connected to a distributed intrafascicular multielectrode (DIME) system consisting of a trifurcated lead attached to 15 LIFEs implanted longitudinally inside fascicles of the median and ulnar nerves. Stimulation parameters and power are transcutaneously communicated via an RF coil to the receiving antenna of the implanted neurostimulator. (B) The subject was seated on a chair with the left residual forearm and the right arm on a table in front of him. A custom 3-button keyboard and a control knob were placed next to the subject's right hand. A computer screen was placed in front of him at eye level. The keyboard was used to provide percept responses, while the knob was used to adjust various stimulation parameters at different stages of the study. LIFE=Longitudinal intrafascicular electrode; PC=Personal computer; RF=Radiofrequency
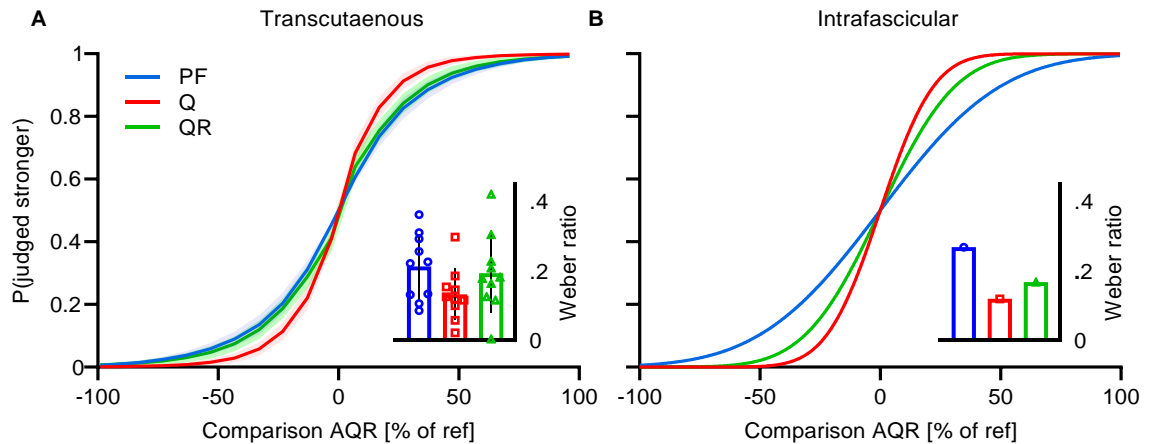
Figure 15. Psychometric functions relating percept intensity discrimination performance to changes in charge-rate. The curves indicate the probability of judging the presented stimuli correctly, i.e., stronger, same or weaker than the reference during modulation of PF (blue), Q (red) and QR (green). (A) Combined psychometric curves from 10 able-bodied subjects. Solid lines represent the mean performance across subjects for each stimulation condition. Shaded area denotes the SEM. (Inset) Weber ratios for all able-bodied subjects were consistent across the stimulation conditions (one-way ANOVA, p = 0.1639). Symbols denote all data; bars denote the mean ± SD. (B) Percept intensity discrimination performance for intrafascicular stimulation in a subject with a transradial amputation. (Inset) Weber ratios for PF, Q and QR modulation were comparable to those of able-bodied subjects across the stimulation conditions (one sample t test, p = 0.10, 0.61, and 0.50). PF=Pulse Frequency; Q=Charge; QR=Charge Rate.
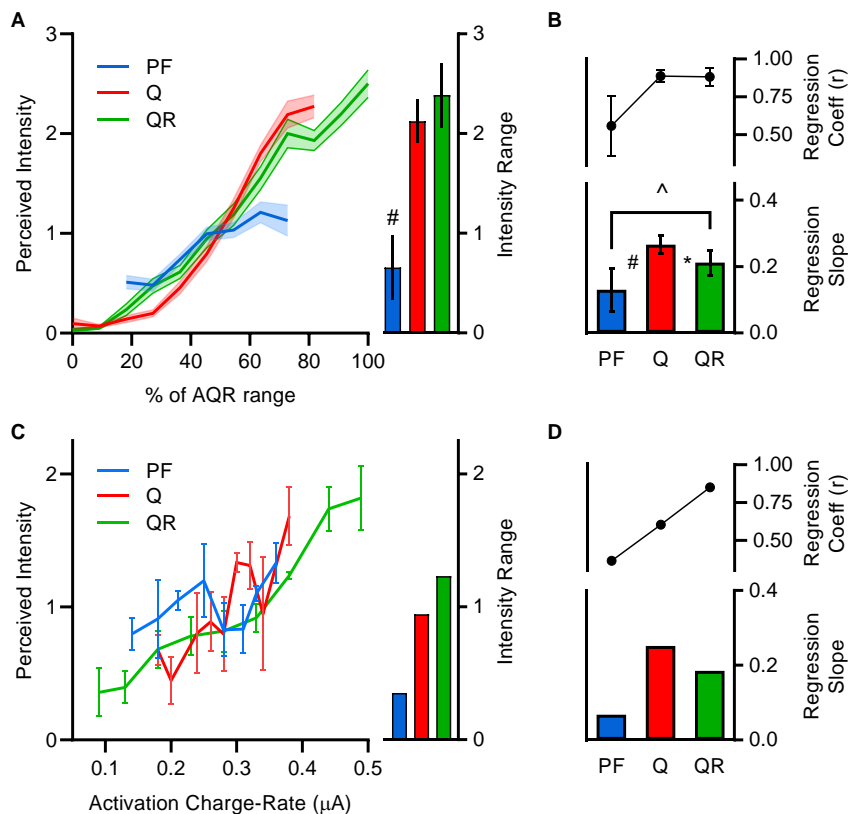
Figure 16. Stimulation charge-rate influences percept intensity. Ratings were normalized by dividing open-ended reports of perceived strength levels by the grand mean rating on their respective blocks, after manipulations of PF (blue), Q (red) or QR (green) as the combination of PF and Q. (A) Normalized perceived intensity as a function of the activation charge-rate range used for each subject. Solid lines indicate the mean ratings across 10 able-bodied subjects (n = 3 ratings per level from each subject) for each stimulation condition. Shaded area denotes the SEM. (Inset) Normalized intensity ranges (mean ± SD) across all able-bodied subjects showing a narrower range during PF modulation than for Q and QR (post hoc Tukey). (B) Comparison of regression slopes and regression coefficients (mean ± SD across subjects) obtained when varying PF, Q, or QR. Slopes were different for all conditions. Intensity was correlated to both Q and QR modulation. (C) Normalized perceived intensity as a function of activation charge-rate for intrafascicular stimulation in a subject with a transradial amputation. Solid lines indicate mean ratings (n = 3 ratings per level); error bars denote the SEM. (Inset) Normalized intensity ranges showing a narrower range during PF modulation. (D) Comparison of regression slopes and regression coefficients obtained when varying PF, Q, or QR during intrafascicular stimulation. Slopes were different for all conditions. Intensity was strongly correlated to QR modulation. (*p<0·05, ^ p<0·01, # p<0·001). See Figure 15 for definitions.

CHAPTER 5

CLOSING THE LOOP: FUNCTIONAL BENEFITS OF ENHANCED ARTIFICIAL PERCEPTS

5.1 Introduction

As commercially available prosthetic technology is limited by the lack of sensory feedback from the prosthesis, individuals with upper-limb amputation have to rely on visual and sound cues to perform simple control tasks such as grasping an object without crushing it. This results in substantial functional deficits (Pylatiuk et al., 2007, Antfolk et al., 2013, Cordella et al., 2016) which impacts quality of life and often leads to prosthesis abandonment (Biddiss and Chau, 2007a, Peerdeman et al., 2011b). For decades, researchers have studied the use of mechanical (Colella et al., 2019, Pena et al., 2019) and electro-tactile (Franceschi et al., 2017, Geng et al., 2018) sensory substitution to convey some prosthesis usage information (e.g. grasp force) through an alternate sensory channel by delivering tactile information at specific locations on the user's skin. However, the percept modality and location mismatch of substitution feedback often limits its efficacy and increases the user's cognitive load and response time (Zhang et al., 2015, Pena et al., 2019). Alternatively, electrical stimulation of residual nerves with implantable electrodes has been demonstrated to provide individuals with amputation with intuitive sensory feedback, resulting in functional and psychological benefits (Dhillon et al., 2005, Schiefer et al., 2015, Wendelken et al., 2017, Petrini et al.,

2018). However, the invasive nature of the device implantation procedures is not acceptable to all (Resnik et al., 2019).

Surface electrical neurostimulation is a non-invasive alternative for providing somatotopically-matched sensory feedback. In this approach, electrical pulses delivered from electrodes on the forearm skin have been shown to activate afferent pathways in the median and ulnar nerves, evoking distally referred sensations (D'Anna et al., 2017). However, traditional methods for surface stimulation are hampered by inadequate electrode and stimulation parameter fitting, poor selectivity, limited percept modulation, and distracting sensations due to localized charges activating tactile afferents in the skin close to the electrodes (Shin et al., 2018, D'Anna et al., 2017). These sensations can be hard to ignore, affecting the overall performance of the sensory feedback.

An enhanced surface electrical neurostimulation (eSENS) platform that is able to elicit distally-referred tactile percepts while avoiding the local sensations and skin discomfort associated with the large charge densities in traditional methods has been previously developed and is described in Chapter 3. Able-bodied subjects received interleaved current pulses from surface electrodes strategically distributed around their right wrist, using a Channel-hopping Interleaved Pulse Scheduling (CHIPS) strategy. This strategy leverages the combined influence of sub-threshold pulses to deliver functional stimulation to the nerve, evoking distally referred sensations more efficiently and comfortably than traditional methods. This provided evidence that the novel CHIPS strategy addresses some of the issues

hindering surface stimulation from being adopted as a viable option for intuitive sensory feedback. A bio-inspired charge-rate encoding strategy was evaluated during psychophysical studies described in Chapter 4. Implementation of this encoding strategy demonstrated enhancement of the range and gradation of evoked percept intensities with the eSENS platform. This strategy could be used to provide relevant sensory information during functional tasks. The relationship between the stimulation parameters used for this encoding strategy allowed for the implementation of "user-in-the-loop" (UiTL) calibration routines to streamline the stimulation parameter fitting process.

Sensory feedback is important when exploring and acting on the physical world. When grasping objects, cutaneous mechanoreceptors in the fingers provide relevant information about their characteristics and how much force is being used to grasp them (Johansson and Flanagan, 2007). One of the design goals of the eSENS platform is to restore this crucial ability by non-invasively evoking intuitive tactile percepts as replacement feedback after loss of sensory function. For individuals with amputation, this feedback could help improve the functionality of prosthetic limbs, enabling them to classify the physical properties of different objects, and perform fine control of grasp force outputs without the need for visual or auditory feedback (Antfolk et al., 2013). Other applications such as teleoperation of mobile robotic devices (e.g. military explosive disposal, remote surgery) and interactions within virtual and augmented reality environments (e.g. gaming, training, social interactions) may also benefit from the provision of tactile feedback

to execute virtual or remote tasks with high precision, without the need for cumbersome haptic hardware.

The goal of the study described here was to investigate the ability of the eSENS platform to convey graded and discriminable levels of sensory information for intuitive haptic feedback during functional tasks. To this end, two different functional task paradigms were developed to assess the functional benefits afforded by the enhanced haptic feedback on the subject's ability to (1) grasp and classify virtual objects with different size and hardness characteristics and (2) perform graded closed-loop control of virtual grasp force outputs. It was hypothesized that functional classification of different virtual grasping force profiles delivered by the eSENS platform would be better than chance. This was tested by quantifying the rate at which able-bodied subjects successfully classified different virtual objects according to their perceived size and hardness. It was also hypothesized that graded control of virtual grasp force outputs would be significantly better in the presence of grasp force feedback from the neurostimulator. This was tested by quantifying the ability of able-bodied subjects to accurately reach different target force levels by controlling the virtual force outputs with a proportional control joystick. Results from these functional studies provide compelling evidence that the tactile percepts delivered by the eSENS platform, with the implementation of the CHIPS strategy and charge-rate encoding, could be readily utilized by able-bodied subjects to complete functional tasks without the need for visual feedback. The task-related information provided by this

sensory feedback approach could also be used to close the loop between individuals with upper limb amputations and their prosthesis.

5.2 Methods

This study was intended to investigate the ability of the eSENS platform to convey task-related sensory feedback to able-bodied subjects. The potential functional benefits afforded by the supplementary feedback were assessed in a series of grasp profile classification and graded force control studies.

All experiments were double-blinded with randomized presentations of virtual object profiles and grasp force targets.

5.2.1 Subjects

Written informed consent was obtained from 4 right-handed adult subjects (2 males, 2 females, mean age ±SD: 27±4.7) in compliance with the Institutional Review Board of Florida International University which approved this study protocol. All prospective subjects were screened prior to the study to determine eligibility. Subjects were able-bodied, with no sensory disorders or any self-reported condition listed as a contraindication for transcutaneous electrical stimulation (pregnancy, epilepsy, lymphedema, or cardiac pacemaker) (Rennie, 2010).

5.2.2 Electrical Stimulation

Median nerve stimulation was delivered transcutaneously by four self-adhesive hydrogel electrodes (Rhythmlink International LLC, Columbia, SC) placed around the subject's right wrist. A multi-channel programmable, optically isolated benchtop

bio-stimulator (TDT IZ2-16H, Tucker-Davis Technologies, Alachua FL USA) was used to deliver charge-balanced, current-controlled biphasic rectangular pulses following the CHIPS strategy. The stimulator was controlled by a TDT Synapse stimulation control environment with a custom MATLAB (v2019b, MathWorks Inc, Natick, MA) program. Additional information regarding the surface electrical neurostimulation procedure can be found in Chapter 3.

5.2.3 Experiment Setup

Subjects were seated on a chair with both arms on a table in front of them (Figure 17). Their right forearm was thoroughly cleaned with a wet wipe and fitted with a distributed set of surface electrodes around their right wrist. The right forearm was placed on a support pad on the table with their hand's palmar surface parallel to the vertical plane. A computer screen was located in front of the subject at eye level. The screen displayed instructions, visual cues of the target levels and, in trials that used visual feedback, a visual indicator of performance. A custom 3-button keyboard and a control knob were placed on the table during the stimulation parameter fitting procedure (Figure 17). The keyboard was used to provide percept responses, while the knob was used to adjust various stimulation parameters at different stages of the stimulation fitting process. The knob was set to control stimulation parameter values within safe levels. The keyboard and knob were removed upon completion of the stimulation fitting process.

During the functional studies, a Leap Motion Controller (Ultraleap, Mountain View CA USA) was placed on the right side of the table, while a custom made proportional control joystick was placed on the left side (Figure 17). The Leap

Motion controller is an optical hand-tracking module that was used to capture the movements of the subject's hand during the virtual object classification studies. The joystick was used by the subject to reach different virtual grasp force target levels during the graded force control studies. Subjects were encouraged to drink water before and during the experiment to increase skin hydration. They were instructed to concentrate throughout the experiment but were encouraged to stretch and move their hand during periodic breaks to prevent discomfort. They were also asked about their comfort levels, or if additional breaks were needed after each task.

5.2.4   Stimulation Parameter Fitting

Pulse Amplitude (PA) thresholds were obtained from all subjects under five different Pulse Width (PW) values (300μs to 700μs, at 100μs intervals). The order of the pulse widths was randomized across all subjects. During the PA threshold determination procedure, subjects triggered the delivery of a pulse train with constant 5Hz Pulse Frequency (PF) by pressing the "Go" button on a keyboard, and then used a custom control knob to adjust the PA (from 0μA to 3000μA) to find the lowest possible level that evoked a percept. These responses were used to derive the strength-duration (SD) profile for each subject. The stimulation pulse amplitude used throughout this study was set to 50% above the percept threshold ($1.5 \times PA_{th}$) at a PW of 500μs.

Conveying a wide range of graded percept intensities was achieved by adjusting both PW and PF simultaneously, along their operating ranges (charge-rate

encoding). The lower and upper limits of these operating ranges were also determined through a similar subject-controlled calibration routine.

First, stimulation was delivered at a fixed PF of 100Hz while instructing the subjects to use the knob to explore a wide range of PW (from 100μs to 800μs) to find the lowest possible level that evoked a reliable percept, and the highest possible level that did not cause discomfort. Lastly, the stimulation PW was set to the midpoint of the recently obtained PW range, and the subjects were again instructed to use the knob to explore a wide range of PF (from 30Hz to 300Hz) to find the lowest possible frequency that was not perceived as pulsating (fusion), and the level at which the perceived stimulation intensity did not change (saturation). Once the range limits were obtained, the stimulation fitting was complete. A questionnaire was used to interrogate the perceived modality, quality and location of the evoked sensations along the fitted parameter range. Additional information regarding the stimulation parameter fitting procedure can be found in Chapter 4.

5.2.5 Virtual Object Classification Task

Virtual object classification tasks were completed to determine whether subjects were able to distinguish between different percept intensity profiles designed to emulate grasping forces during manipulation of various objects of different size and hardness. Six unique virtual profiles were created for this study (Table 3). These included all possible combinations of two size levels (small, large) and three hardness levels (soft, medium, hard).

Table 3. Virtual object profiles used during the classification tasks

Virtual Object	Uncompressed Size (mm)	Compressed Size (mm)
Small-Soft (SS)	40	12
Small-Medium (SM)	40	28
Small-Hard (SH)	40	38
Large-Soft (LS)	80	24
Large-Medium (LM)	80	56
Large-Hard (LH)	80	78

During these tasks, the subject's right hand and fingers were tracked in real time using a Leap Motion tracking module that was placed in front of them. A custom MATLAB algorithm was used to parse the hand tracking data from the Leap Motion software (Orion 3.2.1 SDK) and calculate the subject's hand aperture distance (linear distance between the thumb pad and the average horizontal position of the index, middle and ring finger pads; Figure 18A). The hand aperture data was used to determine whether the subjects were making contact with a virtual object of a preset size and hardness. If the hand aperture was equal or less than the virtual object's uncompressed size (Figure 18B), the algorithm estimated the amount of object compression and resulting grasping force. The full compressive range of the virtual object was linearly mapped to the full range of percept intensities. Hard objects were assigned a small compressive range to allow the stimulation to reduce the chances of a sharp increase in stimulation intensity.

Each virtual grasp trial began with the subject opening their right hand to an aperture of >10cm and placing it in front of the sensor. Once the hand was detected in place, they were asked to slowly close it until they began feeling the stimulation (i.e. the hand aperture matched the virtual object size). The subjects were

instructed to "squeeze" the virtual object and pay attention to how the perceived stimulation intensity was ramped up. For instance, squeezing a hard object would ramp up the perceived grasp force much faster than a more compressible, softer object. Subjects were encouraged to open and close their hand as many times as needed to determine the object size and hardness, within a period of 60 seconds. Subjects were instructed to report the perceived size and hardness of the virtual object. For example, if subjects perceived they were grasping a large object that felt soft, they would say "large and soft". Subjects were blindfolded to prevent any visual feedback of hand aperture.

The experiment started with a practice block in which all unique profiles were presented and identified to the subject twice. Each subject then completed 2 experimental blocks of 18 non-repeating, randomized virtual grasp trials (6 repetitions per profile), resulting in a total of 36 double-blinded presentations. Subjects were allowed to take as many breaks as they needed. For each trial, the subject's response was compared to the virtual object profile used. The frequency of correct responses (success rate) was used as the performance variable.

Statistical Analysis

One-sample t-tests were performed to determine if the success rate was significantly greater than chance. During virtual object classification, the chance of correctly identifying the object size or hardness alone was 50% and 33.3% respectively, while the chance of correctly identifying size and hardness together was 16.7%.

5.2.6 Graded Grasp Force Control Task

Tests for graded control of virtual grasp force outputs were conducted to evaluate the subject's ability to utilize the feedback delivered by the eSENS platform to control virtual grasp force outputs in a graded manner in the absence of visual feedback. Subjects used a proportional control joystick (Figure 19A) with their left hand to adjust the level of grasp force applied by an invisible virtual hand. Briefly, the position of the joystick (degree of deflection) was proportionally mapped to the rate of change of virtual grasp force. A randomized scaling factor was added to the proportional control map, resulting in subtle changes to the rate of change of force in each trial. The full range of grasp force outputs of the virtual hand was linearly mapped to the full range of intensities perceived by the subject on their right hand.

Subjects were presented a target value of the grasp force output of the virtual hand on a computer display (Figure 19B) and asked to match that target by adjusting the level of grasp force with the proportional control joystick; subjects verbally indicated acquisition of the target by saying "there". The display consisted of a white thermometer bar scaled to the full virtual force range. A moving bar provided absolute feedback of the grasp force level. The moving bar was not visible during the "no visual feedback" condition. A target zone box (target level ± 7%) was used to show a target value of 20, 40, 60, or 80%.

Each trial consisted of a series of target presentations over a range of 0 to 100% of the maximum percept intensity range. The sequence of target values in a given

trial was drawn from a set of pre-specified sequences that were varied across trials. Target sequences alternated between 0% and a non-zero level (20, 40, 60, or 80%). An experiment block consisted of 33 trials in which the target alternated between different levels presented randomly. A single experimental sequence started with a block of practice trials to familiarize the subject with the information provided in the experimental display while receiving visual and stimulation feedback together (STIM+VISION). The practice block was followed by two blocks of control trials for each condition without visual feedback: No Stimulation feedback (NO-STIM) and Stimulation feedback only (STIM) in which only the target zone box was shown. Periodic breaks were interspersed among the experiment blocks.

Data Processing

Data from these trials included the target level and continuous measurements of virtual grasp force levels. The value of the grasp force output achieved was determined as the average of the measured values obtained over the last 250 ms for each target (match level). Match error was set to zero when the match level was inside the target zone (target level ± 7%); otherwise, match error was calculated as the distance from the match level to the nearest target zone border. The time it took to reach each target level was also recorded. These data sets provided quantitative measures of the quality of control actions afforded by the feedback from the eSENS platform.

Statistical Analysis

To assess the impact of sensory feedback on the ability of the subject to control the virtual force outputs in a graded manner, a two-way repeated measures ANOVA with Bonferroni multiple pairwise post-hoc comparisons was used to assess the effects of stimulation and target value on performance ($p < .05$). Only data from 20, 40, 60, and 80% target level trials were considered in this analysis

5.3 Results

Four able-bodied subjects received transcutaneous stimulation from a neurostimulation platform enhanced by the novel CHIPS strategy. This approach evoked comfortable distally referred sensations of tingle, pressure and vibration in the general area innervated by the sensory fibers in the median nerve (palmar surface, index, middle, and part of the ring finger). All subjects selected the appropriate stimulation amplitude levels, and operating ranges for Q and PF with a subject-controlled calibration routine. Percept intensity was encoded by modulating charge-rate (QR) over an average range spanning from 1.17 ± 1.43μA to 139.62.97 ± 24.10μA. All surface electrodes had impedance values (mean ± SD) of around 27.34 ± 1.43 kΩ, which remained stable for all subjects throughout the study. No uncomfortable or local sensations, and no side effects like irritation or redness of the skin were observed in any of the able-bodied subjects.

5.3.1 Subjects Successfully Classified Virtual Objects by Their Size and Hardness with Feedback from eSENS

Subjects were able to integrate percept intensity information delivered by the neurostimulator as they grasped virtual objects (Figure 20A) in front of them to successfully determine their size and hardness, (Figure 20B). During an experimental session, each of six virtual object profiles was presented six times, for 36 double-blinded presentations. Subjects were able to differentiate between large and small objects much better than chance, with an average success rate (mean ± SD) of 98.61 ± 2.77%, $p < 0.0001$. Subjects successfully classified virtual objects by their hardness with success rates significantly greater than chance for large objects (70.83 ± 23.70%, $p < 0.001$) and small objects (54.17 ± 26.71%, $p = 0.019$). All subjects successfully classified both object size and hardness combined, with success rates significantly greater than chance (62.5 ± 17.84%, $p < 0.005$).

5.3.2 Subjects Demonstrated Graded Control of Virtual Grasp Force with Feedback from eSENS

Subjects were able to guide their control actions in a graded manner to reach virtual grasp force target levels with sensory feedback enabled (i.e. the STIM condition) in the absence of visual feedback (Figure 21). Error was set to zero when the match level was inside the target zone (± 7%); otherwise, error was calculated as the distance from the match level to the nearest target zone border. The match level (mean ± SD) was significantly lower with STIM (filled bars) than

NO-STIM (empty bars) for target levels of 20%, 40% and 60% ($F_{1,23}$= 29.59, p<0.0001, n=24 per target). Match levels were significantly different between adjacent target levels 40% and 60% with STIM (p=0.0029) and between adjacent target levels 20% and 40% with NO-STIM (p=0.0271). Shaded red boxes indicate the target zone for each target level (Figure 21B). The error (mean ± SD) was significantly lower with STIM than NO-STIM (8.66 ± 3.77% and 30.84 ± 15.03%, respectively; $F_{1,23}$= 41.21, p<0.0001, n=24 per target). More specifically, the error was lower with STIM for target levels of 20%, 40% and 60% (p<0.0001; Figure 21C). In average, subjects took significantly longer to attempt each target (Figure 21D) with STIM (5.63 ± 0.2 s) than with NO-STIM (2.26 ± 0.5 s), regardless of the target level ($F_{1,23}$= 89.18, p<0.0001, n=24 per target).

5.4 Discussion

This study sought to determine if able-bodied subjects could utilize feedback delivered by an enhanced surface electrical neurostimulation (eSENS) platform to successfully classify the perceived physical characteristics of virtual objects, and execute graded control of virtual grasp force outputs. Able-bodied subjects received transcutaneous stimulation from surface electrodes around the wrist. The stimulation performance was enhanced by the novel CHIPS strategy, and charge-rate intensity encoding. This resulted in comfortable distally referred sensations with a wide range of graded intensities, in the areas of the hand innervated by the median nerve afferents. The size and hardness of different virtual objects were encoded by changes in the intensity of the artificial percept during a grasping

112

action such that the object's full compressive range contained the full range of percept intensities. In a similar way, percept intensities were mapped to the full range of grasp forces from the virtual hand during graded control tasks. Subjects successfully recognized virtual objects by their size and hardness combined about 67% of the time, which was much better than chance. Subjects were also able to use the feedback information to reach different target levels without visual feedback with significantly lower errors than when the stimulation was turned off.

The information delivered by the neurostimulator, however limited, should be intuitive and not distracting to reduce cognitive loading. It should provide relevant feedback that would enable the user to make control decisions and reduce error, allowing for closed-loop control of their own actions or the actions of an external device such as a prosthetic limb, thus affording functional advantages of the user. While the virtual object classification task did not explicitly require the subject to perform graded control actions, the grasping action they performed while exploring the object's characteristics was guided by the feedback they received from the stimulator. At first, subjects were instructed to squeeze the object slowly to appreciate its perceived compliance and size. When exhausting the full compressive range of a soft or medium hardness object, subjects typically reversed course and began to open the hand (Figure 20A), suggesting that they perceived the object as fully compressed. Subjects were asked to squeeze the object multiple times without specifying a hand-closing speed. It is unclear whether hand-closing speed may play a role in classification performance. In addition, subjects often reported perceiving the virtual object as something between a

sphere and a cube that conformed to their hand. This could be because the stimulation only delivered information about the size and hardness based solely on hand aperture tracking. Therefore, no changes in object characteristics were perceived after wrist rotation or changing hand positions. Tracking the aperture of individual fingers as well as the hand position may allow for more complex virtual object manipulation information to be delivered by the neurostimulator. Finally, most subjects reported feeling confused at first by the lack of object resistance, especially for large-hard and large-medium objects. However, all of them reported that this feeling subsided during the classification tasks, suggesting that subjects were able to internalize the feedback as compression force.

Performance results from the graded control tasks suggest that feedback from the eSENS platform affords functional advantages to the subjects by providing relevant information to inform their control actions. As seen in Figure 21A, subjects used sensory feedback to correct their error when moving past the target. Because of this corrective action, subjects generally took significantly longer to complete control tasks in the presence of stimulation feedback, regardless of the target level. In contrast, absence of stimulation or visual feedback also meant that subjects did not receive error cues, thus reducing or preventing corrective actions, which in turn reduced task durations.

In the context of sensory feedback from prostheses, the evoked tactile information delivered by the eSENS platform could enable individuals with amputation to better control myoelectric prostheses and potentially promote user acceptance and

embodiment of the prosthetic device, as long as no stimulation-induced motor activation or artifact affects the performance of the myoelectric control system. In addition to the previously mentioned prosthetics applications, the feedback delivered by the eSENS platform may also be used to provide haptic information for many teleoperation applications, and other situations in which the user could benefit from feedback about manipulation and interactions within virtual, augmented, and real environments.

Teleoperation of mobile robots has been widely used to perform remote surgical procedures, explore constricted or dangerous environments, transport and dispose dangerous substances, and carry out firefighting and rescue missions. Some military and police applications include advanced unmanned aerial and terrestrial vehicles, and robotics for explosive device disposal, minimizing risk to personnel (Kot and Novak, 2018). Immersive virtual and augmented reality technologies allow users to interact with virtual environments and even other individuals. This expanding field has had a large influence within the gaming industry, has been widely used for development of surgical training protocols, data visualization and manipulation in scientific research, and for expanding the options of social interaction within virtual worlds. A desired feature of teleoperation systems and virtual or augmented reality environments is interaction transparency. This is when users cannot distinguish between operating in a local or real environment, and a distant or virtual environment. A critical component of transparency is the provision of the necessary sensory feedback, including visual, auditory and haptic cues (Preusche and Hirzinger, 2007). Teleoperators typically

control the remote devices out of direct sight, relying on data from sensors and cameras. This requires a complex combination of the operator's cognitive, perceptual, and motor skills (Lathan and Tracey, 2002). The lack of intuitive feedback from these devices can limit the operator's ability to perform complicated manipulation tasks, especially when trying to complex components such as a manipulator arm with many degrees of freedom. Traditional mechanical haptic feedback interfaces for teleoperation or virtual interaction purposes are limited by the hardware design (Giachritsis et al., 2009). The size and weight of these devices can be restrictive and could have an effect on feedback perception. This problem can be exacerbated when multiple devices are coupled together to increase the amount of haptic information conveyed to the user.

The eSENS platform has the potential to provide more intuitive haptic feedback without the restrictive design of traditional wearable mechanical feedback systems. The evoked sensations can be used to replicate real-world interaction forces in order to enhance virtual object manipulation tasks and improve operation of remote-controlled devices. Additionally, this feedback can be used to provide information that is not available in the physical world, such as force limit indicators that serve as training cues to enhance force skill learning during precise telesurgery tasks and surgical simulations (Morris et al., 2007).

The information delivered by the feedback system could be further expanded by implementing multi-channel stimulation schemes where multiple electrode pairs targeting different parts of the nerve, evoke percepts in different areas of the hand.

116

These enhanced percepts could be used to replicate complex interactions with different types of objects and provide more realistic object manipulation cues that go beyond size and hardness, including object shape, weight and texture, as well as event cues such as object slippage or breakage, thus enabling users to execute virtual or remote manipulation tasks with high precision.

5.4.1 Limitations

Prior to this work, we evaluated various vibrotactile sensory substitution approaches as potential options for delivering task-related feedback (Pena et al., 2019). Although sensory information delivered by these approaches could be distinguished during simple discrimination tasks, they performed poorly during functional tasks such as graded control of the force output from a myoelectric prosthetic hand, as they seem to require extensive learning and remapping. It was also evident that myoelectric control of grasp force outputs was a rather difficult task, even for experienced myoelectric users (Williams, 2011, Carey et al., 2015, Cordella et al., 2016). The high demands imposed by a difficult control scheme seems to mask the potential benefits provided by an already unintuitive sensory feedback approach. Based on these experiences, this work adopted surface electrical stimulation to deliver task-related sensory feedback, as it is capable of evoking more intuitive somatotopically-matched percepts. However, in contrast with previous studies, this work did not utilize a myoelectric prosthetic hand to assess closed-loop control performance. Instead, a proportional control joystick was used to mitigate for potential masking effects of myoelectric limb control expertise in closed-loop control performance. In addition, the hand used to control

117

the joystick was contralateral to the stimulation, as to avoid motion of the stimulated wrist. Future studies should investigate closed-loop control performance with a myoelectric hand, ipsilateral to the stimulation.

Another limitation of the graded control experiments in this study was that the direction of target approach was not controlled. That is, subjects were allowed to oscillate around the target until they sensed they had reached it using the feedback from the eSENS platform. This precluded analysis of the effect of approach direction on performance. This also meant that the tasks completed by the subjects were not representative of typical daily life activities, where reaching force targets with one attempt is often required. Future studies could use a single attempt method in which subjects are instructed to approach the target from one direction and stop once they feel they have reached it.

This work presents the first assessment of the eSENS platform as a method to deliver intuitive haptic feedback during functional tasks. While additional studies are required to investigate whether additional sensory channels can be added (e.g. delivering proprioceptive feedback to the ulnar nerve), these functional studies demonstrated that the artificial sensory feedback delivered by the eSENS platform may help improve the functionality of prosthetic limbs, enhance teleoperation performance and enable individuals to execute virtual or remote manipulation tasks with high precision without relying solely on visual or auditory cues.

A Stimulation Fitting Setup

B Functional Task Setup
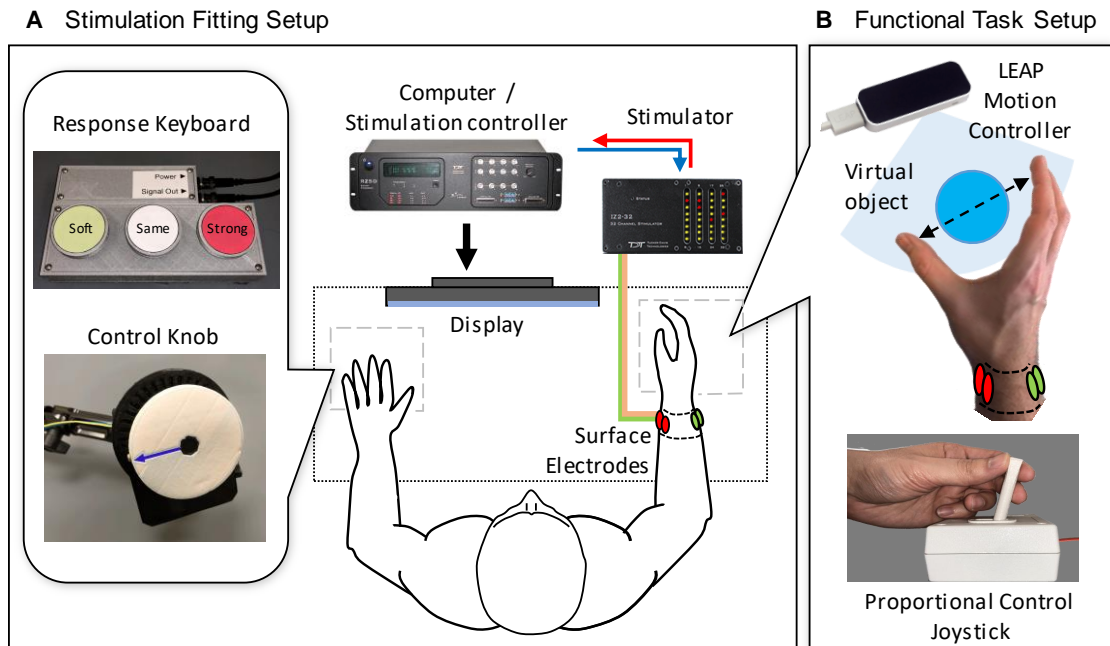
Figure 17. Experimental setup for stimulation fitting and functional tasks. Subjects were seated on a chair and fitted with the surface stimulation platform using the CHIPS strategy. A screen in front of the subject displayed visual cues and feedback signals. (A) A custom 3-button keyboard and a control knob were placed on the table during the stimulation parameter fitting procedure only. (B) During the functional studies, a hand aperture tracking device (LEAP Motion Controller) was placed on the right side of the table, while a custom-made proportional control joystick was placed on the left side.
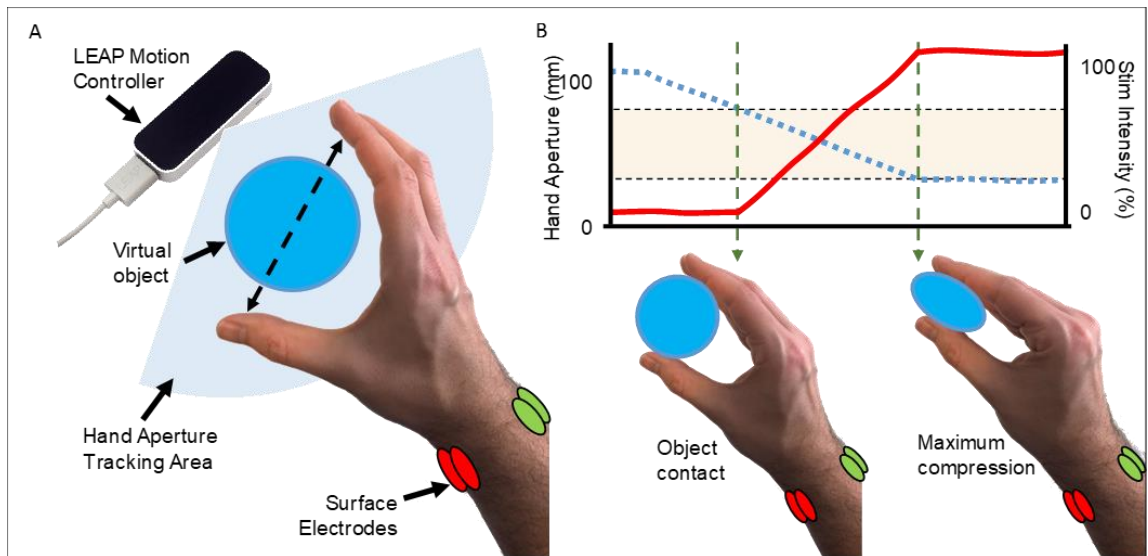
Figure 18. Hand aperture tracking during virtual object classification tasks.
(A) A Leap Motion Controller tracked the subject's hand aperture distance, which was the linear distance between the thumb pad and the average horizontal position of the index, middle and ring finger pads (denoted by the dashed line). (B) The hand aperture data (top; dotted trace) was used to determine object contact (bottom left) and compression (bottom right), and to estimate the resulting grasping force (top; solid trace). The full compressive range of the virtual object (top; shaded region) was linearly mapped to the full range of percept intensities.
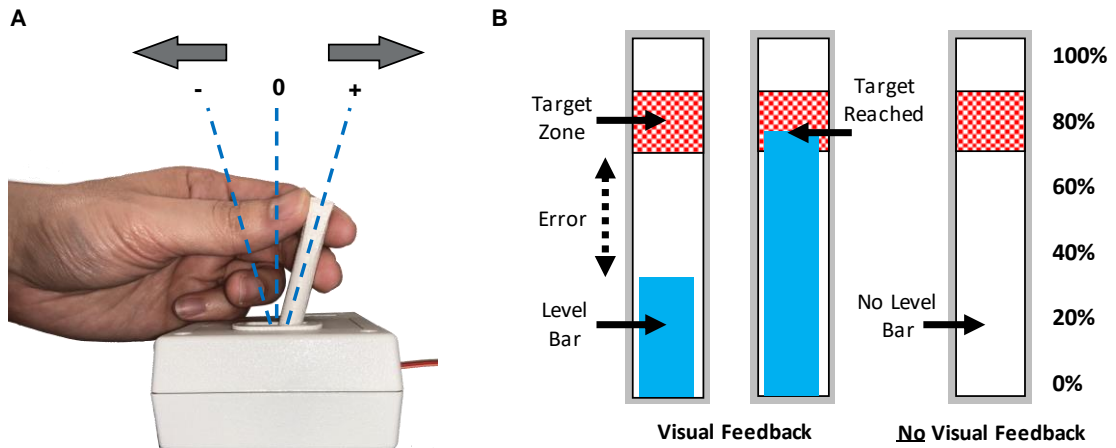
Figure 19. Control of virtual grasp force levels during graded control tasks.
(A) The proportional control joystick used by the subjects to increase (+) or decrease (-) virtual grasp force levels. The rate of change of force was proportional to the degree of deflection of the joystick. (B) Computer display consisting of a "thermometer" with a moving level bar (for visual feedback only), and a ± 7% target zone centered at one of 6 different target levels.
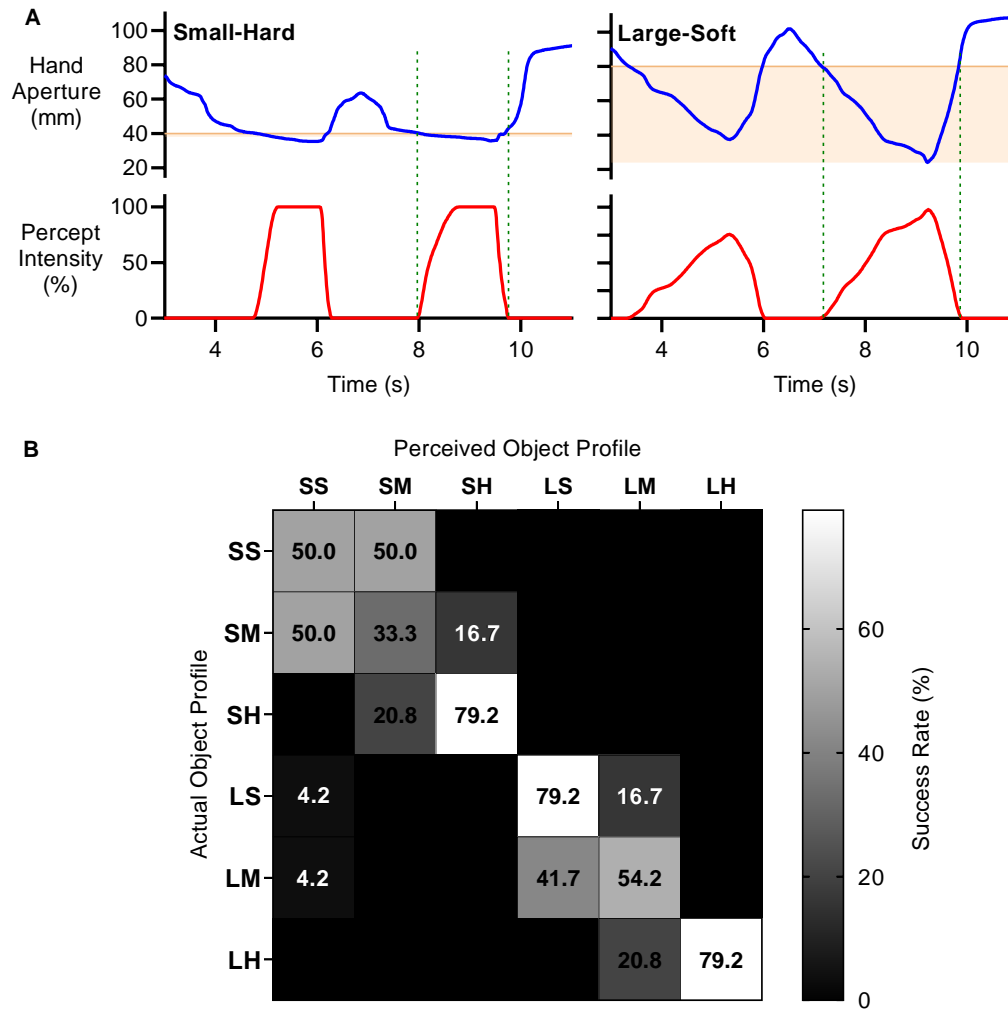
Figure 20. Feedback of grasp force profiles enables identification of virtual object size and hardness in able-bodied subjects. (A) Example of hand aperture (solid blue) and virtual grasp force profile (dashed red) traces recorded from one subject when grasping a small, hard object (left) and a large, soft object (right). The shaded region highlights the object's compressive range. The dashed green vertical lines represent the object contact and release times. (B) Confusion matrices quantifying the perceived size and hardness combined (left-right), in relation with the ground truth (up-down). The average success rate was calculated across all subjects based on 6 virtual object profiles presented to each subject 6 times, for a total of 36 object presentations. SS=Small-Soft; SM=Small-Medium; SH=Small-Hard; LS=Large-Soft; LM=Large-Medium; LH=Large-Hard.
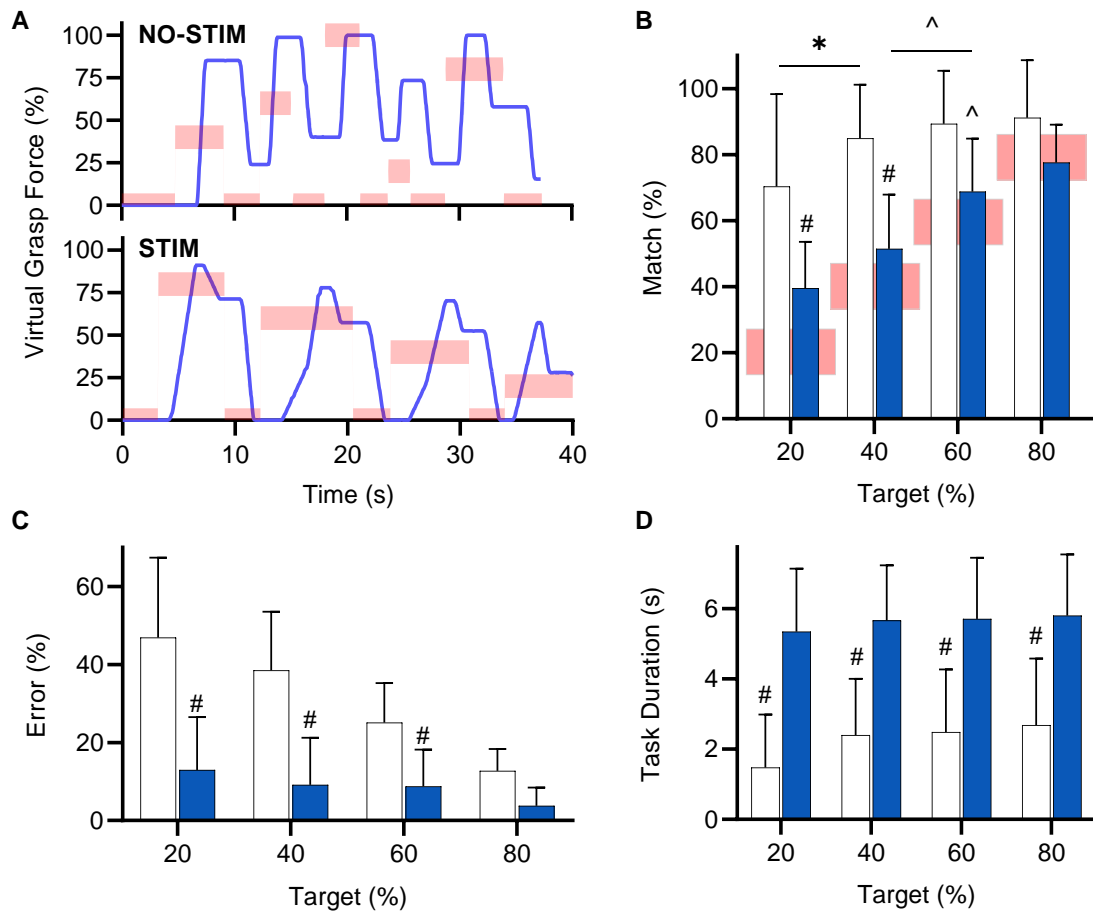
Figure 21. Stimulation improves the ability to achieve target levels of virtual grasp force. (A) Examples of graded control trials showing how one subject attempted to match a series of target levels during the NO-STIM (top) and STIM (bottom) feedback conditions. The solid blue trace indicates the match level over time. The shaded red boxes indicate the target zone sequences for those specific trials. (B) Match level (mean ± SD) was significantly lower with STIM (blue/filled bars) than NO-STIM (empty bars) for target levels of 20%, 40% and 60%; and significantly different between adjacent target levels 40% and 60% with STIM and between adjacent target levels 20% and 40% with NO-STIM. Shaded red boxes indicate the target zone for each target level. (C) Error (mean ± SD) was significantly lower with STIM for target levels of 20%, 40% and 60%. (D) Task durations were significantly longer with STIM than with NO-STIM, regardless of the target level. Comparisons in panels B-D used two-way repeated measures ANOVA with Bonferroni multiple pairwise post-hoc comparisons (*p<0·05, ^ p<0·01, # p<0·001).

CHAPTER 6

CONCLUSIONS AND FUTURE WORK

6.1 Summary

An enhanced surface electrical neurostimulation (eSENS) platform has been developed and evaluated to address the need for a non-invasive approach capable of selectively eliciting comfortable distally referred tactile percepts, with a wide range of graded intensities that are meaningful and could serve as an intuitive somatotopically-matched sensory feedback platform during functional tasks. The platform utilizes a novel Channel-hopping Interleaved Pulse Scheduling (CHIPS) strategy that leverages the combined influence of short, sub-threshold interleaved current pulses to deliver supra-threshold stimulation levels within the tissue, thus eliciting enhanced tactile percepts while avoiding the discomfort associated with localized charge densities. A set of "User-in-the-loop" (UiTL) calibration routines were developed to streamline the stimulation parameter fitting process. A bio-inspired charge-rate encoding strategy was implemented to enhance the range and gradation of percept intensities evoked by the stimulation. Together, these strategies help enhance the stimulation comfort, selectivity, and percept modulation capabilities of the platform, enabling it to provide more intuitive haptic feedback without limitations of sensory substitution feedback systems and traditional transcutaneous stimulation approaches.

These enhanced stimulation-evoked percepts can be used to simulate real-world interaction cues during virtual object manipulation tasks, providing realistic feedback that may enable users to execute virtual tasks with high precision and improve teleoperation of robotic devices. Implementation of multi-channel stimulation schemes could allow for the expansion of tactile information by evoking percepts in different areas of the hand to replicate complex interactions with different types of objects.

The CHIPS strategy was assessed computationally and experimentally. A computational model of human median nerve afferents within the wrist was used to develop and characterize the novel pulse-scheduling scheme before implementation within the stimulation platform. Able-bodied human studies were performed to evaluate the performance of this strategy, and compare it with traditional methods. The encoding strategy and UiTL calibration routines were evaluated during psychophysical studies with surface stimulation in able-bodied subjects and intrafascicular stimulation in an individual with a transradial amputation. Finally, a series of functional studies with able-bodied subjects evaluated the functional benefits afforded by the enhanced feedback on their ability to determine the size and hardness of virtual objects, and perform graded control of virtual grasp force without visual feedback. These studies showed that the eSENS platform is capable of delivering a wide range of comfortable and graded referred percepts that can be utilized to complete precise functional tasks.

6.2 Conclusions

The following conclusions on the performance and abilities of the enhanced surface electrical neurostimulation platform can be drawn based on the results presented in the previous chapters.

- *The channel-hopping interleaved pulse scheduling strategy was able to elicit enhanced tactile percepts while avoiding the distracting sensations and discomfort associated with localized charge densities.* Able-bodied subjects received electrical stimulation from a distributed set of surface electrodes around their right wrist, evoking distally referred sensations in the general area of the hand innervated by the sensory fibers in the median nerve. The combined influence of the shorter, sub-threshold pulses interleaved across two independent channels resulted in percept thresholds that were within the range of thresholds found with larger pulses under traditional single-channel stimulation. This enables the use of smaller electrodes to increase selectivity while avoiding the larger charge densities associated with them. This effect was reduced after introduction of large delays between interleaved pulses, as they seemed to attenuate the influence of the leading pulse on the fiber membrane at the time of arrival of the trailing pulse. This pulse scheduling strategy addresses some of the primary issues hindering traditional surface stimulation methods. Implementation of this strategy within an array of spatially distributed electrodes may allow for improved stimulation fitting and targeting. The ability to deliver enhanced tactile percepts enables the use of this platform

to study the neural mechanisms of natural touch, explore multiple neuromodulation strategies for conveying intuitive and discriminable percepts, and potentially deliver stimulation therapies to treat various pain conditions.

- *Implementation of a charge-rate encoding strategy within the eSENS platform resulted in fine intensity discrimination and a wider dynamic range of percept intensities than frequency modulation alone.* Modulation of charge-rate was accomplished by adjusting pulse charge and pulse frequency simultaneously, along their operating ranges. These ranges were obtained through a subject-controlled calibration routine that was developed to simplify the exploration of the parameter-space. This charge-rate mapping scheme was found to be a strong predictor for graded intensity perception during both transcutaneous and intrafascicular neurostimulation. Its implementation within the stimulation platform seems to be capable of influencing fiber population recruitment as well as the firing rate within the recruited fiber population, with psychophysical outcomes comparable to implanted neural interfaces. This suggests that the eSENS platform has the potential to serve as a testbed for studying neural code and developing neuromodulation strategies for intuitive sensory feedback in able-bodied subjects before deployment in implantable systems. Importantly, this encoding strategy could be used to enhance the intensity mapping of functional information such as the grasping force of a prosthetic hand.

- *The tactile percepts delivered by the eSENS platform, with the implementation of the CHIPS strategy and charge-rate encoding, could be readily utilized by able-bodied subjects to complete functional tasks without the need for visual feedback.* The performance of the stimulation platform was enhanced by the novel CHIPS strategy, and charge-rate intensity encoding was used to convey task-related information that allowed able-bodied subjects to successfully recognize virtual objects by their size and hardness, and to reach different virtual grasp force target levels without visual feedback. Feedback from this platform may help improve the functionality of prosthetic limbs, enhance teleoperation performance and enable individuals to execute virtual or remote manipulation tasks with high precision without relying solely on visual or auditory cues.

The channel-hopping interleaved pulse scheduling strategy proved to be a viable approach to deliver current pulses transcutaneously to selectively stimulate sensory fibers within the median nerve, while avoiding the more superficial tactile afferents located under the electrodes. When two independent current sources are arranged in an interfering configuration, the sequential, interleaved delivery of a short pulse from each source would result in the summation of the individual pulse durations. In other words, the interference region would experience the effects of a single, longer stimulation pulse capable of activating nearby fibers. The distribution of current within the tissue depends on the stimulation amplitude, electrode dimensions and tissue properties, among other factors. This distribution can be shaped by enabling additional electrodes within a single current source

(virtually changing the surface area) and modulating the current amplitude to adjust the location of the interference region. This enables the stimulation strategy to steer the percept area. It is possible that the CHIPS strategy could be also applied with extraneural interfaces such as cuff electrodes used for sensory stimulation and functional neuromuscular stimulation. The fascicular structure of the nerve and the insulating properties of its connective tissue are known to impair the ability of cuff electrodes to selectively stimulate small populations of fibers, albeit to a much lesser degree than surface stimulation. Some have attempted to overcome this limitation by reshaping the nerve, increasing the number of electrodes, or by selecting specific electrodes to shape the electric field (Schiefer et al., 2005). The performance of the latter approach could be further enhanced by implementing the CHIPS strategy not only to avoid activating fibers closer to the electrode contacts, but also to reduce localized charge densities that could cause tissue damage and electrode degradation.

Implementation of this enhanced surface neurostimulation platform shows that it is possible to artificially influence the intensity code transcutaneously with psychophysical responses comparable to more invasive methods. The charge-rate relationship was leveraged to enable fast and accurate stimulation parameter fitting with minimal intervention from the experimenter. The platform utilized an interactive program that collected the subject's responses at different stages of the fitting process, generating a subject-specific stimulation profile that was later used during functional tasks. The subject only provided responses for percept threshold, and the lower and upper bounds for pulse charge and frequency. This reduced the

duration of the fitting process significantly, compared to classic iterative psychophysical methods used during development stages.

The development of an enhanced surface stimulation platform with these capabilities is significant in that it may allow for wide adoption of surface neurostimulation for chronic restoration of sensory function in individuals with amputation, and could serve as a testbed to study the neural mechanisms of natural touch and develop advanced neuromodulation strategies in able-bodied subjects before deployment in implantable systems. The enhanced features of this neurostimulation platform may also allow for its implementation beyond prosthetics applications. For instance, the stimulation-evoked percepts from the eSENS platform could serve as haptic feedback for teleoperation of complex surgical robotic devices, as well as remote control of unmanned aerial and terrestrial vehicles designed to minimize risk to civilian and military personnel during unsafe activities from emergency rescue and firefighting missions, to transport and disposal of explosives or dangerous substances. The eSENS platform could also be used to provide more realistic and intuitive feedback during manipulation and interactions within virtual, augmented, and real environments. These include haptic feedback for gaming, surgical procedure training, physical and neurological rehabilitation and social interactions within virtual worlds without the cumbersome restrictions of traditional haptic hardware. Additionally, it may be possible to expand the capabilities of this platform to deliver targeted neuromodulation therapies for peripheral neuropathies, including neuropathic pain and sensory deficits secondary to intermediate carpal tunnel syndrome injury.

6.3 Limitations

While the performance of the eSENS platform seems promising, all the strategies presented in this work were developed and tested around the peripheral nerves of able-bodied subjects at the wrist level. This location provides a flexible, yet stable setting for exploring the feasibility of the pulse scheduling strategy since the median nerve can be found approximately 1 cm under the skin of the volar wrist. This allows access to mostly afferent fibers that innervate the radial aspect of the palm, and the tips of the thumb, index and middle fingers, while avoiding most of the motor fibers within the median nerve. These strategies may be readily implemented to restore sensory function to individuals with distal transradial amputation or wrist disarticulation, given that the residual nerves are still accessible. However, it is unclear whether these strategies could be translated to other individuals with amputations at other levels. It may be possible to implement these strategies within an array of electrodes distributed around the upper arm, targeting the nerves along the medial side, beneath the short head of the biceps brachii. While stimulation near the elbow is more difficult in able-bodied subjects as it can cause muscle activation, individuals with elbow disarticulation and above-elbow amputations would not necessarily experience these. Furthermore, patients undergoing pre-planned amputation could elect to have nerve relocation procedures to make the median and ulnar nerves more accessible via surface electrodes.

This work did not directly evaluate how different wrist positions affected the stimulation performance. Evidence from previous studies with transcutaneous

stimulation (D'Anna et al., 2017, Shin et al., 2018) show some degree of position dependency, where percept intensity, modality or location is affected by limb posture, e.g. intensity decreases with shoulder adduction, which could impact the usefulness of the feedback signal. Delivering focal stimulation with the CHIPS strategy could potentially exacerbate position dependency as the stimulation would be focused on smaller areas of the nerve. Therefore, the percept areas on the hand would be more likely to change due to nerve motion. However, anecdotal evidence during the evaluation of the CHIPS strategy suggests that percept intensity and location was less susceptible to wrist flexion and extension than with traditional single-channel stimulation. Moreover, subjects reported stable percepts during the virtual object grasping tasks, which required some degree of wrist and finger motion when performing the task. Nonetheless, future studies should be performed to systematically evaluate the evoked percepts at different wrist and elbow positions and under different stimulation conditions in order to assess whether further improvements are needed before this approach could be readily used in real-world environments. A potential mitigating action for motion dependency would be to implement multi-site stimulation with redundant electrodes to target neighboring nerve areas to reduce motion dependency.

Another limitation of the work presented here was that only one sensory channel (i.e. median nerve) was explored. Technical limitations of the stimulator used in this study prevented the implementation of the CHIPS strategy to target two nerves simultaneously. Being able to deliver simultaneous stimulation to both median and ulnar nerves could potentially allow for two or more distinctive streams of

information to be delivered simultaneously, encoding different feedback modalities such as vibration, pressure, touch, slippage, and proprioception, allowing users to better discern information about object size and stiffness, and facilitating the closed loop control required for fine grasping tasks. This could be addressed with a stimulator capable of controlling at least two pairs of independent sources with independent stimulation parameters, with the caveat that channels targeting different nerves might temporally interfere if placed too close to each other.

6.4 Future work

The work presented here aimed to develop and implement an enhanced surface electrical neurostimulation platform capable of selectively eliciting comfortable distally referred tactile percepts, with a wide range of graded intensities that are meaningful, and could be readily utilized to complete functional tasks. The eventual goal of this work was to deliver a neurostimulation platform that is robust enough to serve as a testbed for advanced neurotechnologies, and for chronic therapies and restoration of sensory function secondary to nerve damage or amputation. Assessing the performance of the stimulation strategies on percept enhancement functional benefits provided some evidence of the potential to achieve this goal. It also elucidated some of the limitations that must be addressed before a robust platform is possible.

The targeting performance of the CHIPS strategy could be improved by delivering the stimulation from an electrode array in which subsets of electrodes are selected to optimize the stimulation effectiveness and comfort (Shin et al., 2018).

Computational modeling could be used to estimate the potential distribution resulting from different electrode arrangements (Kuhn et al., 2009, Goffredo et al., 2014, Gaines et al., 2018) as well as amplitudes and timing of each stimulation pulse to optimize the location of the stimuli summation region (Cao and Grover, 2017, Grossman et al., 2017). The user-controlled calibration routines could be used for sequential exploration of sensory responses from multiple combinations of stimulating electrodes within the array. These responses, combined with results from computational models could be used to optimize the active electrode selection, predict the most likely location of the target nerve within the treatment area, and create user-specific stimulation profiles.

The stimulation patterns capable of producing natural percepts are not well documented in the literature. Producing natural patterns of activation may require the ability to provide localized stimulation in an asynchronous manner. Further enhancement of the surface electrical neurostimulation platform could include the implementation of more complex stimulation patterns that could help avoid the unnatural percepts thought to be caused by synchronous activation within a population of different fibers (Ochoa and Torebjörk, 1980, Mogyoros et al., 2000), thus evoking more natural sensations similar to what was recently demonstrated with intraneural stimulation in amputees (Tan et al., 2014). Future work could evaluate different patterning strategies, from sinusoidal or pseudorandom jitter to more advanced neuromorphic models that mimic healthy receptor behavior (Saal and Bensmaia, 2015) to generate time-variant patterns for modulating both charge and frequency.

6.5 Final remarks

In conclusion, an enhanced surface electrical neurostimulation platform to deliver comfortable and intuitive sensory feedback was developed and evaluated in a series of psychophysical and functional studies in able-bodied subjects. The novel channel-hopping interleaved pulse scheduling strategy was able to evoke enhanced percepts while avoiding the discomfort associated with localized charge densities. Implementation of the charge-rate encoding strategy resulted in enhanced range and gradation of percept intensities and a streamlined stimulation fitting process. Finally, feedback delivered by this enhanced surface electrical neurostimulation platform could be readily utilized to complete functional tasks. Extensive work is still required prior to implementation of this platform for chronic neuromodulation therapies and restoration of sensory function after nerve damage or amputation. However, the work presented here serves as an important step towards use of this enhanced neurostimulation platform, its novel strategies, and experimental methods to benefit neuroscience research beyond clinical applications and further our understanding of the sensory neural code and the nervous system at large.

REFERENCES

ANANI, A. B., IKEDA, K. & KORNER, L. M. 1977. Human Ability to Discriminate Various Parameters in Afferent Electrical Nerve-Stimulation with Particular Reference to Prostheses Sensory Feedback. *Med Biol Eng Comput,* 15**,** 363-373.

ANDERSON, D. N., DUFFLEY, G., VORWERK, J., DORVAL, A. D. & BUTSON, C. R. 2019. Anodic stimulation misunderstood: preferential activation of fiber orientations with anodic waveforms in deep brain stimulation. *Journal of Neural Engineering,* 16**,** 016026.

ANTFOLK, C., D'ALONZO, M., ROSEN, B., LUNDBORG, G., SEBELIUS, F. & CIPRIANI, C. 2013. Sensory feedback in upper limb prosthetics. *Expert Rev Med Devices,* 10**,** 45-54.

BANKS, W. P. & COLEMAN, M. J. 1981. Two subjective scales of number. *Percept Psychophys,* 29**,** 95-105.

BEHRENS, B. J. 2006. *Physical agents theory and practice: laboratory manual,* Philadelphia, F.A. Davis.

BIDDISS, E., BEATON, D. & CHAU, T. 2007. Consumer design priorities for upper limb prosthetics. *Disabil Rehabil Assist Technol,* 2**,** 346-57.

BIDDISS, E. A. & CHAU, T. T. 2007a. Upper limb prosthesis use and abandonment: a survey of the last 25 years. *Prosthet Orthot Int,* 31**,** 236-57.

BIDDISS, E. A. & CHAU, T. T. 2007b. Upper limb prosthesis use and abandonment: A survey of the last 25 years. *Prosthetics and Orthotics International,* 31**,** 236-257.

BRUNTON, E. K., SILVEIRA, C., ROSENBERG, J., SCHIEFER, M. A., RIDDELL, J. & NAZARPOUR, K. 2019. Temporal Modulation of the Response of Sensory Fibers to Paired-Pulse Stimulation. *IEEE Transactions on Neural Systems and Rehabilitation Engineering,* 27**,** 1676-1683.

CALDWELL, D. J., CRONIN, J. A., WU, J., WEAVER, K. E., KO, A. L., RAO, R. P. N. & OJEMANN, J. G. 2019. Direct stimulation of somatosensory cortex results in slower reaction times compared to peripheral touch in humans. *Sci Rep,* 9**,** 3292.

CAO, J. & GROVER, P. 2017. STIMULUS: Noninvasive Dynamic Patterns of Neurostimulation using Spatio-Temporal Interference. *bioRxiv*.

CAREY, S. L., LURA, D. J., HIGHSMITH, M. J., CP & FAAOP 2015. Differences in myoelectric and body-powered upper-limb prostheses: Systematic literature review. *J Rehabil Res Dev,* 52**,** 247-62.

CAUNA, N. 1956. Nerve supply and nerve endings in Meissner's corpuscles. *American Journal of Anatomy,* 99**,** 315-350.

CHARKHKAR, H., SHELL, C. E., MARASCO, P. D., PINAULT, G. J., TYLER, D. J. & TRIOLO, R. J. 2018. High-density peripheral nerve cuffs restore natural sensation to individuals with lower-limb amputations. *Journal of Neural Engineering,* 15.

CLEMENTE, F., VALLE, G., CONTROZZI, M., STRAUSS, I., IBERITE, F., STIEGLITZ, T., GRANATA, G., ROSSINI, P. M., PETRINI, F. & MICERA, S. 2019. Intraneural sensory feedback restores grip force control and motor coordination while using a prosthetic hand. *Journal of Neural Engineering,* 16**,** 026034.

COLELLA, N., BIANCHI, M., GRIOLI, G., BICCHI, A. & CATALANO, M. G. 2019. A Novel Skin-Stretch Haptic Device for Intuitive Control of Robotic Prostheses and Avatars. *Ieee Robotics and Automation Letters,* 4**,** 1572-1579.

CORDELLA, F., CIANCIO, A. L., SACCHETTI, R., DAVALLI, A., CUTTI, A. G., GUGLIELMELLI, E. & ZOLLO, L. 2016. Literature review on needs of upper limb prosthesis users. *Front Neurosci,* 10**,** 209.

CORNSWEET, T. N. 1962. The Staircase-Method in Psychophysics. *Am J Psychol,* 75**,** 485-491.

CRUCCU, G., AMINOFF, M. J., CURIO, G., GUERIT, J. M., KAKIGI, R., MAUGUIERE, F., ROSSINI, P. M., TREEDE, R. D. & GARCIA-LARREA, L. 2008. Recommendations for the clinical use of somatosensory-evoked potentials. *Clinical Neurophysiology,* 119**,** 1705-1719.

D'ALONZO, M., CLEMENTE, F. & CIPRIANI, C. 2015. Vibrotactile stimulation promotes embodiment of an alien hand in amputees with phantom sensations. *IEEE Trans Neural Syst Rehabil Eng,* 23**,** 450-7.

D'ANNA, E., PETRINI, F. M., ARTONI, F., POPOVIC, I., SIMANIC, I., RASPOPOVIC, S. & MICERA, S. 2017. A somatotopic bidirectional hand prosthesis with transcutaneous electrical nerve stimulation based sensory feedback. *Sci Rep,* 7.

DAVIS, T. S., WARK, H. A., HUTCHINSON, D. T., WARREN, D. J., O'NEILL, K., SCHEINBLUM, T., CLARK, G. A., NORMANN, R. A. & GREGER, B. 2016. Restoring motor control and sensory feedback in people with upper extremity amputations using arrays of 96 microelectrodes implanted in the median and ulnar nerves. *J Neural Eng,* 13**,** 036001.

DHILLON, G. S. & HORCH, K. W. 2005. Direct neural sensory feedback and control of a prosthetic arm. *IEEE Trans Neural Syst Rehabil Eng,* 13**,** 468-472.

DHILLON, G. S., KRUGER, T. B., SANDHU, J. S. & HORCH, K. W. 2005. Effects of short-term training on sensory and motor function in severed nerves of long-term human amputees. *J Neurophysiol,* 93**,** 2625-33.

DORGAN, S. J. & REILLY, R. B. 1999. A model for human skin impedance during surface functional neuromuscular stimulation. *IEEE Transactions on Rehabilitation Engineering,* 7**,** 341-348.

ELDABE, S., BUCHSER, E. & DUARTE, R. V. 2015. Complications of Spinal Cord Stimulation and Peripheral Nerve Stimulation Techniques: A Review of the Literature. *Pain Med,* 17**,** 325-336.

FIX, J. D. 1995. *Neuroanatomy*, Williams & Wilkins.

FLESHER, S. N., COLLINGER, J. L., FOLDES, S. T., WEISS, J. M., DOWNEY, J. E., TYLER-KABARA, E. C., BENSMAIA, S. J., SCHWARTZ, A. B., BONINGER, M. L. & GAUNT, R. A. 2016. Intracortical microstimulation of human somatosensory cortex. *Sci Transl Med,* 8**,** 361ra141-361ra141.

FORST, J. C., BLOK, D. C., SLOPSEMA, J. P., BOSS, J. M., HEYBOER, L. A., TOBIAS, C. M. & POLASEK, K. H. 2015. Surface electrical stimulation to evoke referred sensation. *J Rehabil Res Dev,* 52**,** 397-406.

FRANCESCHI, M., SEMINARA, L., DOSEN, S., STRBAC, M., VALLE, M. & FARINA, D. 2017. A System for Electrotactile Feedback Using Electronic Skin and Flexible Matrix Electrodes: Experimental Evaluation. *IEEE Trans Haptics,* 10**,** 162-172.

GABRIEL, C. 1996. Compilation of the dielectric properties of body tissues at RF and microwave frequencies. King's coll london (United Kingdom) dept of physics.

GAINES, J. L., FINN, K. E., SLOPSEMA, J. P., HEYBOER, L. A. & POLASEK, K. H. 2018. A model of motor and sensory axon activation in the median nerve using surface electrical stimulation. *Journal of computational neuroscience,* 45**,** 29-43.

GENG, B., DONG, J., JENSEN, W., DOSEN, S., FARINA, D. & KAMAVUAKO, E. 2018. *Psychophysical Evaluation of Subdermal Electrical Stimulation in Relation to Prosthesis Sensory Feedback*.

GENG, B., YOSHIDA, K., GUIRAUD, D., ANDREU, D., DIVOUX, J.-L. & JENSEN, W. 2019. Computerized "Psychophysical Testing Platform" to Control and Evaluate Multichannel Electrical Stimulation-Based Sensory Feedback. *Direct Nerve Stimulation for Induction of Sensation and Treatment of Phantom Limb Pain.* River Publishers.

GENG, B., YOSHIDA, K. & JENSEN, W. 2011. Impacts of selected stimulation patterns on the perception threshold in electrocutaneous stimulation. *J Neuroeng Rehabil,* 8**,** 9.

GEORGE, J. A., BRINTON, M. R., COLGAN, P. C., COLVIN, G. K., BENSMAIA, S. J. & CLARK, G. A. 2020. Intensity Discriminability of Electrocutaneous and Intraneural Stimulation Pulse Frequency in Intact Individuals and Amputees. *arXiv preprint arXiv:2001.08808*.

GIACHRITSIS, C., BARRIO, J., FERRE, M., WING, A., ORTEGO, J. & IEEE 2009. *Evaluation of Weight Perception During Unimanual and Bimanual Manipulation of Virtual Objects,* New York, Ieee.

GODLOVE, J. M., WHAITE, E. O. & BATISTA, A. P. 2014. Comparing temporal aspects of visual, tactile, and microstimulation feedback for motor control. *J Neural Eng,* 11**,** 046025.

GOFFREDO, M., SCHMID, M., CONFORTO, S., BILOTTI, F., PALMA, C., VEGNI, L. & D'ALESSIO, T. 2014. A two-step model to optimise transcutaneous electrical stimulation of the human upper arm. *Compel-the International Journal for Computation and Mathematics in Electrical and Electronic Engineering,* 33**,** 1329-1345.

GOODWIN, A. W. & WHEAT, H. E. 2004. Sensory signals in neural populations underlying tactile perception and manipulation. *Annu. Rev. Neurosci.,* 27**,** 53-77.

GRACZYK, E. L., SCHIEFER, M. A., SAAL, H. P., DELHAYE, B. P., BENSMAIA, S. J. & TYLER, D. J. 2016. The neural basis of perceived intensity in natural and artificial touch. *Sci Transl Med,* 8**,** 362ra142.

GROSSMAN, N., BONO, D., DEDIC, N., KODANDARAMAIAH, S. B., RUDENKO, A., SUK, H. J., CASSARA, A. M., NEUFELD, E., KUSTER, N., TSAI, L. H., PASCUAL-LEONE, A. & BOYDEN, E. S. 2017. Noninvasive Deep Brain Stimulation via Temporally Interfering Electric Fields. *Cell,* 169**,** 1029-1041 e16.

HINES, M. L. & CARNEVALE, N. T. 1997. The NEURON simulation environment. *Neural Comput,* 9**,** 1179-1209.

HORCH, K., MEEK, S., TAYLOR, T. G. & HUTCHINSON, D. T. 2011. Object discrimination with an artificial hand using electrical stimulation of peripheral tactile and proprioceptive pathways with intrafascicular electrodes. *IEEE Trans Neural Syst Rehabil Eng,* 19**,** 483-489.

JOHANSSON, R. S. & FLANAGAN, J. R. 2007. Tactile sensory control of object manipulation in human, volume Handbook of the Senses: Vol. 5-Somatosensation. Elsevier.

JOHANSSON, R. S. & FLANAGAN, J. R. 2009. Coding and use of tactile signals from the fingertips in object manipulation tasks. *Nature Reviews Neuroscience,* 10**,** 345-359.

JOHNSON, K. O., YOSHIOKA, T. & VEGA–BERMUDEZ, F. 2000. Tactile functions of mechanoreceptive afferents innervating the hand. *Journal of Clinical Neurophysiology,* 17**,** 539-558.

JOHNSON, M. I., PALEY, C. A., HOWE, T. E. & SLUKA, K. A. 2015. Transcutaneous electrical nerve stimulation for acute pain. *Cochrane Database of Systematic Reviews*.

JOUCLA, S., GLIERE, A. & YVERT, B. 2014. Current approaches to model extracellular electrical neural microstimulation. *Front Comput Neurosci,* 8**,** 13.

KANDEL, E. R., SCHWARTZ, J. H., JESSELL, T. M., SIEGELBAUM, S. A. & HUDSPETH, A. J. 2000. *Principles of neural science*, McGraw-hill New York.

KOT, T. & NOVAK, P. 2018. Application of virtual reality in teleoperation of the military mobile robotic system TAROS. *International Journal of Advanced Robotic Systems,* 15.

KUHN, A., KELLER, T., LAWRENCE, M. & MORARI, M. 2010. The influence of electrode size on selectivity and comfort in transcutaneous electrical stimulation of the forearm. *IEEE Trans Neural Syst Rehabil Eng,* 18**,** 255-62.

KUHN, A., KELLER, T., MICERA, S. & MORARI, M. 2009. Array electrode design for transcutaneous electrical stimulation: A simulation study. *Med Eng Phys,* 31**,** 945-951.

LAPICQUE, L. 1909. Definition experimentale de l'excitabilite. *Soc Biol,* 77**,** 280-283.

LATHAN, C. E. & TRACEY, M. 2002. The effects of operator spatial perception and sensory feedback on human-robot teleoperation performance. *Presence-Teleoperators and Virtual Environments,* 11**,** 368-377.

MARASCO, P. D., KIM, K., COLGATE, J. E., PESHKIN, M. A. & KUIKEN, T. A. 2011. Robotic touch shifts perception of embodiment to a prosthesis in targeted reinnervation amputees. *Brain,* 134**,** 747-758.

MCINTYRE, C. C., RICHARDSON, A. G. & GRILL, W. M. 2002. Modeling the excitability of mammalian nerve fibers: influence of afterpotentials on the recovery cycle. *Journal of Neurophysiology,* 87**,** 995-1006.

MELZACK, R. & WALL, P. D. 1965. Pain mechanisms: a new theory. *Science,* 150**,** 971-9.

MERRILL, D. R., BIKSON, M. & JEFFERYS, J. G. 2005. Electrical stimulation of excitable tissue: design of efficacious and safe protocols. *J Neurosci Methods,* 141**,** 171-98.

MIALL, R. C., ROSENTHAL, O., ØRSTAVIK, K., COLE, J. D. & SARLEGNA, F. R. 2019. Loss of haptic feedback impairs control of hand posture: a study in chronically deafferented individuals when grasping and lifting objects. *Exp Brain Res,* 237**,** 2167-2184.

MICERA, S. & NAVARRO, X. 2009. Bidirectional interfaces with the peripheral nervous system. *Int Rev Neurobiol,* 86**,** 23-38.

MOBERG, E. 1964. Aspects of Sensation in Reconstructive Surgery of the Upper Extremity. *JBJS,* 46**,** 817-825.

MOGYOROS, I., BOSTOCK, H. & BURKE, D. 2000. Mechanisms of paresthesias arising from healthy axons. *Muscle & Nerve: Official Journal of the American Association of Electrodiagnostic Medicine,* 23**,** 310-320.

MOGYOROS, I., KIERNAN, M. C. & BURKE, D. 1996. Strength-duration properties of human peripheral nerve. *Brain,* 119 (Pt 2)**,** 439-47.

MORRIS, D., TAN, H., BARBAGLI, F., CHANG, T. & SALISBURY, K. Haptic Feedback Enhances Force Skill Learning. Second Joint EuroHaptics Conference and Symposium on Haptic Interfaces for Virtual Environment and Teleoperator Systems (WHC'07), 22-24 March 2007 2007. 21-26.

MUNIAK, M. A., RAY, S., HSIAO, S. S., DAMMANN, J. F. & BENSMAIA, S. J. 2007. The neural coding of stimulus intensity: linking the population response of mechanoreceptive afferents with psychophysical behavior. *J Neurosci,* 27**,** 11687-11699.

NELSON, R. J. 2001. *The somatosensory system: Deciphering the brain's own body image*, CRC Press.

OCHOA, J. L. & TOREBJÖRK, H. 1980. Paraesthesiae from ectopic impulse generation in human sensory nerves. *Brain: a journal of neurology,* 103**,** 835-853.

ORTIZ-CATALAN, M., WESSBERG, J., MASTINU, E., NABER, A. & BRÅNEMARK, R. 2019. Patterned Stimulation of Peripheral Nerves Produces Natural Sensations With Regards to Location but Not Quality. *IEEE Transactions on Medical Robotics and Bionics,* 1**,** 199-203.

P. SLOPSEMA, J., M. BOSS, J., A. HEYBOER, L., M. TOBIAS, C., P. DRAGGOO, B., E. FINN, K., J. HOFF, P. & H. POLASEK, K. 2018. *Natural Sensations Evoked in Distal Extremities Using Surface Electrical Stimulation*.

PARÉ, M., SMITH, A. M. & RICE, F. L. 2002. Distribution and terminal arborizations of cutaneous mechanoreceptors in the glabrous finger pads of the monkey. *Journal of Comparative Neurology,* 445**,** 347-359.

PECKHAM, P. H. & KNUTSON, J. S. 2005. Functional electrical stimulation for neuromuscular applications. *Annu Rev Biomed Eng,* 7**,** 327-60.

PEERDEMAN, B., BOERE, D., WITTEVEEN, H., HUIS IN TVELD, R., HERMENS, H., STRAMIGIOLI, S., RIETMAN, H., VELTINK, P. & MISRA, S. 2011a. Myoelectric forearm prostheses: State of the art from a user-centered perspective. *The Journal of Rehabilitation Research and Development,* 48**,** 719-738.

PEERDEMAN, B., BOERE, D., WITTEVEEN, H., IN'T VELD, R. H., HERMENS, H., STRAMIGIOLI, S., RIETMAN, H., VELTINK, P. & MISRA, S. 2011b. Myoelectric forearm prostheses: State of the art from a user-centered perspective. *Journal of rehabilitation research and development,* 48**,** 719-737.

PENA, A. E., KUNTAEGOWDANAHALLI, S. S., ABBAS, J. J., PATRICK, J., HORCH, K. W. & JUNG, R. 2017. Mechanical fatigue resistance of an implantable branched lead system for a distributed set of longitudinal intrafascicular electrodes. *Journal of Neural Engineering,* 14**,** 066014.

PENA, A. E., RINCON-GONZALEZ, L., ABBAS, J. J. & JUNG, R. 2019. Effects of vibrotactile feedback and grasp interface compliance on perception and control of a sensorized myoelectric hand. *PLoS One,* 14**,** e0210956.

PETERSEN, B. A., NANIVADEKAR, A. C., CHANDRASEKARAN, S. & FISHER, L. E. 2019. Phantom limb pain: peripheral neuromodulatory and neuroprosthetic approaches to treatment. *Muscle & Nerve,* 59**,** 154-167.

PETRINI, F. M., VALLE, G., STRAUSS, I., GRANATA, G., DI IORIO, R., D'ANNA, E., CVANCARA, P., MUELLER, M., CARPANETO, J., CLEMENTE, F., CONTROZZI, M., BISONI, L., CARBONI, C., BARBARO, M., IODICE, F., ANDREU, D., HIAIRRASSARY, A., DIVOUX, J. L., CIPRIANI, C., GUIRAUD, D., RAFFO, L., FERNANDEZ, E., STIEGLITZ, T., RASPOPOVIC, S., ROSSINI, P. M. & MICERA, S. 2018. Six-months assessment of a hand prosthesis with intraneural tactile feedback. *Ann Neurol.*

PHILLIPS, J., JOHANSSON, R. & JOHNSON, K. 1990. Representation of braille characters in human nerve fibres. *Exp Brain Res,* 81**,** 589-592.

PREUSCHE, C. & HIRZINGER, G. 2007. Haptics in telerobotics: Current and future research and applications. *The Visual Computer: International Journal of Computer Graphics,* 23**,** 273-284.

PYLATIUK, C., SCHULZ, S. & DODERLEIN, L. 2007. Results of an Internet survey of myoelectric prosthetic hand users. *Prosthet Orthot Int,* 31**,** 362-70.

RATTAY, F. 1989. Analysis of models for extracellular fiber stimulation. *IEEE Trans Biomed Eng,* 36**,** 676-82.

REDMOND, B., AINA, R., GORTI, T. & HANNAFORD, B. Haptic characteristics of some activities of daily living. 2010 IEEE Haptics Symposium, 25-26 March 2010 2010. 71-76.

REILLY, J. P. & DIAMANT, A. M. 2011. *Electrostimulation: theory, applications, and computational model,* Artech House.

RENNIE, S. 2010. Electrophysical Agents - Contraindications And Precautions: An Evidence-Based Approach To Clinical Decision Making In Physical Therapy. *Physiotherapy Canada,* 62**,** 1-80.

RESNIK, L., BENZ, H., BORGIA, M. & CLARK, M. A. 2019. Patient perspectives on benefits and risks of implantable interfaces for upper limb prostheses: a national survey. *Expert Rev Med Devices,* 16**,** 515-540.

RUTTEN, W. L., VAN WIER, H. J. & PUT, J. H. 1991. Sensitivity and selectivity of intraneural stimulation using a silicon electrode array. *IEEE Trans Biomed Eng,* 38**,** 192-8.

SAAL, H. P. & BENSMAIA, S. J. 2014. Touch is a team effort: interplay of submodalities in cutaneous sensibility. *Trends Neurosci,* 37**,** 689-697.

SAAL, H. P. & BENSMAIA, S. J. 2015. Biomimetic approaches to bionic touch through a peripheral nerve interface. *Neuropsychologia*.

SATO, K. & TACHI, S. Design of electrotactile stimulation to represent distribution of force vectors. 2010 IEEE Haptics Symposium, 2010. IEEE, 121-128.

SCHIEFER, M., TAN, D., SIDEK, S. M. & TYLER, D. J. 2015. Sensory feedback by peripheral nerve stimulation improves task performance in individuals with upper limb loss using a myoelectric prosthesis. *J Neural Eng,* 13**,** 016001.

SCHIEFER, M., TAN, D., SIDEK, S. M. & TYLER, D. J. 2016. Sensory feedback by peripheral nerve stimulation improves task performance in individuals with upper limb loss using a myoelectric prosthesis. *J Neural Eng,* 13**,** 016001.

SCHIEFER, M. A., GRACZYK, E. L., SIDIK, S. M., TAN, D. W. & TYLER, D. J. 2018. Artificial tactile and proprioceptive feedback improves performance and confidence on object identification tasks. *PLoS One,* 13**,** e0207659.

SCHIEFER, M. A., TRIOLO, R. J., DURAND, D. M. & TYLER, D. J. Modeling selective stimulation with a flat interface nerve electrode for standing neuroprosthetic systems. Neural Engineering, 2005. Conference Proceedings. 2nd International IEEE EMBS Conference on, 2005. IEEE, 356-359.

SHIN, H., WATKINS, Z., HUANG, H., ZHU, Y. & HU, X. 2018. Evoked Haptic Sensations in the Hand via Non-Invasive Proximal Nerve Stimulation. *J Neural Eng*.

SPENCER, T. C., FALLON, J. B. & SHIVDASANI, M. N. 2018. Creating virtual electrodes with 2D current steering. *Journal of Neural Engineering,* 15.

STANDRING, S., ELLIS, H., HEALY, J., JOHNSON, D., WILLIAMS, A., COLLINS, P. & WIGLEY, C. 2005. Gray's anatomy: the anatomical basis of clinical practice. *American Journal of Neuroradiology,* 26**,** 2703.

STEVENS, S. S. 1956. The direct estimation of sensory magnitudes: Loudness. *Am J Psychol,* 69**,** 1-25.

STRAUSS, I., VALLE, G., ARTONI, F., D'ANNA, E., GRANATA, G., DI IORIO, R., GUIRAUD, D., STIEGLITZ, T., ROSSINI, P. M., RASPOPOVIC, S., PETRINI, F. M. & MICERA, S. 2019. Characterization of multi-channel intraneural stimulation in transradial amputees. *Sci Rep,* 9**,** 19258.

TACKMANN, W., SPALKE, G. & OGINSZUS, H. 1976. Quantitative histometric studies and relation of number and diameter of myelinated fibres to

electrophysiological parameters in normal sensory nerves of man. *J Neurol,* 212**,** 71-84.

TAN, D. W., SCHIEFER, M. A., KEITH, M. W., ANDERSON, J. R., TYLER, J. & TYLER, D. J. 2014. A neural interface provides long-term stable natural touch perception. *Sci Transl Med,* 6**,** 257ra138.

TAYLOR, M. M. & CREELMAN, C. D. 1967. PEST: Efficient Estimates on Probability Functions. *Journal of the Acoustical Society of America,* 41**,** 782-787.

THOTA, A. K., KUNTAEGOWDANAHALLI, S., STAROSCIAK, A. K., ABBAS, J. J., ORBAY, J., HORCH, K. W. & JUNG, R. 2015. A system and method to interface with multiple groups of axons in several fascicles of peripheral nerves. *J Neurosci Methods,* 244**,** 78-84.

VALERIO, I. L., DUMANIAN, G. A., JORDAN, S. W., MIOTON, L. M., BOWEN, J. B., WEST, J. M., PORTER, K., KO, J. H., SOUZA, J. M. & POTTER, B. K. 2019. Preemptive Treatment of Phantom and Residual Limb Pain with Targeted Muscle Reinnervation at the Time of Major Limb Amputation. *J Am Coll Surg,* 228**,** 217-226.

VANDERAH, T. & GOULD, D. J. 2015. *Nolte's The Human Brain E-Book: An Introduction to its Functional Anatomy*, Elsevier Health Sciences.

WEBER, A. I., SAAL, H. P., LIEBER, J. D., CHENG, J.-W., MANFREDI, L. R., DAMMANN, J. F. & BENSMAIA, S. J. 2013. Spatial and temporal codes mediate the tactile perception of natural textures. *Proceedings of the National Academy of Sciences,* 110**,** 17107-17112.

WEISS, G. 1990. Sur la possibilite de rendre comparables entre eux les appareils servant a l'excitation electrique. *Arch Ital Biol,* 35**,** 413-445.

WENDELKEN, S., PAGE, D. M., DAVIS, T., WARK, H. A. C., KLUGER, D. T., DUNCAN, C., WARREN, D. J., HUTCHINSON, D. T. & CLARK, G. A. 2017. Restoration of motor control and proprioceptive and cutaneous sensation in humans with prior upper-limb amputation via multiple Utah Slanted Electrode Arrays (USEAs) implanted in residual peripheral arm nerves. *J Neuroeng Rehabil* 14**,** 121.

WESSELINK, W. A., HOLSHEIMER, J. & BOOM, H. B. 1999. A model of the electrical behaviour of myelinated sensory nerve fibres based on human data. *Med Biol Eng Comput,* 37**,** 228-35.

WICHMANN, F. A. & HILL, N. J. 2001. The psychometric function: I. Fitting, sampling, and goodness of fit. *Percept Psychophys,* 63**,** 1293-1313.

WILLIAMS, T. W. 2011. Progress on stabilizing and controlling powered upper-limb prostheses. *J Rehabil Res Dev,* 48**,** IX-XIX.

ZHANG, D., XU, H., SHULL, P. B., LIU, J. & ZHU, X. 2015. Somatotopical feedback versus non-somatotopical feedback for phantom digit sensation on amputees using electrotactile stimulation. *J Neuroeng Rehabil,* 12**,** 44.

ZIEGLER-GRAHAM, K., MACKENZIE, E. J., EPHRAIM, P. L., TRAVISON, T. G. & BROOKMEYER, R. 2008. Estimating the prevalence of limb loss in the United States: 2005 to 2050. *Arch Phys Med Rehabil,* 89**,** 422-429.

VITA

ANDRES PENA

Born, Los Teques, Miranda, Venezuela

2005-2010	B.S, Electrical Engineering Florida International University Miami, Florida
2011-2013	B.S, Biomedical Engineering Florida International University Miami, Florida
2011-2013	Biomedical Technology Specialist Aplimed Medical Miami, Florida
2011-2013	Network Field Engineer Engineering Information Center Florida International University Miami, Florida
2011-2013	Research Assistant Adaptive Neural Systems Laboratory Florida International University Miami, Florida
2013-2015	NSF Bridge to Doctorate Fellow Florida International University Miami, Florida
2013-2020	Doctoral Candidate Florida International University Miami, Florida
2015-2017	Teaching Assistant Florida International University Miami, Florida

PUBLICATIONS AND PRESENTATIONS

Pena, A. E., Kuntaegowdanahalli, S. S., Jung, R., & Abbas, J. J. (2014, February). Modular multi-channel inline connector system to link electrodes to percutaneous leads or an implanted electrical device. (Poster) 2014 DARPA RE-NET Program Review, Scottsdale, AZ

Pena, A. E., Kuntaegowdanahalli, S. S., Abbas, J. J., & Jung, R. (2014, June). Fatigue testing of longitudinal intrafascicular electrodes as a peripheral nerve interface. In Neuromodulation, 17(5), e103. Issn Print: 1094-7159. Annual Neural Interface Conference, Dallas TX

Pena, A. E., Kuntaegowdanahalli, S. S., Abbas, J. J., & Jung, R. (2015, October). Mechanical fatigue testing of an implantable intrafascicular electrode system. (Poster) Annual Society for Neuroscience Conference, Chicago, IL

Pena, A. E., Rincon-Gonzalez, L., Aguilar, D., Abbas, J. J., & Jung, R. (2016, November). A sensory substitution system for providing grasping force and hand opening feedback from a sensorized myoelectric hand. (Poster) Annual Society for Neuroscience Conference, San Diego, CA

Pena, A. E., Rincon-Gonzalez, L., Abbas, J. J., & Jung, R. (2017, November). Effect of vibrotactile feedback and hand interface compliance on grasp force and hand opening. Oral Presentation at the Annual Society for Neuroscience Conference, Washington, DC

Pena, A. E., & Jung, R. (2018, February). Longitudinal Intrafascicular Electrodes (LIFEs): Restoring Sensation with a Neural-Enabled Prosthetic Hand System for Home Use: A First-in-Human Study. Oral Presentation at the Electrodes Session of the 2018 DARPA HAPTIX Program Review Meeting, Charleston, SC

Pena, A. E., & Jung, R. (2018, April). The Bioethics of Implantable Biohybrid Systems. Oral Presentation at the 9th International Conference on Ethics in Biology, Engineering & Medicine, Miami, FL

A Pena, L Herran, R Jung. Enhanced Non-invasive Peripheral Nerve Stimulation for Sensory Restoration and Neuropathic Pain Treatment. Abstract #MHSRS-19-01649 – Rehabilitation Following Limb Trauma and Amputation, (Poster) Military Health Systems Research Symposium. August 19-22, 2019, Kissimmee, FL, USA

Pena, A. E., Kuntaegowdanahalli, S. S., Abbas, J. J., Patrick, J., Horch, K. W., & Jung, R. (2017). Mechanical fatigue resistance of an implantable branched lead system for a distributed set of longitudinal intrafascicular electrodes. Journal of neural engineering, 14(6), 066014. https://doi.org/10.1088/1741-2552/aa814d

Pena, A. E., Rincon-Gonzalez, L., Abbas, J. J., & Jung, R. (2019). Effects of vibrotactile feedback and grasp interface compliance on perception and control of a sensorized myoelectric hand. PloS one, 14(1), e0210956. https://doi.org/10.1371/journal.pone.0210956